

ECO-FRIENDLY CUSHIONING FOAM FROM NATURAL RUBBER FOR
THAI FRESH PRODUCE



A Thesis Submitted in Partial Fulfillment of the Requirements for the
Degree of Master of Engineering in Materials Engineering
Suranaree University of Technology
Academic Year 2022

โปมกันกระแทกที่เป็นมิตรกับสิ่งแวดล้อมจากยางธรรมชาติสำหรับ
ผลิตภัณฑ์ไทย



วิทยานิพนธ์นี้เป็นส่วนหนึ่งของการศึกษาตามหลักสูตรปริญญาวิศวกรรมศาสตรมหาบัณฑิต
สาขาวิชาวิศวกรรมวัสดุ
มหาวิทยาลัยเทคโนโลยีสุรนารี
ปีการศึกษา 2565

ECO-FRIENDLY CUSHIONING FOAM FROM NATURAL RUBBER FOR
THAI FRESH PRODUCE

Suranaree University of Technology has approved this thesis submitted in partial fulfillment of the requirements for a Master's Degree.

Thesis Examining Committee

C. Deepsertkul

(Asst. Prof. Dr. Chantima Deepsertkul)

Chairperson

T. Trongsatitkul

(Asst. Prof. Dr. Tatiya Trongsatitkul)

Member (Thesis Advisor)

Kasama Jarukumjorn

(Assoc. Prof. Dr. Kasama Jarukumjorn)

Member (Thesis Co-advisor)

Saowapa Chaiwong

(Assoc. Prof. Dr. Saowapa Chaiwong)

Member (Thesis Co-advisor)

Supakij Suttiruengwong

(Assoc. Prof. Dr. Supakij Suttiruengwong)

Member

Nitinat Suppakarn

(Asst. Prof. Dr. Nitinat Suppakarn)

Member

Sukanya Aiamla-or

(Dr. Sukanya Aiamla-or)

Member

Chatchai Jothityangkoon

(Assoc. Prof. Dr. Chatchai Jothityangkoon)

Vice Rector for Academic Affairs and
Quality Assurance

Pornsiri Jongkol

(Assoc. Prof. Dr. Pornsiri Jongkol)

Dean of Institute of Engineering

เกวลิน จิตรโคกกรวด : โฟมกันกระแทกที่เป็นมิตรกับสิ่งแวดล้อมจากยางธรรมชาติสำหรับ
ผลิตผลสดไทย (ECO-FRIENDLY CUSHIONING FOAM FROM NATURAL RUBBER FOR
THAI FRESH PRODUCE). อาจารย์ที่ปรึกษา : ผู้ช่วยศาสตราจารย์ ดร.ตติยา ตรงสถิตกุล,
122 หน้า.

คำสำคัญ : โฟมจากน้ำยางธรรมชาติ กระบวนการต้นลอป การใช้ไมโครเวฟช่วยทำให้ยางคงรูป การ
ย่อยสลายทางชีวภาพ บรรจุภัณฑ์ ประสิทธิภาพการกันกระแทก การทดสอบการสั่นสะเทือน

วิทยานิพนธ์นี้มุ่งเน้นพัฒนาโฟมกันกระแทกที่เป็นมิตรกับสิ่งแวดล้อมจากน้ำยางธรรมชาติ
ด้วยกระบวนการต้นลอปร่วมกับการให้ความร้อนด้วยไมโครเวฟช่วยในขั้นตอนการทำให้ยางคงรูป
นอกจากนี้ศึกษาผลคอมโพสิตของโฟมยางธรรมชาติและเส้นใยธรรมชาติเพื่อปรับปรุงอัตราการย่อย
สลายทางชีวภาพของโฟมกันกระแทก โฟมยางกันกระแทกถูกทดสอบเพื่อใช้เป็นบรรจุภัณฑ์ปฐมภูมิ
สำหรับผลิตผลสดของไทยสำหรับป้องกันความเสียหายที่อาจเกิดระหว่างการขนส่ง

ขั้นตอนแรก ตัวแปรการขึ้นรูปสำหรับกระบวนการทำให้ยางคงรูปถูกปรับให้เหมาะสมเพื่อลด
พลังงานและเวลา ศึกษากำลังการฉายรังสีไมโครเวฟ (450 600 และ 800 วัตต์) และระยะเวลา (4 6
และ 8 นาที) โดยปัจจัยอื่นๆ ควบคุมให้คงที่ (ความเร็วในการปั่นน้ำยางที่ 1,250 รอบต่อนาที ด้วย
เวลา 6 นาที) การตรวจสอบโครงสร้างด้วยตาเปล่าพบว่า การฉายรังสีไมโครเวฟที่กำลังไฟ 600 วัตต์
เป็นเวลา 6 นาที ทำให้ได้การคงรูปที่สม่ำเสมอที่สุดของโฟมยางจากน้ำยางธรรมชาติ นอกจากนี้ศึกษา
ผลของความเร็วในการปั่น (650 950 1,250 1,550 และ 1,850 รอบต่อนาที) และเวลาในการปั่น (2
4 6 8 และ 10 นาที) สำหรับขั้นตอนการขึ้นรูปโฟม และปริมาณสารทำให้เกิดฟอง (1.50 3.00 และ
4.50 ส่วนในร้อยส่วนของยาง) จากผลการทดลองพบว่าสภาวะต่างๆ ที่ใช้ในการศึกษานี้ให้โฟมยางที่มี
ความแตกต่างกันเพียงเล็กน้อยของโครงสร้างโฟม ความหนาแน่น ความแข็ง ความทนแรงอัด และค่า
สัมประสิทธิ์การรับแรงกระแทก สภาวะของการปั่นที่ความเร็ว 1,250 รอบต่อนาที เป็นเวลา 6 นาที
และสารทำให้เกิดฟอง 4.50 ส่วนในร้อยส่วนของยางถูกเลือกสำหรับการผลิตโฟมยางธรรมชาติกัน
กระแทกแบบตาข่ายและคอมโพสิต เนื่องจากโฟมที่มีความหนาแน่นต่ำที่สุด

การผลิตโฟมกันกระแทกแบบตาข่ายทำโดยการใช้แม่พิมพ์ที่สร้างด้วยการพิมพ์ 3 มิติ การ
ออกแบบตาข่าย (รูปแบบและขนาด) คล้ายกับโฟมกันกระแทกทางการค้าเพื่อจุดประสงค์ในการ
เปรียบเทียบประสิทธิภาพของโฟมทั้งสองชนิด โฟมยางจากยางธรรมชาติคอมโพสิตที่มีเส้นใยใบไม้
คาดหวังว่ามีอัตราการย่อยสลายทางชีวภาพที่เร็วกว่าโฟมยางที่ไม่มีการใส่เส้นใย เส้นใยใบไม้ขนาด 90

ถึง 106 ไมโครเมตร ที่ปริมาณต่างๆ (0.00 2.50 5.00 7.50 และ 10.00 ส่วนในร้อยส่วนของยาง) ถูกใส่เข้าไปในโพลีเมอร์จากยางธรรมชาติหลังจากขั้นตอนการทำให้เกิดฟอง ผลการศึกษาพบว่าขนาดเซลล์ของโพลีเมอร์ ความหนาแน่น ความแข็ง ความทนแรงอัด สัมประสิทธิ์การกันกระแทก และการยุบตัวเนื่องจากแรงอัดของโพลีเมอร์จากน้ำยางธรรมชาติเพิ่มขึ้นตามการเพิ่มขึ้นของปริมาณเส้นใยใบไม้ ในทางตรงกันข้าม ความหนาแน่นของพันธะการเชื่อมขวางมีแนวโน้มลดลง เมื่อปริมาณเส้นใยใบไม้เพิ่มขึ้น นอกจากนี้มีการใช้วิธีการฝังดินเป็นเวลา 24 สัปดาห์เพื่อตรวจสอบอัตราการย่อยสลายทางชีวภาพของโพลีเมอร์คอมโพสิต หลังจากการฝังดิน ผลการทดลองแสดงให้เห็นว่าอัตราการย่อยสลายทางชีวภาพช่วงเริ่มต้นของโพลีเมอร์คอมโพสิตเพิ่มขึ้นอย่างมีนัยสำคัญตามปริมาณของเส้นใยใบไม้ที่ใช้ ผลการทดลองนี้สอดคล้องกับการเปลี่ยนแปลงของลักษณะทางกายภาพและสัณฐานวิทยา โครงสร้างทางเคมี และสมบัติเชิงกล

การทดสอบประสิทธิภาพของโพลีเมอร์จากน้ำยางธรรมชาติและโพลีเมอร์คอมโพสิตในการเป็นบรรจุภัณฑ์กันกระแทกเปรียบเทียบกับโพลีเมอร์ทางการค้า (โพลีเอทิลีนแบบขยาย) ผ่านการทดสอบบรรจุภัณฑ์กับฝรั่งภายใต้สภาวะการขนส่งเหิน (ความเร่ง 8.826 เมตรต่อวินาทีกำลังสอง ความถี่ 13.5 เฮิรตซ์ เป็นเวลา 40 นาที) หลังการขนส่ง ฝรั่งถูกเก็บในห้องเย็นที่อุณหภูมิ 20 องศาเซลเซียส เป็นเวลา 4 วัน พบว่าฝรั่งที่ไม่มีโพลีเมอร์กันกระแทกมีพื้นที่ช้ำมากที่สุด ในขณะที่ฝรั่งที่บรรจุในโพลีเมอร์คอมโพสิตที่ไม่มีเส้นใยใบไม้มีรอยช้ำน้อยที่สุด ซึ่งเทียบเคียงได้และ/หรือดีกว่าฝรั่งที่บรรจุในโพลีเมอร์เชิงพาณิชย์เล็กน้อย ผลที่ได้สอดคล้องอย่างดีกับการส่งผ่านเปอร์เซ็นต์ที่ต่ำของตัวอย่างทั้งสอง

โพลีเมอร์กันกระแทกที่เป็นมิตรกับสิ่งแวดล้อมที่พัฒนาขึ้นในงานนี้ได้รับการพิสูจน์แล้วว่าเป็นทางเลือกทางเลือกที่ดีเพื่อใช้ทดแทนโพลีเมอร์ทางการค้า โพลีเมอร์กันกระแทกที่เป็นมิตรกับสิ่งแวดล้อมในด้านต่างๆ ประกอบด้วย วัตถุประสงค์ กระบวนการผลิต ประสิทธิภาพในการกันกระแทก และการเสื่อมสภาพหลังอายุการใช้งาน โดยงานนี้ยังเป็นการเพิ่มมูลค่าให้กับยางธรรมชาติซึ่งเป็นผลิตภัณฑ์ทางการเกษตรที่สำคัญชนิดหนึ่งของไทยอีกด้วย

สาขาวิชาวิศวกรรมพอลิเมอร์

ปีการศึกษา 2565

ลายมือชื่อนักศึกษา... เกวลิน จิตรโกกกร

ลายมือชื่ออาจารย์ที่ปรึกษา... T. Sangpatitkul

ลายมือชื่ออาจารย์ที่ปรึกษาร่วม... นาย ก. ก.

ลายมือชื่ออาจารย์ที่ปรึกษาร่วม... นาย ข. ข.

KEAVALIN JITKOKKRUAD: ECO-FRIENDLY CUSHIONING FOAM FROM NATURAL RUBBER FOR THAI FRESH PRODUCE. THESIS ADVISOR: ASST. PROF. TATIYA TRONGSATITKUL, Ph.D., 122 PP.

Keyword: Natural rubber latex foam/ Dunlop process/ Microwave assisted vulcanization/ Biodegradation/ Packaging/ Cushion performance/ Vibration test

The focus of this thesis was to develop an eco-friendly cushion made from natural rubber latex (NRL) using the Dunlop process coupled with microwave-assisted vulcanization. Additionally, composite of the NRL foam with natural fiber was studied with the aim to enhance the cushion's foam biodegradation rate. The cushion foam was tested to be used as primary packaging for Thai fresh produce to prevent any damage that might occur during transportation.

Firstly, the processing parameters for the vulcanizing process were optimized to reduce energy and time. The microwave irradiation powers (450, 600, and 800 W) and time (4, 6, and 8 min) were studied, with other factors being held constant (stirring speed of 1,250 rpm for 6 min). The visual observation suggested that microwave irradiation at 600 W for 6 min was optimal as it yielded the most uniform curing of the NRL foam. Additionally, the effects of stirring speed (650, 950, 1,250, 1,550, and 1,850 rpm) and time (2, 4, 6, 8, and 10 min) for foaming step and foaming agent content (1.50, 3.00, and 4.50 parts) were studied. The results revealed that the various conditions used in this study yielded the foams with slight differences in terms of foam structure, density, hardness, compressive strength, and cushion coefficient. The condition of a stirring speed of 1,250 rpm for 6 min and a foaming agent of 4.50 phr was selected for fabricating NRL foam net and its composite as it yielded a foam with lowest density.

The fabrication of NRL foam net was made possible by using 3D printed mold. The net design (shape and size) was similar to that of the commercial foam net with the purpose to compare their performance. The NRL foam composite with BLF was expected to possess the faster biodegradation rate as compared to the NRL foam without one. The bamboo leaf fiber (BLF) with the size range of 90 to 106 μm at various

contents (0.00, 2.50, 5.00, 7.50, and 10.00 phr) were added into the NRL foam after the foaming step. The results suggested the foam's cells size, density, hardness, compressive strength, cushion coefficient, and compression set of the NRL foam samples increased as a function of the increasing BLF content. In contrast, the crosslink density showed the decreasing trend as the BLF content increased. In addition, the soil burial method of 24 weeks was used to investigate the biodegradation rate of the NRL foam composites. After of soil burial, the results revealed that the initial biodegradation rates of the foam composites increased significantly with the amount of BLF used. This result was well agreed with the changes in physical and morphological characteristics, chemical structure and, mechanical properties.

The performance of NRL foam and its composites as a cushioning packaging was evaluated against the commercial foam (expanded polyethylene foam) via pack test of guava under the simulated vibration condition (an acceleration of 8.826 m/s^2 at a frequency of 13.5 Hz for 40 min). After the vibration conditioning, the guavas were then stored in a cold room at $20 \text{ }^\circ\text{C}$ for 4 days. It was found that guava without cushioning foam had the most bruising area, while the guava packed in the NRL foam without BLF had the least bruise which was comparable and/or slightly better than that of packed in the commercial foam. The result was in a good agreement with the low percentage transmission of the two samples.

The eco-friendly foam cushions developed in this work was proven to be a good alternative to replace the commercial one. They were eco-friendly in various aspects including raw material, process, cushion performance, and degradation after service life. This work also added the value to the natural rubber which was one of the main agricultural products of Thailand.

School of Polymer Engineering

Academic Year 2022

Student's Signature Keavalin Jitkokkrud

Advisor's Signature T. Trongsatitkul

Co-advisor's Signature Kasana Janakunich

Co-advisor's Signature Sayan Y

ACKNOWLEDGEMENTS

I wish to thank the Center of Excellence in Petrochemical and Materials Technology (PETROMAT) for scholarship and financial support in the High Performance and Smart Materials (HPSM) program. I appreciate the resources and facilities provided by Mea Fah Luang University and Suranaree University of Technology.

My thesis advisor, Asst. Prof. Dr. Tatiya Trongsatitkul, is the most significant figure in my academic career at Suranaree University of Technology, and I would like to convey my sincere gratitude to her. I would like to thank my thesis co-advisors, Assoc. Prof. Dr. Kasama Jarukumjorn and Assoc. Prof. Dr. Saowapa Chaiwong for their invaluable guidance, suggestions, and encouragement during this research. My thanks go to Asst. Prof. Dr. Chantima Deeprasertkul, Assoc. Prof. Dr. Supakij Suttiruengwong, Asst. Prof. Dr. Nitinat Suppakarn, and Dr. Sukanya Aiamla-or for their helpful suggestions and guidance as thesis examining committee member.

I also want to thank the entire Suranaree University of Technology Laboratory staff for their assistance and support with my project.

Finally, I want to express my gratitude to all of my professors and peers for their support and encouragement.

Last but not least, without my family's assistance throughout my time as a student at Suranaree University of Technology, I would not have been able to graduate.

KEAVALIN JITKOKKRUAD

TABLE OF CONTENTS

	Page
ABSTRACT (THAI).....	II
ABSTRACT (ENGLISH).....	III
ACKNOWLEDGEMENTS.....	V
TABLE OF CONTENTS.....	VI
LIST OF TABLES.....	X
LIST OF FIGURES.....	XI
CHAPTER	
1. INTRODUCTION.....	1
1.1 Background.....	1
1.2 Research objectives.....	6
1.3 Scope and limitation of the study.....	7
2. LITERATURE REVIEWS.....	8
2.1 Cushioning materials.....	8
2.2 NRL foam fabrication technique.....	8
2.3 Cell foam structure.....	9
2.3.1 Open-cell foam.....	9
2.3.2 Closed-cell foam.....	10
2.4 Key parameters affecting foam density.....	11
2.4.1 Mechanical foaming agent.....	11
2.4.2 Chemical foaming agent.....	11
2.5 Heating technique for NRL foam vulcanization.....	11
2.6 Cushion performance of material.....	12
2.7 Biodegradability of NRL foam.....	12

TABLE OF CONTENTS (Continued)

	Page
2.7.1 Effect of fiber on enhancing biodegradability of NRL foam.....	12
2.7.2 Effect of crosslink density on biodegradability of NRL foam.....	13
3. RESEARCH METHODOLOGY.....	14
3.1 Materials and methods.....	14
3.1.1 Materials.....	14
3.1.2 Preparation of bamboo leaf fiber.....	15
3.1.3 Preparation of rapid silicone mold.....	15
3.1.4 Fabrication of NRL foam via the Dunlop process together with microwave-assisted vulcanization technique.....	16
3.1.5 Fabrication of NRL foam composites via the Dunlop process together with microwave-assisted vulcanization technique.....	17
3.1.6 Characterization.....	18
3.1.6.1 Bulk density.....	18
3.1.6.2 Morphology.....	18
3.1.6.3 Hardness.....	19
3.1.6.4 Mold shrinkage.....	19
3.1.6.5 Compression set.....	19
3.1.6.6 Compression test.....	20
3.1.6.7 Cushion coefficient.....	21
3.1.6.8 Biodegradation study.....	21

TABLE OF CONTENTS (Continued)

	Page
3.1.6.9 Crosslink density.....	22
3.1.6.10 Pack test (Simulated vibration transportation).....	23
3.1.6.11 Percentage transmissibility.....	25
3.1.6.12 Statistical analysis.....	25
4. RESULTS AND DISCUSSION.....	26
4.1 Process optimization and formulation of eco-friendly cushioning packaging foam fabrication from natural rubber latex using the Dunlop process coupled with microwave- assisted vulcanization.....	26
4.1.1 Effect of foaming time.....	27
4.1.1.1 Bulk density.....	27
4.1.1.2 Morphology.....	28
4.1.1.3 Compression test.....	29
4.1.2 Effect of stirring speed.....	30
4.1.2.1 Bulk density.....	30
4.1.2.2 Morphology.....	31
4.1.2.3 Compression test.....	32
4.1.3 Effect of potassium oleate content.....	33
4.1.3.1 Bulk density.....	33
4.1.3.2 Morphology.....	33
4.1.3.3 Compression test.....	34
4.1.3.4 Cushion coefficient.....	35

TABLE OF CONTENTS (Continued)

	Page
4.2 Effect of BLF content on foam properties and biodegradability of NRL foam composite.....	37
4.2.1 Appearance and design of the NRL foam cushion.....	38
4.2.2 Mold shrinkage.....	39
4.2.3 Bulk density.....	40
4.2.4 Morphology and cell structure analysis.....	41
4.2.5 Hardness.....	45
4.2.6 Compression set.....	46
4.2.7 Compression test.....	48
4.2.8 Crosslink density.....	50
4.2.9 Biodegradation study.....	52
4.2.9.1 Appearance.....	52
4.2.9.2 Weight loss.....	53
4.2.9.3 Fourier transform infrared (FTIR) analysis.....	56
4.2.9.4 Compression test.....	60
4.3 Evaluate the cushion performance of eco-friendly NRL foam using a vibration condition in pack test.....	61
4.3.1 Cushioning properties and percentage transmission.....	62
4.3.2 Appearance.....	63
5. CONCLUSIONS AND RECOMMENDATIONS.....	66
REFERENCES.....	68
APPENDIX.....	78
List of publications.....	79
BIOGRAPHY.....	122

LIST OF TABLES

Table	Page
3.1	Formulation of NRL foam at various foaming agents and BLF contents.....14
4.1	Physical appearance of NRL foam at various microwave irradiation conditions.....27
4.2	Properties of NRL foam prepared using different foaming times and at a constant speed of 1,250 rpm.....28
4.3	Properties of NRL foam prepared using different stirring speeds and at a constant time of 8 min.....31
4.4	Properties of NRL foam prepared using different foaming agent.....35
4.5	Cushion coefficient (C) at 50% strain of NRL foam at various foaming agent...37
4.6	Foam properties of EPE-FN and NRL-FN-BLFs.....42
4.7	Cushion coefficient at 50% strain of a commercial cushion foam compared to the eco-friendly cushion NRL-FN at various BLF contents.....51
4.8	Crosslink density and swelling ratio of the NRL foam composite at various BLF contents.....51
4.9	Appearance and micrograph of cushion foams before soil burial (0 weeks) and after soil burial (24 weeks).....54
4.10	IR bands assignment of NRL, BLF, and NRL composite.....57
4.11	Guava appearance on day 0 and day 4 of simulated vibration Transportation.....64
4.12	Thickness, energy (E), cushion coefficient (C) and percentage transmissibility (P_T) of five treatments.....65

LIST OF FIGURES

Figure	Page
2.1	Dunlop process.....9
2.2	Open-cell foam structure.....10
2.3	Closed-cell foam structure.....10
3.1	The appearance and shape of bamboo leaf fibers: (a) photograph; (b) SEM micrograph at a 100× magnification.....15
3.2	Schematic for fabricating a rapid silicone mold using 3D printing: (a) 3D model; (b) converting to G-code; (c) 3D printing; (d) inverted mold; and (e) silicone mold.....16
3.3	Biodegradation experiment of cushion foams: (a) plastic box used for soil burial; (b) cushion foam placement.....22
3.4	Guava packaging for simulated vibration transportation.....23
3.5	Vibration simulation test equipment.....24
4.1	SEM micrographs of NRL foam prepared using a constant foaming speed of 1,250 rpm and different foaming times (a) 2 min, (b) 4 min, (c) 6 min, (d) 8 min, and (e) 10 min.....29
4.2	Cell size distribution of NRL foam at foaming speed of 1,250 rpm and different foaming times (a) 2 min, (b) 4 min, (c) 6 min, (d) 8 min, and (e) 10 min.....30
4.3	Physical appearance of NRL foam during foam production at (a) 650 rpm and (b) 1,850 rpm.....31
4.4	SEM micrographs of NRL foam at foaming time of 8 min and various stirring speed (a) 950 rpm, (b) 1,250 rpm, and (c) 1,550 rpm.....32

LIST OF FIGURES (Continued)

Figure		Page
4.5	Cell size distribution of NRL foam at foaming time 8 min and various stirring speeds (a) 950 rpm, (b) 1,250 rpm, and (c) 1,550 rpm.....	32
4.6	SEM micrographs of NRL foam at various potassium oleate contents (a) 1.50 phr, (b) 3.00 phr, and (c) 4.50 phr.....	34
4.7	Cell size distribution of NRL foam at various potassium oleate contents (a) 1.50 phr, (b) 3.00 phr, and (c) 4.50 phr.....	34
4.8	Compressive stress-strain curve of the NRL foam at various foaming agent contents.....	35
4.9	Cushion coefficient-compressive strain curve of the NRL foam at various foaming agents.....	36
4.10	Fabrication and design of NRL-FN: (a) foam net sheet; (b) foam net cylindrical tube; (c) cross-section of EPE-FN; and (d) cross-section of NRL-FN.....	38
4.11	Cushion foam net: (a) EPE-FN; (b) NRL-FN-BLF0.0; (c) NRL-FN-BLF2.5; (d) NRL-FN-BLF5.0; (e) NRL-FN-BLF7.5; (f) NRL-FN-BLF10.0.....	39
4.12	Shrinkage percentage of NRL foam composite at various BLF loading at different shrinkage directions compared with silicone mold size. Significant differences at $p < 0.05$ are shown by different letters. The values represent the mean \pm S.E. of five replicates.....	40
4.13	NRL foam composites morphology at the top surface of specimens (5kx magnification): (a) EPE-FN; (b) NRL-FN-BLF0.0; (c) NRL-FN-BLF2.5; (d) NRL-FN-BLF5.0; (e) NRL-FN-BLF7.5; (f) NRL-FN-BLF10.0.....	43
4.14	Cushion foams morphology at a 50x magnification: (a) EPE-FN; (b) NRL-FN-BLF0.0; (c) NRL-FN-BLF2.5; (d) NRL-FN-BLF5.0; (e) NRL-FN-BLF7.5; (f) NRL-FN-BLF10.0.....	44

LIST OF FIGURES (Continued)

Figure	Page
4.15 Cell size distribution of NRL foam composite with various BLF loadings ($p < 0.05$, $n = 400$): (a) NRL-FN-BLF0.0; (b) NRL-FN-BLF2.5; (c) NRL-FN-BLF5.0; (d) NRL-FN-BLF7.5; (e) NRL-FN-BLF10.0.....	45
4.16 Compression set of NRL foam composite various BLF loading. Significant differences at $p < 0.05$ are shown by different letters. The values represent the mean \pm S.E. of five replicates.....	47
4.17 Stress–strain curve of the cushion foams.....	48
4.18 Cushion coefficient–compressive strain curves of cushion foams.....	50
4.19 Weight loss percentage of EPE-FN, NRL-FN, and NRL-FN-BLFs cushion Foams at various BLF contents over 24 weeks of soil burial times.....	55
4.20 Weight loss percentage of NRL-FN-BLF0.0 (thickness ~ 3 mm) and NRL-FN-BLF0.0 (thickness ~ 2 mm) cushion foams at thickness over 24 weeks of soil burial times.....	56
4.21 FTIR spectra of NRL foam composites before (solid lines) and after (dash lines) soil burial.....	58
4.22 FTIR spectrum of BLF.....	59
4.23 FTIR spectra of NRL foam composites at various BLF contents after soil burial for 24 weeks.....	60
4.24 Compressive strength of 50% after soil burial for 24 weeks of cushion Foam at various soil burial times.....	61

CHAPTER 1

INTRODUCTION

1.1 Background

Plastic waste is one of the most problematic among various materials. The beneficial qualities such as its light weight, durability, inertness, ease of the process, and versatility of plastics have served humans well for several decades. On the other hand, these qualities also lead to an enormous amount of plastic waste accumulation due to the high consumption volume and poor decomposability/degradability. The UN environment program (UNEP) anticipates that plastic will increase by 1,100 million tons in 2,050 from 400 million tons in the present year. Because most plastics are fossil-based materials, the widespread use of these materials adds other concerns to environmental issues, such as the exhaustion of natural resources and global warming (Nilsen-Nygaard et al., 2021). Several key aspects must be considered to effectively address these problems, including product design and material selection to enhance recyclability (Roithner, Cencic, & Rechberger, 2022), strict regulation enforcement (Ncube, Ude, Ogunmuyiwa, Zulkifli, & Beas, 2021), and proper education of the public (Filho et al., 2021) are examples of how to remedy the situation sustainably.

Because plastics are versatile materials, they are used in several industries, such as automotive, construction, home appliances, electronics, and packaging (Faraca & Astrup, 2019). The proper management of plastic product waste requires an understanding of their natures, including the type of materials used, how they are made, how they are used, service life, and post-consumer disposal. Among all plastic products, approximately 36% is used in packaging. Single-use items such as food and drink containers are made up of the most share of waste. Although rigid plastic packaging, such as bottles, boxes, trays, and cups, has been successfully recycled (Horodytska, Valdés, & Fullana, 2018), 85% of plastic packaging waste is discarded as

uncontrolled waste or in landfills (Programme, 2018). These problematic wastes are mainly flexible packaging, such as plastic films and bags, as well as cushioning materials. These types of packaging are difficult to collect as they are very thin or/and low in bulk density. They are also difficult to separate (multi-layer film) and once contaminated, they are also difficult to clean. Recycling these plastics waste is often logistically and economically unfeasible. For example, cushion foam nets for fresh produce protect the goods during transportation. Once the produce arrives customers, the cushion is discarded even though it could have been reused or recycled. The cost to retrieve, collect, and transport back to the packaging location is cumbersome and requires combined efforts from several parties.

Plastics used to fabricate cushion foam nets for fresh produce are mainly made from expanded polystyrene foam (EPS) and expanded polyethylene foam (EPE). With the foam structure, they are exceptionally light and able to absorb mechanical shock, vibration, and impact forces that occur during transportation. Fresh fruit covered with proper cushion materials are therefore protected from mechanical damage. Together with good cold-chain management, the fruit's appearance, quality, and nutrients can be preserved (Li, 2021). Cushioning is thus a crucial part of a packaging system. However, to reduce the negative impact of the synthetic foams (Georges, Lacoste, & Damien, 2018; Sohn, Kim, Kim, Ryu, & Cha, 2019), many countries have placed restrictions on their use. This includes laws imposed by local and state governments on single-use packaging at the end of its life cycle. Consequently, an alternative cushion that is eco-friendly and possesses a good cushion performance is in great demand.

To substitute the current nondegradable polystyrene and polyethylene packaging materials, researchers have focused on using biodegradable polymers, such as polylactic acid (PLA), poly(lactic-co-glycolic acid) (PLGA), polybutylene adipate terephthalate, (PBAT), and poly(3-hydroxybutyrate-co-3-hydroxyvalerate) (PHBV) (Vroman & Tighzert, 2009). However, these polymers are substantially more expensive compared to conventional petroleum-based polymers (Ke & Sun, 2003), such as high-

density polyethylene (HDPE), low-density polyethylene (LDPE), and polypropylene (PP), etc. The lack of processability and, even less so, their cushioning performance information lead to the unsuccessful use of these biodegradable polymers. Blends of biodegradable polymers and conventional polymers, such as HDPE/PLA (Torres-Huerta et al., 2019), PLA/PP (Hamad, Kaseem, & Deri, 2011) and PLA/LDPE (Trongsatitkul & Chaiwong, 2017), etc., have also been investigated. Their practicality and implementation, as well as environmental impacts, are yet to be evaluated.

Another interesting alternative for cushioning materials is natural rubber (NR). NR is harvested from the rubber tree (*Hevea brasiliensis*) in latex (Mahathaninwong et al., 2021; Prasopdee & Smitthipong, 2020). NR is, therefore, bio-based material that comes from a renewable resource and is inherently biodegradable (Garrison, Murawski, & Quirino, 2016). In fact, a NR product may undergo degradation via one or a combination of several degradation modes, including mechanical degradation, oxidation, photodegradation, thermal degradation, and/or biodegradation (Jedruchniewicz, Ok, & Oleszczuk, 2021). Previous works have been done to prevent the degradation of a NR product to extend its service life. Now degradation of NR is appreciatively viewed as a solution for environmental pollution. Foam products of NR have been used as mattresses, pillows (Prasopdee & Smitthipong, 2020; Suksup, Sun, Sukatta, & Smitthipong, 2019), cushions (Mahathaninwong et al., 2021), padding foam (Syahrin, Zunaida, Hakimah, & Nuraqmar, 2020), etc. The natural rubber latex (NRL) foam possesses unique properties such as lightweight, good thermal insulation, good sound absorption, excellent elasticity, good cushioning performance, and biodegradability (Phomrak, Nimpaiboon, Newby, & Phisalaphong, 2020; Suethao, Phongphanphanee, Wong-Ekkabut, & Smitthipong, 2021; Suksup et al., 2019). Our research team is interested in using NRL foam as cushion material for fresh produce.

Generally, the NRL foam can be fabricated using a Dunlop or Talalay process. The Dunlop process has been widely used as it is a simpler process with a lower production cost and is more energy efficient than those of the Talalay process (Sirikulchaikij, Kokoo, & Khangkhamano, 2020). The Dunlop process steps include

incorporation of the air and some chemicals into the latex via a mechanical method to create and stabilize the foam structure before vulcanization. Heating in the vulcanization step may use either a conventional hot air oven and a microwave oven (Ariff, Afolabi, Salmazo, & Rodriguez-Perez, 2020). The recent trend of replacing conventional heating with microwave irradiation is due to the advantages of the later process. For the microwave heating, the heat generated in the product results from the conversion of electromagnetic energy to thermal energy (Tang & Resurreccion Jr, 2009). Because of the direct interaction between the microwave and the heated article, energy transfer occurs more efficiently. Thus, microwave heating provides a significantly faster heating rate, resulting in shorter vulcanization time, higher production rate, and less time and energy consumption compared to conventional heating (Ahmad Zauzi, Ariff, & Khimi, 2019; Ariff et al., 2020). We have successfully optimized the microwave irradiation condition for making the NRL foam (Jitkokkruad, Jarukumjorn, Chaiwong, & Trongsatitkul, 2021). The study showed the promising and important finding that the use of microwave heating could reduce vulcanization time by 15 folds (from 90 min (Sirikulchaikij et al., 2020) to 6 min (Jitkokkruad et al., 2021)). Using microwave irradiation for NRL foam fabrication is, therefore, fundamentally making the foam product more eco-friendly.

To further improve the eco-friendly attributes of NRL foam, enhancing its biodegradation rate is considered. Even though NR is fully degraded, the degradation time of rubber products could be up to several decades. The relatively long degradation time may lead to environmental pollution as landfill sites become too limited (Gillen & Clough, 1997; Jedruchniewicz et al., 2021). A biodegradable filler may be added to the NRL to reduce such issues. Natural fillers, such as rice husk (Ramasamy, Ismail, & Manusamy, 2013; Ramasamy, Ismail, & Munusamy, 2015), fiber of banana, coir, bagasse (Mursalin, Islam, Moniruzzaman, Zaman, & Abdullah, 2018), oil palm fiber (Tomyangkul, Pongmuksuwan, Harnnarongchai, & Chaochanchaikul, 2016), sisal (Alvarez, Fraga, & Vazquez, 2004), bamboo (Lokesh, Kumari, Gopi, & Loganathan, 2020), and kenaf (Kudori & Ismail, 2019; Srisuwan, Jarukumjorn, & Suppakarn, 2018)

have been added to polymer matrixes. Several research groups have reported that the addition of natural fibers contributed to the enhancement of biodegradability for the polymer products (Ramasamy et al., 2015).

Bamboo is one of the most common plants available in Asian countries. It is one of the fastest-growing plants, is widely accessible, considered a sustainable resource (Ameram, Afiq Che Agoh, Idris, & Ali, 2018; Mohd Nazri & Sapawe, 2020), and is strong and lightweight (Surip, Khalil, Wan Othman, & Jawaid, 2013). Bamboo leaf is the by-product of growing bamboo trees. It is high in fiber, protein, and silica content and can be used for bamboo tea, bamboo beer, livestock feed, medicinal aids, aromatherapy, and essential oils (Lewis Bamboo, 2022). Research and development has found bamboo leaves to be a good carbon source. They can be made into aerogel, silica nanoparticles, adsorbents, and composites. Adding bamboo leaf fiber (BLF) into NRL foam should positively affect the environment, society, and the economy (Yuan et al., 2021). However, limited information is available regarding how the BLF affects the cushion performance of NRL foam, especially for fresh produce packaging applications.

Therefore, the aim of this studies to develop eco-friendly cushioning packaging foam from the NRL. We used the Dunlop process together with microwave-assisted vulcanizing for NRL foam fabrication. Firstly, optimize microwave irradiation conditions (power and time). The power and time are 450, 600, and 800 W and 4, 6, and 8 min, respectively were investigated. In addition, the foaming time (2, 4, 6, 8, and 10 min) and stirring speed (950, 950, 1,250, 1,550, and 1,850 rpm) were investigated as parameters of foam structure, density, hardness, and compressive strength. Then, the foam was reduced in bulk density using potassium oleate (K-oleate) at various contents (1.50, 3.00, and 4.50 phr). The lowest foam density was chosen for eco-friendly cushioning packaging foam fabrication.

The BLF was added to the NRL foam due to its ability to enhance the biodegradability of the foam. The main focus was to investigate the effect of BLF contents (0.00, 2.50, 5.00, 7.50, and 10.00 phr) on physical and mechanical properties,

cushion coefficient (C), and biodegradability. The NRL foam composite was prepared into a net shape similar to that of commercial foam. The NRL foam composites were compared to a commercial EPE cushion net in terms of foam density, hardness, morphology, cushion coefficient (C), and biodegradability. Additionally, the mold shrinkage, compression set, number of cells per unit volume, and average cell size of the composites were studied. The NRL foam composite was tested for biodegradability using the soil burial method for a duration of 24 weeks (6 months). The degradation results of the NRL foam composites were analyzed by weight loss, chemical structure, foam appearance, morphology, compressive strength, and crosslink density. The pack test was simulated in vibration mode for transportation (using an acceleration of 8.826 m/s^2 at a frequency of 13.5 Hz for 40 min). Guava was represented as fresh produce in the sphere model. The guava was wrapped in a foam net. After a vibration test for 4 days, the foam was followed by the bruising area and the percentage of transmission that occurred with guava.

1.2 Research objectives

1.2.1 Process optimization and formulation of eco-friendly cushioning packaging foam fabrication from natural rubber latex using the Dunlop process coupled with microwave-assisted vulcanization.

1) To investigate the critical microwave heating parameters including microwave irradiation power and time on NRL foam structure and foam appearance.

2) To study effect of foaming time, stirring speed, and foaming agent content on foam structure, density, hardness, compressive property and cushion coefficient.

1.2.2 To study effect of BLF content on foam properties and biodegradability of NRL foam composite.

1) To study effect of BLF content on foam structure, density, hardness, mold shrinkage, compressive property, compression set, cushion coefficient, and crosslink density of NRL foam composite. 2) To study biodegradability of NRL foam

composite using soil burial method on foam appearance, foam structure, chemical structure, weight loss, and compressive property.

1.2.3 To evaluate the cushion performance of eco-friendly NRL foam using a vibration condition in pack test.

1.3 Scope and limitations of the study

In this work, the study was divided into three main sections including eco-friendly cushioning foam fabrication, biodegradation study of NRL foam composite, and pack test (simulated vibration transportation).

The cushioning packaging from NRL foam was prepared by the Dunlop process and vulcanized using microwave-assisted heating. Microwave irradiation power and time for vulcanization of the NRL foam were varied at 450, 600, and 800 W for 4, 6, and 8 min. In the Dunlop process, NRL foam was prepared with different foaming times (2, 4, 6, 8, and 10 min), stirring speeds (950, 950, 1,250, 1,550, and 1,850 rpm), and foaming agent contents (1.50, 3.00, and 4.50 phr) in the foaming step. Morphology was examined by a scanning electron microscope (SEM). A compressive test was performed using a universal testing machine. The relationship between compressive stress and strain was used to calculate the cushion coefficient of samples.

In the biodegradation study, the effect of BLF contents (0.00, 2.50, 5.00, 7.50, and 10.00 phr) on biodegradability of NRL foam composite were investigated in terms of physical and mechanical properties, weight loss, and chemical structure (FTIR analysis). The foam structure, foam properties, and cushion performance of NRL foam composite were compared with a commercial foam. Moreover, the foam properties such as foam appearance, hardness, mold shrinkage, compressive property, cushion coefficient, compression set, and crosslink density of the NRL foam composites were tested. The crosslink density was calculated using the Flory-Rehner equation.

The cushioning performance was evaluated via pack test in simulated vibration transportation. The bruise area and percentage transmission were analyze.

CHAPTER 2

LITERATURE REVIEWS

2.1 Cushioning materials

Cushions are used to protect fresh produce against mechanical damage while being harvested, handled, stored, or transported. Packaging with cushioning is very effective at reducing vibration/impact damage on the product. Vibration/impact protection of fresh produce is the main aim of packaging but other properties of cushioning materials such as flexibility, environmental compatibility and consumer safety aspects should also be considered. Cushioning materials can be categorized as natural or synthetic, based on their origins. The fundamental role of a cushioning material is to reduce the forces created during sudden contact of one surface with another, which prevents compression or deforming damages and minimizes damaging impact forces (Dubey & Mishra, 2019).

2.2 NRL foam fabrication technique

There are two main techniques used in making NRL foam i.e. Dunlop process and Talalay process. The advantages of using the Dunlop method are that it requires less massive capital investment in its equipment and can achieve higher durability and environmental sustainability in the product (Surya, Kudori, & Ismail, 2019). The fabrication of the NRL foam are shown in Figure 2.1. Generally, Dunlop process is divided into four steps (compound preparation, foaming, gelling, and curing). The compound is stirred by a Hobart mixer at 1,200 rpm to increase volume 10 times from original. The Dunlop process and the Talalay process had similar foam structures. However, the Dunlop process was mainly used in Thailand due to its simplicity and low production costs. Currently, the bubbling process was used and replaced the Talalay process due to the absence of the vacuum and freezing system. In the foaming step, the bubbling process was prepared similarly to the Dunlop process except for

the foaming process (The compound was fed air through a diffuser in the bubble column). The inlet air flow was varied at 20, 50, and 100 cm³/min. Foam structure from the Dunlop process showed non-uniform cell size, irregular shape, and heavily fractured interconnective-cell structure. The bubbling process demonstrated a flawless, crack-free, spherical, interconnected foam network. The cell size of the foam in the bubbling process was smaller than the Dunlop process. The foam density decreased with increasing air flow into the latex compound. Moreover, the compression set and indentation index were increased with increasing air flow rate (Sirikulchaikij et al., 2020).

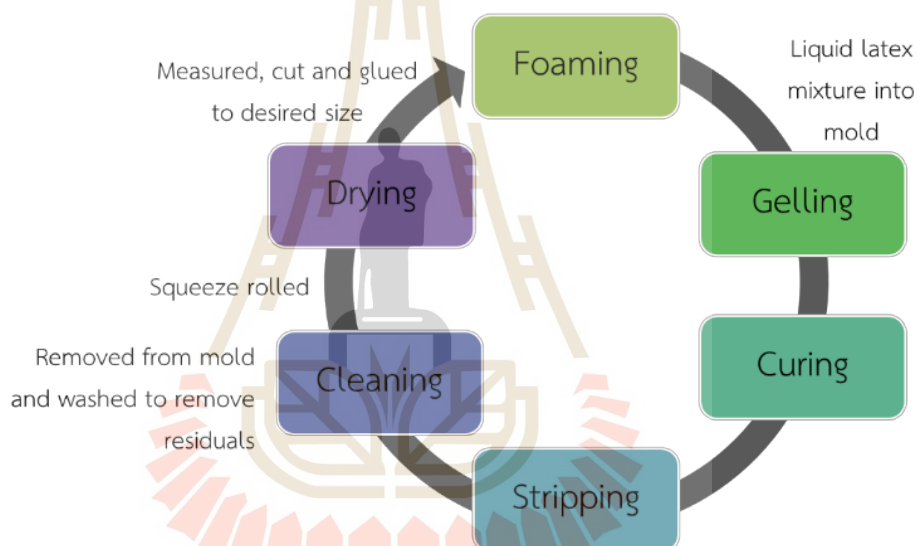


Figure 2.1 Dunlop process (Hui Mei & Singh, 2010)

2.3 Cell foam structure

Cellular foam structure indicates properties of foam. Generally, foam structures are divided into open-cell and closed-cell foams.

2.3.1 Open-cell Foam

Open-cell foam structure is shown in Figure 2.2 The structure is made from the foaming process, which creates a cell network. Foam produced is compressed during impact, air flows through the connected cellular structure and out of the foam. If an open-cell foam is manufactured with smaller cells, the foam cannot be compressed due to the fact that there is less air to exhaust from the material. Moreover, smaller

cells increase the volume of material, making it denser and less able to compress under impact (Goodwin & Young, 2011).

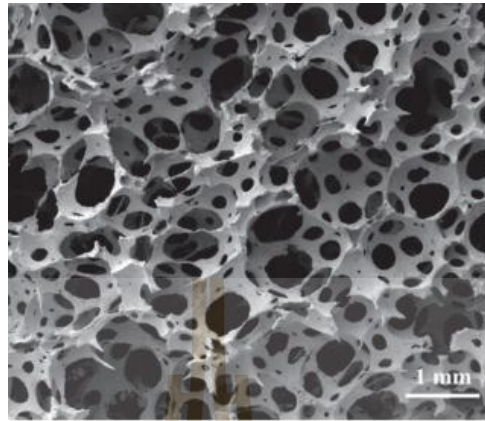


Figure 2.2 Open-cell foam structure (Ariff et al., 2020).

2.3.2 Closed-cell foam

Closed-cell foams are the result of a manufacturing process that allows air to become trapped within the structure of the material. These materials absorb energy by compressing the trapped air during impact. Materials with small cells are denser and have stiffer, or higher, spring constants. Furthermore, the closed-cell structures provide more thermal protection than the open-cell variety (Goodwin & Young, 2011). Closed-cell foam is shown in Figure 2.3.

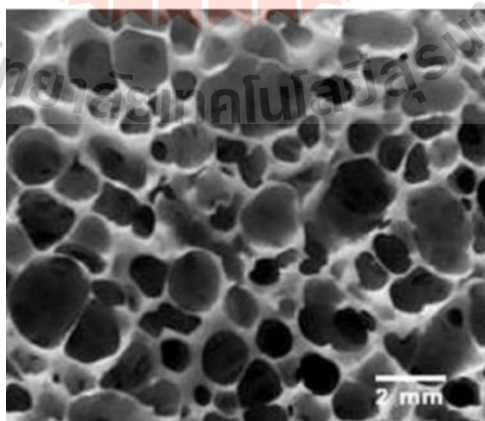


Figure 2.3 Closed-cell foam structure (Najib, Ariff, Bakar, & Sipaut, 2011).

2.4 Key parameters affecting foam density

2.4.1 Mechanical foaming agent

The NRL became extremely porous as a result of the mechanical agitation, or whipping, of the latex into foam. Whipping foam continued to rise until the appropriate density was reached. The NRL foam product was gelled using a gelling agent and poured into a mold. The foam was vulcanized by steam, enhancing its strength and resilience. When the mold opened, the foam was stripped, and then washing and drying were the final steps and completed the foam fabrication (Hui Mei & Singh, 2010).

2.4.2 Chemical foaming agent

Suethao et al., (2021) studied the relationship between the morphology and elasticity of natural rubber foam based on the concentration of the chemical blowing agent (0.90, 1.15, 1.40, and 1.65 phr). In this study, potassium oleate was used as a chemical blowing agent. The formula control was at 1.65 phr of blowing agent. The morphological characteristics of rubber foam turned out to be extremely susceptible to the concentration of the chemical blowing agent. As a result, smaller gas bubbles were produced, and the average cell size of the foam samples decreased as the potassium oleate concentration decreased. Moreover, foam density decreased with the decrease of blowing agent concentration.

2.5 Heating technique for NRL foam vulcanization

Generally, conventional heating is also known as a heat transfer process in which thermal energy is transmitted from outside to inside a sample by conduction. The top of the sample surface receives the most energy, and crosslinking is formed before the foaming process (Ahmad Zauzi et al., 2019).

The conventional heating method uses heat from a hot air oven for the vulcanizing process. NRL foam was vulcanized at temperature of 120°C for 90 minutes (Sirikulchaikij et al., 2020).

Ahmad Zauzi et al., (2019) investigated the foamability of natural rubber via microwave assisted foaming with azodicarbonamide (ADC) as a blowing agent.

Microwave energy can pass through a sample through molecular interactions with electromagnetic fields and generate internal heat. Hence, the foaming and crosslinking processes started from the inside of the samples. Microwave heating had increasingly attracted attention as it gave faster heating times with better heating uniformity.

2.6 Cushion performance of material

Packaging products for use in transportation inevitably suffers from mechanical shock, vibration, and other damage. The cushion material can absorb the energy to reduce external damage and protect goods during transportation. The static compression performance is one of the properties to analyze in the cushion performance of materials. Song et al. (2018) studied the cushion performance of cushion materials composed of EPE and corrugated paperboard. The lowest cushion coefficient, indicated the highest cushion performance of the material. The cushion coefficient was calculated from compression testing. Moreover, the cushion material's performance did not tend to get better with increasing thickness (Song, Zhang, Lu, Zhang, & Zhang, 2018).

2.7 Biodegradability of NRL foam

2.7.1 Effect of fiber on enhancing biodegradability of NRL foam

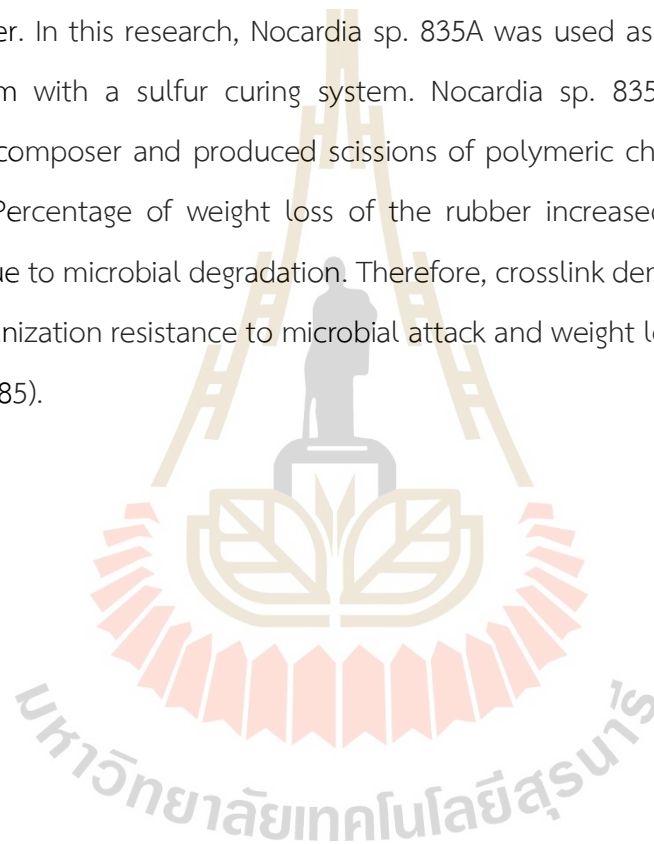
Ramasamy et al., (2015) studied the soil burial, tensile properties, morphology, and biodegradability of (rice huck powder)-filled natural rubber latex foam. The rice huck powder (RHP) was incorporated into the latex foam at different concentrations of 2.5, 5.0, 7.5, and 10.0 phr. The NRL foam composite was buried in soil for 90 days for a biodegradability study. The result showed is that weight loss increased with increasing RHP loading because the RHP enhanced the biodegradability of the NRL foam composite. Tensile strength and elongation at break dropped as the RHP loading increased.

Jayathilaka, Ariyadasa et al., (2020) studied the development of biodegradable natural rubber latex foam by employing corn derivative bio-fillers. Powdered corn grain (CG), corn flour (CF), and corn starch (CS) were used as bio-fillers to improve the biodegradability of the composite. The foam composite was soil burial

for 15 weeks. Mechanical properties and biodegradability of the foam composite depended on starch, protein, and inorganic constituents of bio-fillers. Tensile strength, tear strength, and elongation at break were reduced when the foam composite was buried in soil. The bio-fillers content affected the biodegradability. The biodegradability increased when the content of bio-fillers was increased.

2.7.2 Effect of crosslink density on biodegradability of NRL foam

Tsuchii et al. (1985) investigated the microbial degradation of vulcanized natural rubber. In this research, *Nocardia* sp. 835A was used as a rubber degradation microorganism with a sulfur curing system. *Nocardia* sp. 835A was a very strong microbial decomposer and produced scissions of polymeric chains in natural rubber vulcanized. Percentage of weight loss of the rubber increased as crosslink density decreased due to microbial degradation. Therefore, crosslink density affected the main issue in vulcanization resistance to microbial attack and weight losses (Tsuchii, Suzuki, & Takeda, 1985).



CHAPTER 3

RESEARCH METHODOLOGY

3.1 Materials and methods

3.1.1 Materials

Chemical ingredients and their contents used in the formulation of the NRL foam composites are listed in Table 3.1. The ingredients were supplied by Chemical and Materials Co., Ltd., Bangkok, Thailand. Dried bamboo leaf was purchased from local farmers in Nakhon Ratchasima, Thailand. Guava fruit (*Psidium guajava* L.) cv. Glom Sali was obtained from the Pangha Homestay Orchard, Chiang Rai, Thailand.

Table 3.1 Formulation of NRL foam at various foaming agents and BLF contents.

Ingredients	Functions	Content (phr ⁽¹⁾)
60% High ammonia natural rubber latex (HA Latex)	Matrix	100.00
10% Potassium oleate (K-oleate)	Foaming agent	1.50, 1.50, 3.00, 4.50
50% Sulfur	Vulcanizing agent	2.00
50% Zinc diethylthiocarbonate (ZDEC)	1 st accelerator	2.00
50% Zinc 2 mercaptobenzothiazone (ZDMT)	2 nd accelerator	2.00
50% Wingstay L	Antioxidant	2.00
50% Zinc oxide (ZnO)	Activator	5.00
12.5% Sodium silicofluoride (SSF)	1 st gelling agent	1.00
33% Diphenyl guanidine (DPG)	2 nd gelling agent	1.40
Bamboo leaf fiber (90 - 106 μ m)	Natural fiber	0.00, 2.50, 5.00, 7.50, 10.00

⁽¹⁾ Parts per hundred rubbers.

3.1.2 Preparation of bamboo leaf fiber

Dried bamboo leaf was ground in a fine wood crusher machine (WSC-20, CT, Samut Prakan, Thailand) for 1 h. The ground BLF was then sieved using a vibratory sieve shaker (Analysette 3 Pro, Fritsch, Idar-Oberstein, Germany). BLF fibers in range of 90–106 μm was used. The BLF fiber is shown in Figure 3.1(a). The BLF appeared as greenish particles. SEM micrograph of BLF fiber in Figure 3.1(b) revealed the irregular shape of the BLF particles. To use the BLF in the formula, the prepared fibers were soaked in deionized (DI) water with a 1:1 ratio of fiber to water.

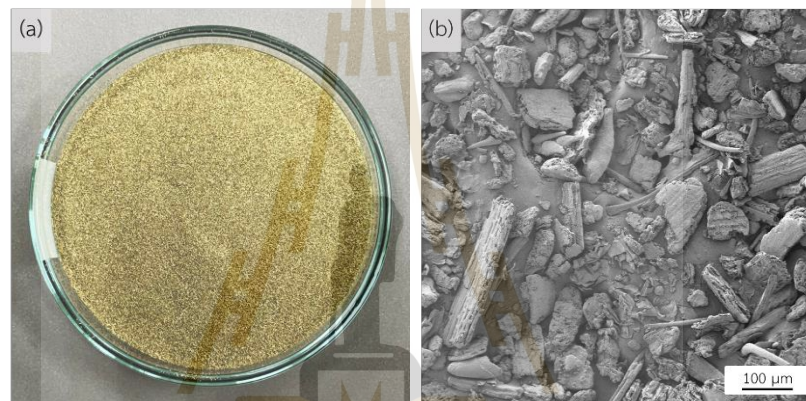


Figure 3.1 The appearance and shape of bamboo leaf fibers: (a) photograph; (b) SEM micrograph at a 100 \times magnification.

3.1.3 Preparation of rapid silicone mold

In this work, 3D printing was used to prepare a master with the desired shape of a cushion net, which was then used for making a negative cavity silicone mold. 3D printing has many benefits. The technique provided flexibility in product and mold design. The process is fast and cost-effective compared to that of a conventional metal mold. The resulting silicone mold was also lightweight, had good heat resistance, and, most importantly, was suitable to be used in a microwave oven. Firstly, the SolidWorks program (Dassault Systèmes, Vélizy-Villacoublay, France) was used to create a 3D model of the cushion net (Figure 3.2(a)). Then a CAD file was generated and converted to G-code using the PrusaSlicer program (Prusa Research, Prague, Czech Republic) (Figure 3.2(b)) before printing (Figure 3.2(c)). PLA filament (Prusament Prusa

Galaxy Black, Prusa Research, Prague, Czech Republic) was used to print the inverted mold via a 3D printer (Original Prusa i3 MK3S, Prusa Research, Prague, Czech Republic). Silicone rubber and hardener, supplied by Infinite Crafts Co., Ltd., Bangkok, Thailand, were mixed before pouring into the inverted mold. The silicone mold was left at room temperature until full setting. The working mold was obtained after the inverted mold was removed. The inverted and silicone molds are shown in Figure 3.2(d) and Figure 3.2(e), respectively.

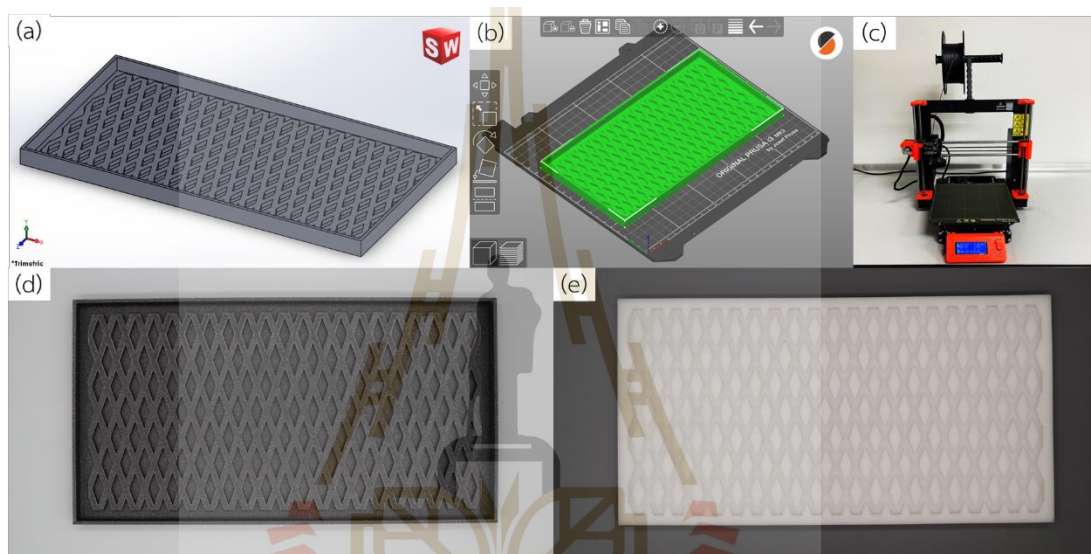


Figure 3.2. Schematic for fabricating a rapid silicone mold using 3D printing: (a) 3D model; (b) converting to G-code; (c) 3D printing; (d) inverted mold; and (e) silicone mold.

3.1.4 Fabrication of NRL foam via the Dunlop process together with microwave-assisted vulcanization technique

The preparation of NRL foam can be divided into 5 steps (reduction ammonia, foaming, gelling, vulcanizing, and drying process). Natural rubber latex (60% high ammonium latex) was stirred by a mechanical stirrer (Eurostar 20 digital, IKA Works, Wilmington, NC, USA) at speed of 300 rpm for 30 min to reduce amount of ammonia in the latex. Chemical ingredients for foaming process i.e. K-oleate, ZDEC, ZMBT, and Wingstay L were incorporated into the reduced ammonia latex. In this foaming step, foaming times were varied from 2, 4, 6, 8, and 10 min at a constant stirrer speed of

1,250 rpm. Then ZnO, DPG, and SSF were added into the NRL compound at speed of 700 rpm for 1 min. After that, NRL compound was gelled by SSF. The gelled foam was poured into a silicone mold (5.5 cm x 5.5 cm x 2.5 cm) at room temperature for 1 h. The foam was vulcanized using a commercial microwave oven (MS23K3513AW/TC, Samsung, Kuala Lumpur, Malaysia) at constant power of 600 W and time of 6 min. Finally, the NRL foam was washed and dried in a hot air oven at 70°C for 24 h.

Similar process was used to study the effect of stirring speeds during the foaming step. The speed was varied from 650, 950, 1,250, 1,550, and 1,850 rpm at a constant foaming time of 8 min. Other parameters in other steps were kept constant.

The effect of foaming agent content was also investigated. The concentrations of K-oleate were 1.50, 3.00, and 4.50. In this study, foaming time and speed were 6 min and 1,250 rpm, respectively.

3.1.5 Fabrication of NRL foam composites via the Dunlop process together with microwave-assisted vulcanization technique

The NRL foam composites were prepared using the Dunlop process to generate a foam structure before curing via microwave irradiation. The process used here was similar to that reported previously with the additional step of adding BLF. Firstly, the NRL was first stirred using a mechanical stirrer. The stirring speed of the first step was 300 rpm for 30 min to reduce the ammonia content in the latex. Secondly, chemical ingredients required for the foaming process, i.e., K-oleate, Sulfur, ZDEC, ZMBT, and Wingstay L were incorporated, and the latex mixture was whipped at a speed of 1250 rpm for 6 min. Thirdly, a soaked bamboo leaf fiber was added to the whipped latex mixture at a speed of 500 rpm for 2 min. The BLF to DI water ratio was 1:1. Finally, ZnO, DPG, and SSF were added to the whipped latex for foam gelation at a speed of 700 rpm for 1 min. The gelled foam was poured into a silicone mold and set at room temperature for 1 h. The foams were vulcanized using the microwave oven. The optimum vulcanization conditions used were microwave irradiation power and time of 600 watts and 6 min, respectively. Finally, the NRL foam product was washed with water and dried in a hot air oven at 70 °C for 4 h.

3.1.6 Characterization

3.1.6.1 Bulk density

Bulk foam density was carried out by measuring the weight and volume the samples. The bulk density of NRL foam can be determined using the following Equation (1) (Syahrin et al., 2020):

$$\text{Bulk density} = \frac{M}{V} \quad (1)$$

Where; M is mass of specimen (kg), V is volume of specimen (m³)

3.1.6.2 Morphology

The cellular morphology of the cushion foams was analyzed using a scanning electron microscope (SEM) (JEOL, JSM6010LV, Japan). Foam sample was prepared from a small piece using a sharp blade. At low magnification, the SEM micrograph was tested at an accelerating voltage of 10 kV. The cross-sectional surfaces of the samples were sputtered and coated with gold for 3 min. At high magnification, the SEM micrographs were taken at an accelerating voltage of 3 kV and a working distance of 6.7–9.8 mm (AURIGA, Zeiss, Germany). The surface and cross-section of NRL foam were sputter-coated with gold at 5.7 nm using a Leica sputter coater (Leica, EM ACE600, Vienna, Austria). The surface and cross-section of the foam samples were investigated.

ImageJ image analyzer software was used to determine the foam's cell size and cell count. For each cell, four lines were drawn across the cell, and the length of each line was measured. For each location or image, at least 100 cells were measured and recorded. Then, cell size distribution and average cell size were determined using a nonlinear curve fit (Gaussian) in the Origin program (OriginLab Corporation, Northampton, MA, USA). Additionally, the cell wall thickness of the cushion foams was measured using ImageJ software (NIH, Bethesda, MD, USA) and reported using average data from five locations of cell wall thickness.

The number of cells per unit volume (N) was evaluated by the average cell size data from ImageJ software and the foam density. Equation (2) was used to calculate the number of cells per unit volume of the NRL foam composite:

$$N = \frac{6}{\pi d^3} \times \frac{\rho_{\text{rubber}}}{\rho_{\text{foam}}} - 1 \quad (2)$$

where N is the number of cells per unit volume, d is the average cell diameter (cm), ρ_{rubber} is a density of the solid rubber (1.09 g/cm³), and ρ_{foam} is the density of the rubber foam (g/cm³) or the bulk density.

3.1.6.3 Hardness

The hardness values of the NRL foam composites were determined using a durometer hardness (Durometer LX-00 Shore OO, X.F, Graigar, Guangdong, China) according to ASTM D2240. The hardness of the cushion foam net was measured on the sample surface. Five measurements on five different locations on each specimen were measured. The reported values were averaged from at least five replicates.

3.1.6.4 Mold shrinkage

The shrinkage of the NRL foam composites can be determined using the following Equation (3). The shrinkage was compared in three dimensions (width, length, and height). The reported values were averaged from at least five replicates.

$$\text{Shrinkage (\%)} = \frac{(X_0 - X_1)}{X_0} \times 100 \quad (3)$$

Where X_0 are the dimensions of mold (mm), X_1 is the dimension of NRL foam composite after vulcanization (mm).

3.1.6.5 Compression set

Compression set measurements were performed by ASTM D1055. A cylindrical specimen with a diameter of 29 mm and a height of 19 mm was prepared using the same processing condition as the NRL composite foam net. Using a compression set apparatus (MonTect, CS3000, Germany), the specimen was

compressed to 50% of its original thickness. The specimen was then placed in a hot air oven at 70 °C for 22 h. Afterward, the specimen was removed from the oven, and the compression set apparatus was removed from the specimen before being left to cool at room temperature for 30 min.

The final thickness of the specimen was measured within 10 min after the cooling step. The compression set was calculated according to Equation (4):

$$C_h = \frac{(t_0 - t_1)}{t_0} \times 100 \quad (4)$$

where C_h is the compression set, t_0 is the original thickness of the specimen (mm), t_1 is the thickness of the specimen after 30 min of removal from the compression set apparatus (mm)

3.1.6.6 Compression test

A compression test of the cushion foam was performed using a universal testing machine (UTM) (Instron 5565, Norwood, MA, USA). The relationship between stress and strain was obtained. The raw data of the compressive stress–strain curve was used to calculate the cushion coefficient. Moreover, Mechanical property of the NRL foam from biodegradation were investigated the compressive strength at 50% compressive strain.

The NRL foam was tested according to ASTM D3574 with a load cell of 5 kN. The NRL foam was prepared specimen approximately 50 mm × 50 mm × 25 mm. The foam specimen was compressed to 50% of each foam original thickness at a crosshead speed of 50 mm/min. At least three specimens were tested and the averaged values were reported.

The NRL composite foam net was cut into a rectangular shape with the dimensions of (width × length × thickness) 100 mm × 100 mm × 3 mm. The test was carried out using the load cell of 1 kN at a crosshead speed of 12 mm/min. The compression test was adapted from the static compression method for packaging buffer material (GB/T 8168-2008) to determine the cushion performance of cushion

materials. The reported results were the averaged values from testing at least five replicates.

3.1.6.7 Cushion coefficient

The cushion coefficient (C) is an ability of a cushion material to absorb the applied energy. The calculation was carried out using the data from the compression test mentioned earlier. The cushion coefficient equation is as follows:

$$C = \frac{\sigma}{e} \times 100 \quad (5)$$

Where σ is the compressive stress (N/mm²), e is the energy absorption of the material (N·mm/mm³), which is estimated from the compressive stress–strain curve using Equation (6):

$$e = \int_0^{\epsilon} \sigma d\epsilon \quad (6)$$

Where ϵ is the compressive strain (mm/mm).

3.1.6.8 Biodegradation study

The soil burial method was used to investigate the effect of BLF content in NRL foam composites on their biodegradability. Square specimens with the size of 50 mm × 50 mm × 3 mm (width × length × thickness) of each NRL composite foam net sample were placed in a box containing planting soil at the dept of 12–15 cm. The 100 L plastic box (500 mm × 770 mm × 43 mm) used was covered with a plastic lid, and small holes of 5 mm in diameter were uniformly drilled on all sides of the box for ventilation. The soil used was planting soil from Suranaree farm, Suranaree University of Technology, Nakhon Ratchasima, Thailand. The plastic boxes filled with soil were placed outdoors beside equipment building 4 (F4) at Suranaree University of Technology, Nakhon Ratchasima, Thailand (Figure 3.3(a)). Figure 3.3(b) depicts the placement of foam samples for burial. The soil's moisture content was maintained at 60–80% (water as needed). The commercial cushion EPE foam net (EPE-FN) was also buried in the soil with the same protocol and condition. The degradation study was carried out over a period of 24 weeks (May–October 2022). Every 4 weeks, five specimens of each sample were taken out from the soil and then washed with water

and dried in a hot air oven at 70 °C for 4 h. These specimens were tested for changes in the foam appearance, morphology, compression property (at 50% strain), and weight loss. The compression property and weight loss values were reported as averaged values calculated from at least three replicates. The weight loss formula is given as Equation (7). The NRL foam were prepared different specimens use at each time interval characterization. An analytical balance with four digits (ML240, Mettler Toledo, Greifensee, Switzerland) was used for the weight loss determination.

$$\text{Weight loss (\%)} = \frac{(W_0 - W_1)}{W_0} \times 100 \quad (7)$$

where W_0 is the sample weight before the test (g) and W_1 is the sample weight after the test (g).

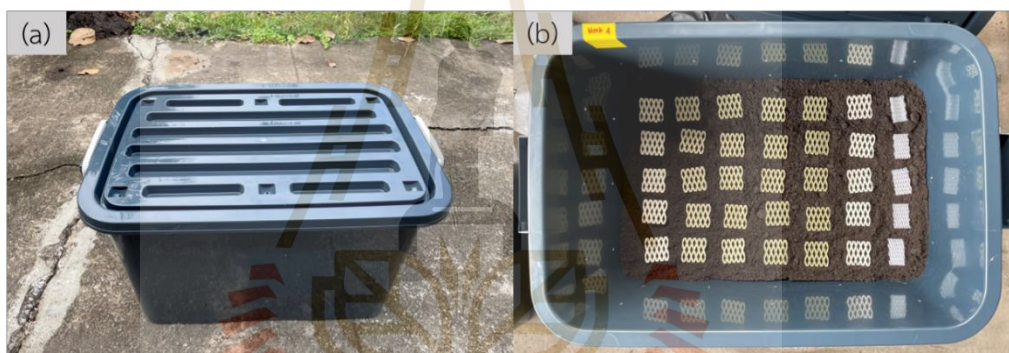


Figure 3.3. Biodegradation experiment of cushion foams: (a) plastic box used for soil burial; (b) cushion foam placement.

3.1.6.9 Crosslink density

Crosslink density was determined using the toluene-swelling method (ASTM D6814-02). The vulcanized foam was prepared in a cubic mold with the size of 15 cm × 15 cm × 10 cm (width × length × thickness). The foam was swollen to equilibrium in toluene for 72 h. The crosslink density was calculated by Flory-Rehner equation according to Equation (8):

$$V_e = \frac{-[\ln(1-V_r) + V_r + \chi_1 V_r^2]}{\left[V_1 \left(\frac{1}{V_r^3} - \frac{V_r}{2} \right) \right]} \quad (8)$$

Where: V_e is the efficient number of chains in the real network per unit volume (mol/cm^3), V_r is the volume fraction at the equilibrium within pure

solvent of polymer in swollen network, V_1 is molar volume of toluene (106.3 cm³/mol), χ_1 is the Flory-Huggins interaction parameter between rubber and toluene (0.391)

$$V_r = \frac{X_r/\rho_r}{\frac{X_r}{\rho_r} + \frac{X_s}{\rho_s}} \quad (9)$$

Where: ρ_s is density of toluene (g/cm³), ρ_r is density of rubber (g/cm³), X_s is mass fraction of toluene (g), X_r is weight of rubber (g)

$$X_s = \frac{\text{Weight of swollen sample (g)} - \text{Weight of original sample (g)}}{\text{Weight of swollen sample (g)}} \times 100 \quad (10)$$

$$X_r = 1 - X_s \quad (11)$$

3.1.6.10 Pack test (Simulated vibration transportation)

Fresh guava was used as a representative of spherical fresh produce for this test. Two guavas without bruises and scratches were chosen, wrapped in foam, and packed into a one-piece folder (OPF) box (4 boxes for 4 replicates). Each box of guava was used to pack two guava fruits (500 grams). The box dimensions used were 10.5 × 18.5 × 8.0 cm³. The guava pack was shown in Figure 3.4. In the testing process, two boxes of guava will be tested at the same time, as shown in Figure 3.5.



Figure 3.4 Guava packaging for simulated vibration transportation.

Vibration testing and setting followed the method of Chaiwong et al. (2021). Briefly, the simulated frequency level (Hz) of vibration transportation for Glom Sali guava fruit was generated using Audacity® recording and editing software (version 3.1.3, The Audacity Team). A power amplifier was used to drive an electrodynamic vibration exciter to enhance the signals and control the level of acceleration. The sampling signal was processed by a three-channel data acquisition

system, and the resulting samples were converted using Fast Fourier Transform (FFT) to produce the frequency spectrum of the signals. A reference accelerometer was attached to the framework, while another two accelerometers were installed inside the OPF box and at the center of a guava fruit. In this study, the vibration condition was examined at acceleration (Grms) (8.826 m/s^2), frequency (13.5 Hz) and vibration duration (40 min). Based on previous simulated vibration testing in guava fruit (Chaiwong et al., 2021), this research addressed peak frequency and high acceleration levels that were representative of severe vibration conditions of simulated transportation. Low intensity vibration at frequency ranges of 10-20 Hz is generally found in actual truck transportation in Thailand (Chonhenchob et al., 2010). Moreover, this vibration condition was a similar range of vibration conditions from an actual truck transportation in other countries such as Japan, Taiwan (Ishikawa, Kitazawa, & Shiina, 2009), Turkey (Karatepe, Karatepe, Çakmak, Karaer, & Ergün, 2009), Spain, France and Italy (Barchi, Berardinelli, Guarnieri, Ragni, & Fila, 2002). While vibration lengths of 40 min were assumed to correspond to road transportation distances of 1,500 km (Acican, Alibaş, & Özelkök, 2007). This was the estimated distance from the north to the south of Thailand to reach domestic markets.

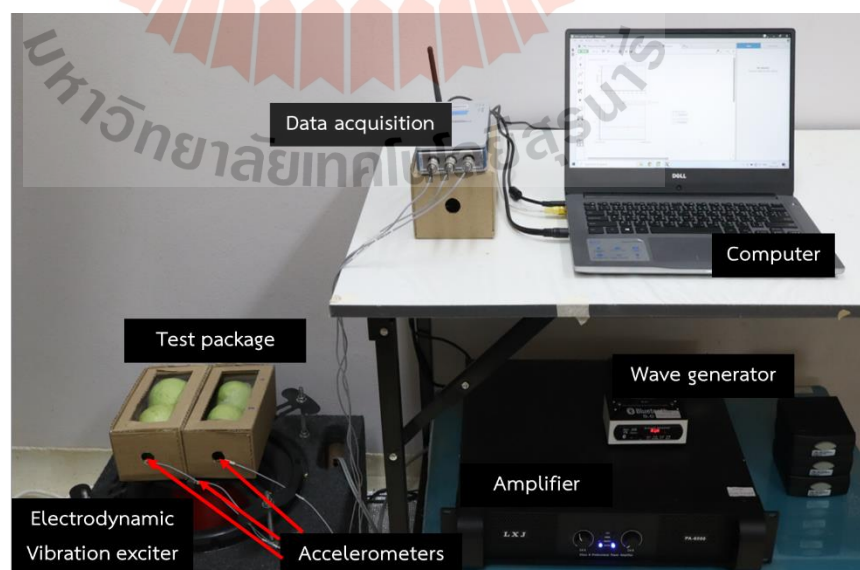


Figure 3.5 Vibration simulation test equipment.

3.1.6.11 Percentage transmissibility (%)

The percentage transmissibility (%) of the cushioning material at frequency 13.5 Hz was calculated using Eq. (13) (Vursavus and Ozguven, 2004; Idah et al., 2012).

$$\text{Percentage Transmission (P}_T\text{) (\%)} = \frac{a_b}{a_t} \times 100 \quad (13)$$

Where P_T is the packaging transmissibility (%), a_b is the measured acceleration on the package (cushion) (m/s^2) and a_t is the applied acceleration from the framework (m/s^2).

3.1.6.12 Statistical analysis

The SPSS software for Windows version 20 (SPSS Inc., Chicago, IL, USA) was implemented to conduct the statistical analysis of the cushion foam properties. Tukey's HSD post-hoc test was used to compare the means of five replicates of bulk density, hardness, mold shrinkage, and compression set, and 400 measurements of average cell size for each cushion foam sample at the 0.05 significance level.

CHAPTER 4

RESULTS AND DISCUSSION

4.1 Process optimization and formulation of eco-friendly cushioning packaging foam fabrication from natural rubber latex using the Dunlop process coupled with microwave-assisted vulcanization

In this work, we used Dunlop process together with microwave-assisted vulcanization for NRL foam fabrication. We first optimized microwave irradiation conditions (power and time). The foaming time and stirring speed using the optimal microwave irradiation condition were investigated.

Optimization of microwave irradiation for vulcanizing NRL foam was performed using different powers (450, 600, and 800 W) and times (4, 6, and 8 min). The physical appearance of the foam vulcanized is shown in Table 4.1. It can be seen that too low in heating energy (low power or time) could lead to unsuccessful curing. Overheating also caused browning at the core of the sample, indicating the degradation of the rubber foam samples. The core of the rubber foam became brown first. This was well agreed with the heat characteristic of microwave irradiation that heated from inside out. This study provided the processing window for curing of the NRL foam. The results indicated that the optimum microwave curing condition of NRL foam was at power of 600 W and time of 6 min where the foams with good foam structure and no degradation were obtained.

This work also aimed to investigate the two important parameters in Dunlop process for making rubber foam from rubber latex using microwave assisted vulcanization. The two parameters were foaming time and stirring speed. In the foaming step, air was whipped into the latex creating air in liquid colloidal dispersion. The stability of the colloid depended on various factors and crucial for controlling the

foam structure in the final product. The volume of the air incorporated into the latex was expected to affect the foam structure. Longer foaming time may increase the air volume in the foam but can also destabilize the colloid, as a consequence, alters the final foam product's properties. The results reported here discussed the effects of foaming time and speed on foaming density, structure, and compressive strength of the NRL foam.

Table 4.1 Physical appearance of NRL foam at various microwave irradiation conditions.

Power (W)	Time (min)		
	4	6	8
450	 Incomplete cured with gel-like edges		
600	 Incomplete cured with gel-like edges	 Fully cured	 Fully cured
800	 Fully cured	 Fully cured	 Over cured and degraded

4.1.1 Effect of foaming time

4.1.1.1 Bulk density

The effect of foaming time on the bulk density of NRL foam is shown in Table 4.2. It can be seen that the bulk density decreased as the foaming

time increased. This was because the longer whipping time (foaming time) allowed greater amount of air to be incorporated into the compound (Hui Mei & Singh, 2010). As a result, the foams prepared using longer foaming time expanded to a greater degree/volume while the weight of the samples was relatively constant.

Table 4.2 Properties of NRL foam prepared using different foaming times and at a constant speed of 1,250 rpm.

Foaming time (min)	Bulk density (kg/m ³)	Cell size (μm)	Number of cell per unit volume (×10 ³ cells/cm ³)	Compressive strength (kPa)	Hardness (Shore OO)
2	420.80 ± 4.03	197.68	155.55	263.30 ± 9.60	55.13 ± 0.12
4	397.95 ± 8.55	170.13	223.15	198.66 ± 9.73	53.87 ± 1.45
6	367.43 ± 6.66	166.98	208.71	171.76 ± 9.89	52.07 ± 2.50
8	355.89 ± 2.99	136.71	362.59	156.01 ± 4.12	48.60 ± 2.62
10	345.23 ± 2.20	127.88	423.55	154.69 ± 1.67	47.80 ± 1.83

4.1.1.2 Morphology

SEM micrographs of a cross-sectional surface of NRL foam at various foaming times are displayed in Figure 4.1. From these images, it could be seen that as the foaming time increased, the cell size of NRL foam decreased, at the same time the number of cells increased as a function foaming time. Cell size distribution of the NRL foam was presented in Figure 4.2. These images gave the insight detail of the foam structure and how they changed as the foaming time increased. Longer foaming time allowed more air to be incorporated with the rubber latex and the mechanical mixing action also generated greater number of foam cell. It could be hypothesized that the large foam cells were initially formed and then disrupted into smaller ones as the mixing continued. The smaller foam cell also resulted in tiny cell wall which was less likely to collapse. On the other hand, the greater number of cells

meant that the cell wall may become thinner and less stable. When the cell foam become smaller but being greater in number, the final properties of the foam depended on the balance of these two characters.

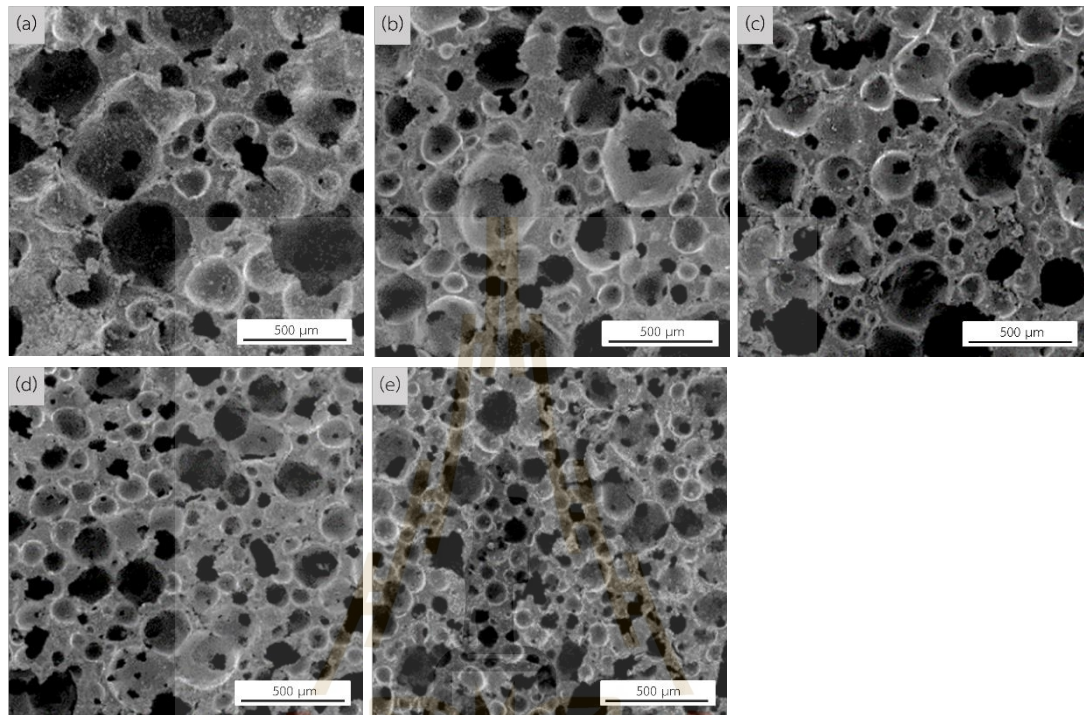


Figure 4.1. SEM micrographs of NRL foam prepared using a constant foaming speed of 1250 rpm and different foaming times (a) 2 min, (b) 4 min, (c) 6 min, (d) 8 min, and (e) 10 min.

4.1.1.3 Compression test

Compressive strength at 50% compressive strain of NRL foam prepared with different foaming times is listed in Table 4.2. Compressive strength of NRL foam decreased with increasing foaming time. This was likely due to the change in the structure of the foams and their density. As previously shown, both higher volume of air, greater number of foam cell can contribute to the lower of the compressive strength. This finding was also recognized by others. Samsudin et al. reported that there was relationship between density and compressive properties of NRF. Higher density resulted in increased compressive strength of NR foam.

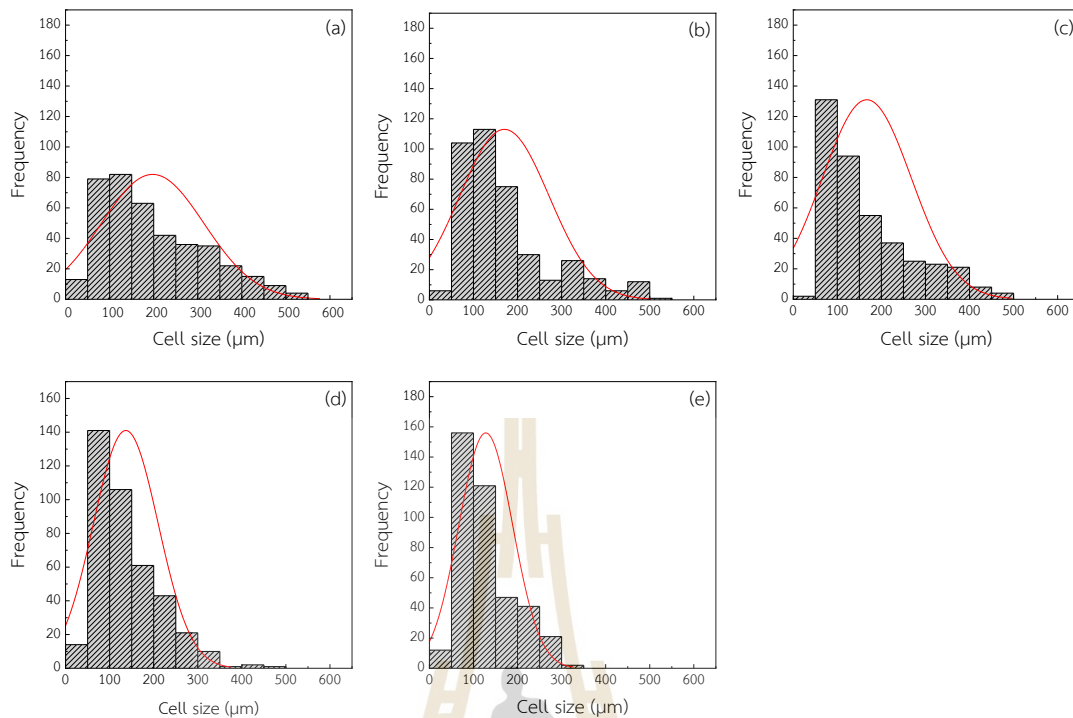


Figure 4.2. Cell size distribution of NRL foam at foaming speed of 1250 rpm and different foaming times (a) 2 min, (b) 4 min, (c) 6 min, (d) 8 min, and (e) 10 min.

4.1.2 Effect of stirring speed

4.1.2.1 Bulk density

In Dunlop process, stirring speed during the foaming process is one of the most important parameters to develop character of a cell foam of NRL foam. Effect of stirring speed in foaming step on bulk density is reported in Table 4.3. Five different foaming speeds were used in the NRL foam preparation (650-1,850 rpm). However, only 3 speeds were successfully used in the NRL foam production. Too low and too high stirring speed created unstable foam bubbles which broke down before the foam can be settled as shown in Figure 4.3. For too low stirring speed at 650 rpm, the air was not enough to create foam cells throughout the sample. The top surface of the foam was dense and burst during vulcanization as moisture vapor in the foam left from the inside. Foam sample at foaming speed of 1,850 rpm after adding SSF in gelling process was presented in Figure 4.3(b). Too high the foaming speed probably destabilized the latex rubber and gooey-rubber paste was obtained. We could

establish processing window for the foaming speed for our system from these results. From Table 4.3, it can be seen that higher speed during foaming step caused the lower in the bulk density of NRL foam. The lower bulk density could be because the higher speed was more efficient in terms of aeration of the latex rubber. The lower bulk density indicated that greater volume of the air was incorporated into the latex at the higher foaming speed but the same amount of time.

Table 4.3 Properties of NRL foam prepared using different stirring speeds and at a constant time of 8 min.

Foaming speed (rpm)	Bulk density (kg/m ³)	Cell size (μm)	Number of cell per unit volume (×10 ³ cells/cm ³)	Compressive strength (kPa)	Hardness (Shore OO)
950	400.73 ± 14.00	201.50	135.79	251.16 ± 7.62	54.80 ± 0.40
1,250	355.89 ± 2.99	136.71	362.59	156.01 ± 4.12	48.60 ± 2.62
1,550	301.14 ± 8.11	181.72	121.56	117.03 ± 5.08	45.40 ± 1.60



Figure 4.3. Physical appearance of NRL foam during foam production at (a) 650 rpm and (b) 1,850 rpm.

4.1.2.2 Morphology

SEM results in Figure 4.4 revealed that cell size of the foams tended to decrease as the stirring speed increased. Again, higher number of foam cell occurred simultaneously with the lower in cell size. It should be noted that at 1,550

rpm stirring speed, the cell structure seemed to open with the presence of smaller cells inside the cell wall itself. This structure could lead to a lowering in the mechanical properties of this NRL foam. Cell size distribution of NRL foam at foaming time 8 min and various stirring speeds is shown in Figure 4.5.

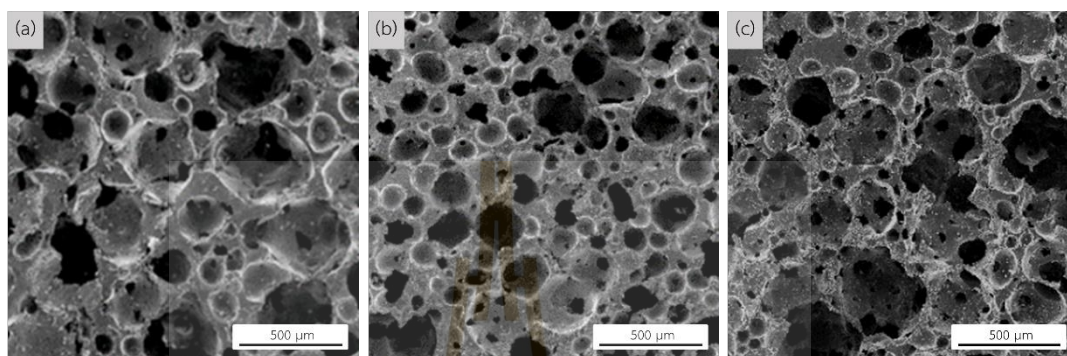


Figure 4.4. SEM micrographs of NRL foam at foaming time of 8 min and various stirring speed (a) 950 rpm, (b) 1,250 rpm, and (c) 1,550 rpm.

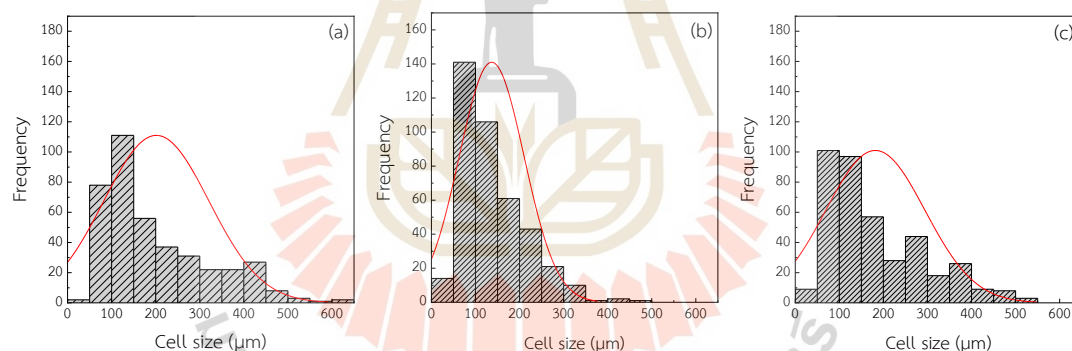


Figure 4.5. Cell size distribution of NRL at foaming time 8 min and various stirring speeds (a) 950 rpm, (b) 1,250 rpm, and (c) 1,550 rpm.

4.1.2.3 Compression test

Compressive strength of NRL foam prepared using different foaming speeds of 950, 1,250, and 1,550 rpm are presented in Table 4.3. At low foaming speed (950 rpm), the foam possessed the highest compressive strength at 50% compressive stain. As the foaming speeds increased to 1,250 and 1,550 rpm, the compressive strength of the foams decreased, continuously. The results may be

caused by the lowered bulk density as well as the changes in the foam structure as described earlier.

This study reported the result of the investigation of two important parameters i.e. time and stirring speed used in foaming step in Dunlop process. The relationship between the cell characteristics, bulk density, and compressive strength of NRL foam was established. The final foam product properties and performance strongly depended on the foam structure, generated during the foaming step. The compressive strength depended on both bulk density and cell morphology. Understanding the parameters affecting the foam structure and properties could lead to the better control and design the foam product to give desired properties suitable for specific applications. Microwave heating is one of the techniques that should be adopted in the near future as it could save significant amount of time and energy during vulcanization process.

4.1.3 Effect of potassium oleate content

In this study, potassium oleate as a chemical foaming agent was added into latex compound at various contents of 4.50, 3.00, and 4.50 phr to reduce the foam density.

4.1.3.1 Bulk density

Foaming agent was used to lessen the NRL foam bulk density. The influence of the foaming agent on foam density is shown in Table 4.4. When the K-oleate concentration increased, the bulk density of NRL foam decreased. That was because the chemical foaming agent generated more gas, which depended on the concentration of the foaming agent in the NRL foam compound (Suethao et al., 2021).

4.1.3.2 Morphology

SEM micrograph and cell size distribution are shown in Figure 4.6 and 4.7 respectively. All NRL foam structures showed an open-cell structure and non-uniform cell size. K-oleate affected foam structure. The cell size was slightly increased with increasing K-oleate content, but the cell number per unit volume decreased. When the foam structure was changed, the foam properties, such as the

compression property and cushion performance, were also changed. The compressive strength at 50% compressive strain (Table 4.4) and cushion performance decreased with increasing cell size. Song et al., (2018) reported that the cushion performance was determined by the cushion coefficient value (Table 4.5), the foam showed high cushion performance when the cushion coefficient was low.

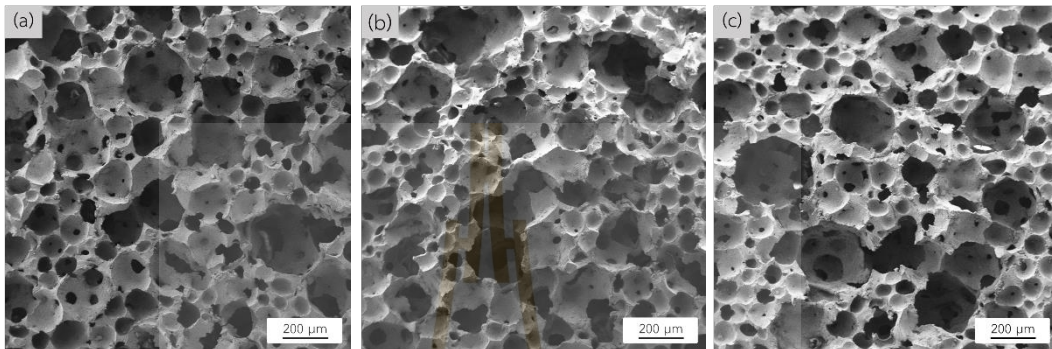


Figure 4.6. SEM micrographs of NRL foam at various potassium oleate contents (a) 1.50 phr, (b) 3.00 phr, and (c) 4.50 phr.

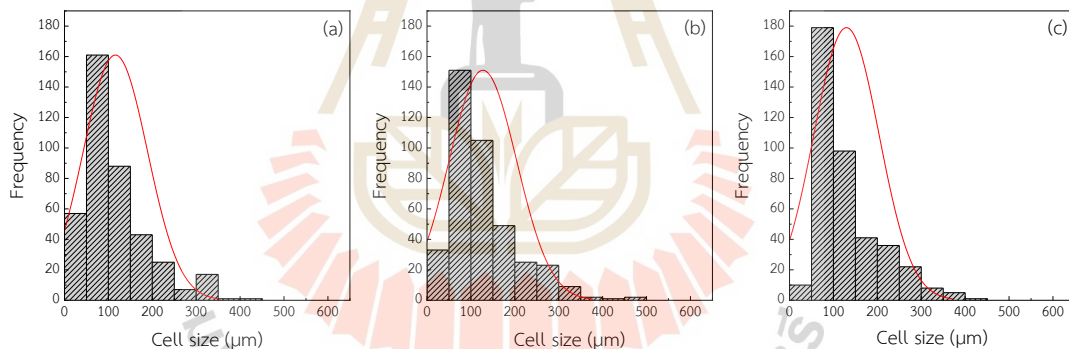


Figure 4.7. Cell size distribution of NRL foam at various potassium oleate contents (a) 1.50 phr, (b) 3.00 phr, and (c) 4.50 phr.

4.1.3.3 Compression test

The open-cell structure, which exhibits a long, flat plateau in the stress-strain graph, determines the elastic collapse stress and the post-collapse behaviour (Suethao et al., 2021). Compressive stress-strain curves are shown in Figure 4.8. The compressive stress was slightly increased when the cell foam space had been collapsed. 50% compressive strength of NRL foam decreased with increasing K-oleate content. The large cell size foam led to lower 50% compressive strength.

Table 4.4. Properties of NRL foam prepared using different foaming agent.

K-oleate content (phr)	Bulk density (kg/m ³)	Cell size (μm)	Number of cell per unit volume (×10 ³ cells/cm ³)	50% Compressive strength (kPa)
1.50 K-oleate	306.23 ± 0.38	83.06 ± 4.63	58.88	78.22 ± 2.87
3.00 K-oleate	288.12 ± 10.49	92.78 ± 4.81	57.32	65.18 ± 0.75
4.50 K-oleate	271.88 ± 5.65	94.47 ± 28.01	22.59	55.92 ± 2.79

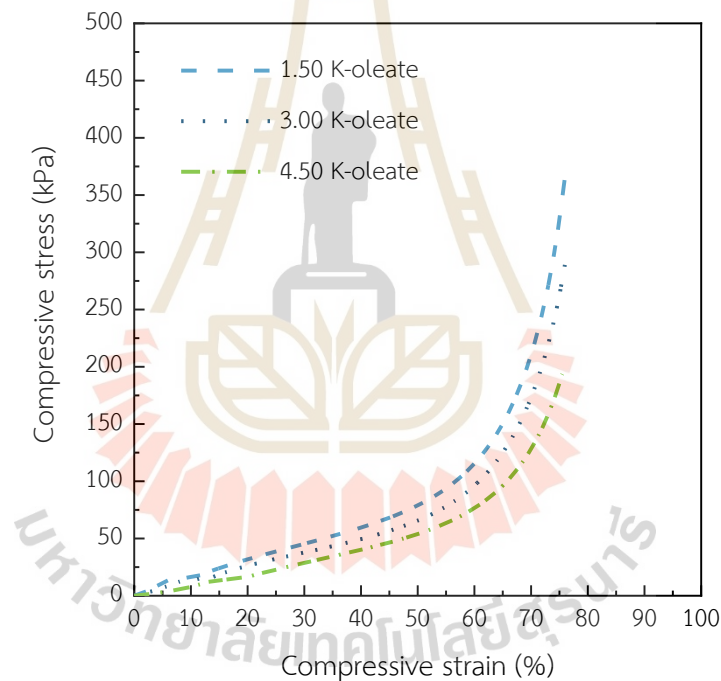


Figure 4.8. Compressive stress-strain curves of the NRL foam at various foaming agent contents.

4.1.3.4 Cushion coefficient

Cushion coefficient indicated cushion performance of the material. Figure 4.8 depicted the cushion coefficient-compressive strain curve of the NRL foam at various foaming agents. The result of cushion coefficient at various foaming agent content was presented in Table 4.5. Cushion coefficient was slightly

decreased with increasing K-oleate content. The lowest cushion coefficient indicated the highest energy absorption or best cushion performance (Song et al., 2018). Therefore, the foam 4.50 phr with K-oleate revealed the best cushion performance due to the lowest cushion coefficient. From the results of this research, the NRL foam presented the lowest foam density using the foaming agent at 4.50 phr but showed the highest cushion performance using the foaming agent at 1.50 phr. However, the cushion coefficient of these NRL foam was not different. The density of the foam product for packaging was important in transportation. Therefore, the low foam density was selected to fabricate eco-friendly cushion foam from the NRL foam in the foam net shape for Thai-fresh produce because its foam presented the best cushion performance.

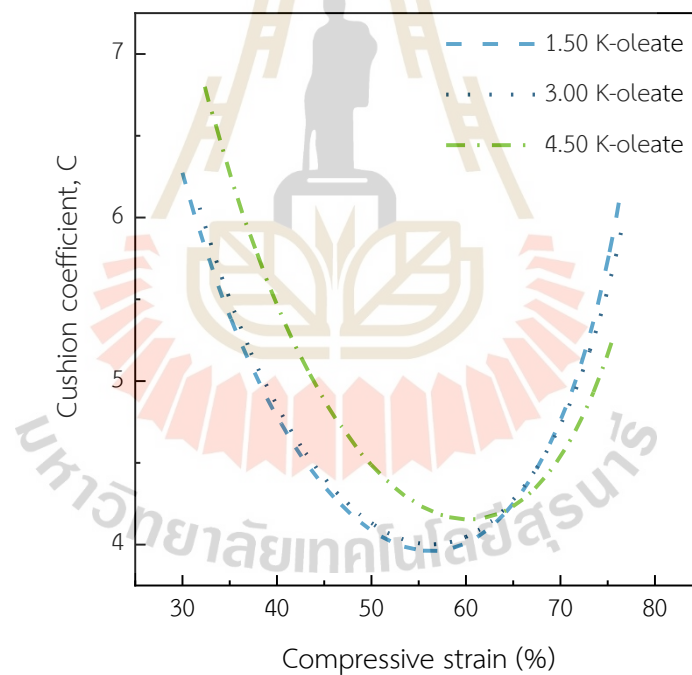


Figure 4.9 Cushion coefficient- compressive strain curve of the NRL foam at various foaming agents.

Table 4.5. Cushion coefficient (C) at 50% strain of NRL foam at various foaming agent.

K-oleate content (phr)	Cushion coefficient (C) at 50% strain
1.50 K-oleate	4.13 ± 0.02
3.00 K-oleate	4.15 ± 0.07
4.50 K-oleate	4.30 ± 0.16

4.2 Effect of BLF content on foam properties and biodegradability of NRL foam composite.

An eco-friendly cushion foam net was developed by the NRL. The aim of this development was to create an alternative cushion for the nonbiodegradable commercial EPE foam net used in fresh produce packaging. The NRL foam net was made from a sustainable resource using an energy-efficient process. Though natural rubber is generally considered inherently biodegradable, an increase in its biodegradation rate is desirable. The addition of BLF to the NRL foam net was mainly to enhance biodegradability. However, adding BLF to NRL may affect several other aspects, including processability, mechanical properties, appearance, and cushion performance. This work was focused on the investigation of the effects of the addition of BLF and its content on NRL foam cushion based on these aspects.

The NRL foam net was fabricated using the Dunlop process with microwave vulcanization. In the Dunlop process, the air was incorporated into the NRL and stabilized with chemicals. The appearance of the resulting NRL foam at this stage was similar to that of whipped cream, which was relatively delicate. Adding dried BLF directly to the compound caused the NRL foam to destabilize and collapse instantly. This could be because the dried BLF absorbed large amounts of moisture from the foam compound, and destroyed the balance of the foamed rubber. Adding the moisture to the BLF, therefore, solved the problem and the NRL composite foams with different BLF contents were successfully fabricated.

Effect of the BLF addition into NRL foams based on their appearance and properties related to the fruit cushion packaging application were discussed.

4.2.1 Appearance and design of the NRL foam cushion

The NRL foam cushion was tested and compared with a conventional EPE foam cushion. A flat net sheet was firstly made (Figure 4.10(a)), and it was rolled to form a tube shape before fastening with rubber glue (Figure 4.10(b)). The final shape of the NRL foam net (NRL-FN) cushion resembled that of the expanded polyethylene foam net (EPE-FN) used commercially (Figure 4.11(a)). It should be noted that the flat net sheet of NRL-FN was comprised of one layer of square-cross-section filaments (Figure 4.10(d)). This design was used to simplify the process of making the prototype cushion foam net. On the other hand, the commercial EPE-FN comprised round cross-section filaments crossing over one another (Figure 4.10(c)).

The NRL-FN with and without BLF are shown in Figure 4.11(b–f). The NRL-FN without BLF was off-white with a slight yellow tint. Adding BLF to the NRL-FN resulted in a green color and its color intensity increased with the BLF content. The green color was the natural color of BLF, as shown previously in Figure 3.1(a).

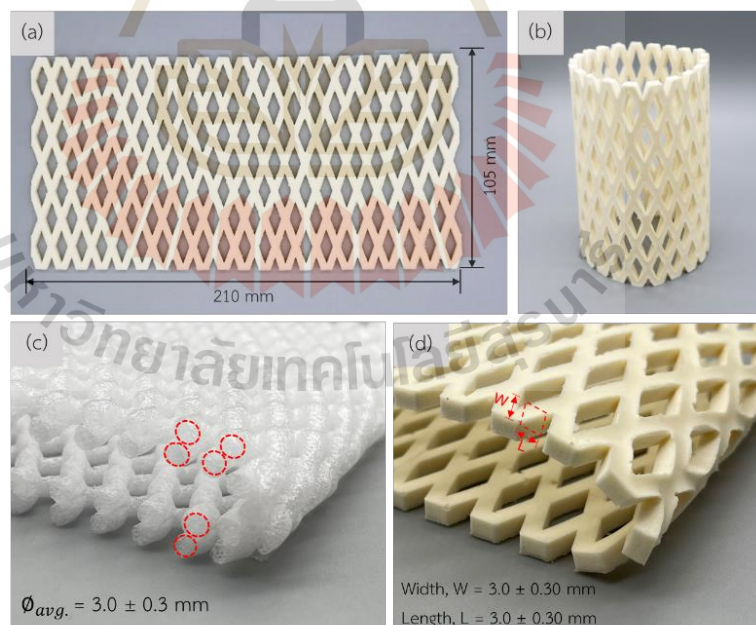


Figure 4.10. Fabrication and design of NRL-FN: (a) foam net sheet; (b) foam net cylindrical tube; (c) cross-section of EPE-FN; and (d) cross-section of NRL-FN.

4.2.2 Mold shrinkage

The shrinkage of cushion foam is an important parameter for cushion packaging design and fabrication. The shrinkage of NR products after vulcanization may have an impact on the final density and performance. The understanding of this shrinkage behavior can also be used to design the mold so the desired shape and dimension of the cushion can be obtained. The shrinkage of NRL-FN at different BLF contents is displayed in Figure 4.12. It could be generally seen that the height direction of all samples showed the highest shrinkage rates compared to the width and length direction. The height shrinkage further increased with increasing BLF content. Whereas, the width and length slightly decreased. The different shrinkages in height from the width and length were plausibly due to freedom of shrinkage from the top and the free surface of the molding foam during fabrication. The height direction presented a higher shrinkage percentage because the free surface of the NR foam was pulled by the BLF weight. The side walls prohibited the changes in the width and length from molding the NR foam and prevented shrinkage in these directions.

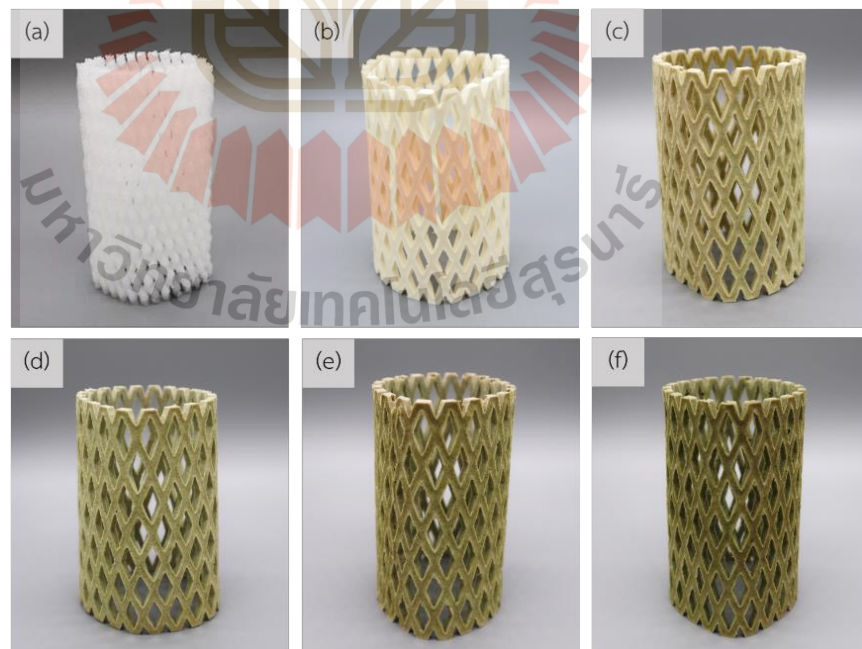


Figure 4.11. Cushion foam net: (a) EPE-FN; (b) NRL-FN-BLF0.0; (c) NRL-FN-BLF2.5; (d) NRL-FN-BLF5.0; (e) NRL-FN-BLF7.5; (f) NRL-FN-BLF10.0.

The higher shrinkage rate was observed when higher filler content was incorporated into the foam (Ramli et al., 2015). Moreover, the addition of filler was most likely to corrupt the foam's cell structure (Mahathaninwong et al., 2021). The effect of BLF incorporation into the NRL-FN and its contents on the bulk density and cell structures are discussed in the following section.

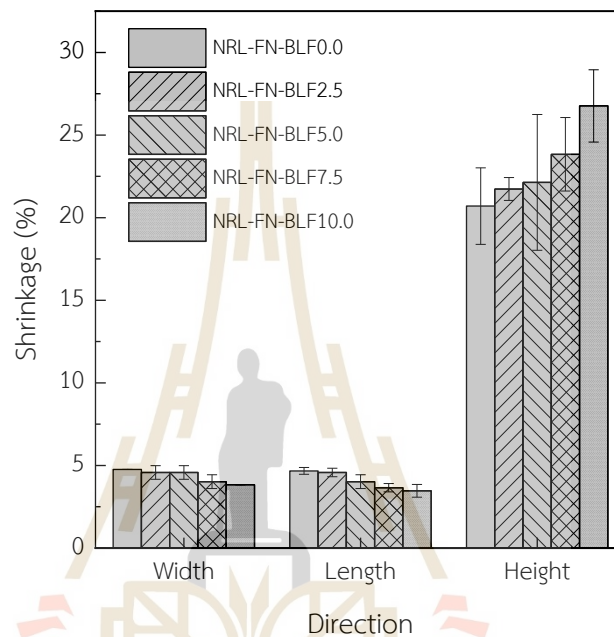


Figure 4.12. Shrinkage percentage of NRL foam composite at various BLF loading at different shrinkage directions compared with silicone mold size. Significant differences at $p < 0.05$ are shown by different letters. The values represent the mean \pm S.E. of five replicates.

4.2.3 Bulk density

In packaging, low bulk density material is preferred due to lower fuel consumption and lower cost of transportation. Table 4.6 shows the bulk density of EPE-FN compared to NRL-FN and NRL-FN-BLFs. It was clear that the density of EPE-FN commercial foam was greatly lower than that of the NRL-FN-BLFs (≥ 10 folds). This was expected as polyethylene (PE) possessed a lower density than NR. In addition, PE had a good melt strength, which was required to fabricate a foam structure with high porosity (large cell and thin wall). SEM micrographs in the following section were good agreement with the bulk density result.

The bulk density of NRL-FN was approximately 265 kg/m^3 . The density was higher than those values reported by Prasopdee and Smitthipong ($\sim 65 \text{ kg/m}^3$) (Torres-Huerta et al., 2019) and Mahathaninwong et al. ($\sim 161.6 \text{ kg/m}^3$) (Hamad et al., 2011). Generally, the low density of NRL foam was achieved by the incorporation of the air into the NR latex or whipping in the Dunlop process (Hui Mei & Singh, 2010). Foaming time, foaming speed (Jitkokkrud et al., 2021), and blowing agent content (Harnnarongchai & Chaochanchaikul, 2015; Suethao et al., 2021) were used to adjust the bulk density of the NRL foam. The differences in the density of the NR forms reported here as compared to others may be due to the different methods and/or equipment used during the aeration process. The addition of the BLF, which possessed higher density than the NRL foam, gave rise to the bulk density of NRL-FN-BLF composites. The presence of BLF also induced a higher degree of shrinkage (Figure 4.11), resulting in an increase in bulk density. A similar result was also found by Zhang, N. and H. Cao when chitin was used to enhance the antibacterial activity in NRL foam. The volume of the air in the NRL foam was decreased because chitin particles agglomerated and destroyed the original cellular structure of the foam cells, resulting in the collapse of the foam and thus increasing the foam bulk density (Zhang & Cao, 2020).

4.2.4 Morphology and cell structure analysis

The foam surface and the foam cell characteristics of the EPE-FN and NRL-FN with and without BLF cushions were studied using SEM. The surfaces of the foam samples are shown in Figure 4.13. The EPE-FN surface shown in Figure 4.13(a) was dense and smooth without any holes or protrusions on the surface. On the other hand, the surface of the NRL-FN and NRL-FN-BLFs (Figure 4.13(b–f)) appeared to be dense and rough with some holes and lumps on the surface of some samples. The addition of BLF to the NRL-FN slightly caused the change in the surface roughness. The roughness increased slightly as a function of BLF content. No obvious fiber was found on the surface. The roughness of the foam surface may implicate its use as cushioning for fresh produce. As the cushion foam surfaces usually directly contact with the fresh

produce's surface, the rough surface may cause bruising damage during transportation. However, several other parameters can also contribute to accrue bruise damage on some fruit, including the foam's hardness, cushion efficiency, fruit firmness, etc. The pack test of the target fruit using cushions with different BLF contents must be done to elucidate the effect of surface roughness of the NRL-FN on surface bruising of the fruit.

Table 4.6. Foam properties of EPE-FN and NRL-FN-BLFs.

Cushion Foams	Bulk Density (kg/m ³)	Hardness (Shore OO)	Number of Cells per Unit Volume (Cells/cm ³)	Average Cell Size (µm)
EPE-FN	18.869 (Song et al., 2018)	29.56 ± 0.65 ^a	-	-
NRL-FN-BLF0.0	264.59 ± 4.64 ^b	28.88 ± 0.61 ^{ab}	63,726.67	93.54 ± 2.64 ^c
NRL-FN-BLF2.5	272.56 ± 5.35 ^{ab}	28.64 ± 0.67 ^b	56,892.56	100.73 ± 4.76 ^c
NRL-FN-BLF5.0	276.99 ± 7.22 ^{ab}	29.08 ± 0.78 ^{ab}	50,968.49	108.06 ± 2.06 ^b
NRL-FN-BLF7.5	281.53 ± 11.60 ^a	29.28 ± 0.67 ^{ab}	51,381.86	115.05 ± 3.66 ^a
NRL-FN-BLF10.0	288.47 ± 12.51 ^a	29.48 ± 0.48 ^b	45,758.51	122.58 ± 4.52 ^a

Note: Significant differences at $p < 0.05$ are shown by different letters. The values represent the mean ± S.E. of five replicates.

SEM micrographs of the cross-sectioned of the samples are shown in Figure 4.14. For EPE-FN (Figure 4.14(a)), the foam appeared to be a closed-cell structure with a very large cell size of 600–900 µm. The cell wall was relatively thin, with a thickness of 2–5 µm. The shape of the foam cell was a polygon with interconnecting thin walls similar to that of the honeycomb structure. SEM micrographs of the NRL-FN foam structure in Figure 4.14(b–f) also revealed a more or less closed-cell structure of a spherical cell morphology with openings on some cell walls when the BLF was increased. Spherical foam cells were found throughout the sample. The spherical foam cells with different sizes were relatively small as compared to that of the EPE-FN. Cell

size was analyzed using the ImageJ program and shown as a cell size distribution curve in Figure 4.15. The average cell size of the samples was calculated and shown in Table 4.6. The difference in cell size of a sample indicated that the air bubbles generated during the Dunlop process were nonuniform. This is a common result of a mechanical foaming technique, such as in the Dunlop process, where poor pore formation regulation is observed (Jedruchniewicz et al., 2021). The cell wall was relatively thick, with a thickness in the range of 10–70 μm . The structures of the obtained NRL foams agreed with the high bulk density results discussed earlier. The lower bulk density of the NRL foam reported by (Garrison et al., 2016; Materials, 2010) was due to the open cell structure of NRL. The polymeric foam can be made into either open or closed-cell foam, depending on the stabilizing agent used (Garrison et al., 2016). The results suggested that our NRL foam could be further optimized to obtain a lower bulk density to make it suitable for packaging applications. However, such a structure may need to prove its ability to withstand the incorporation of BLF.

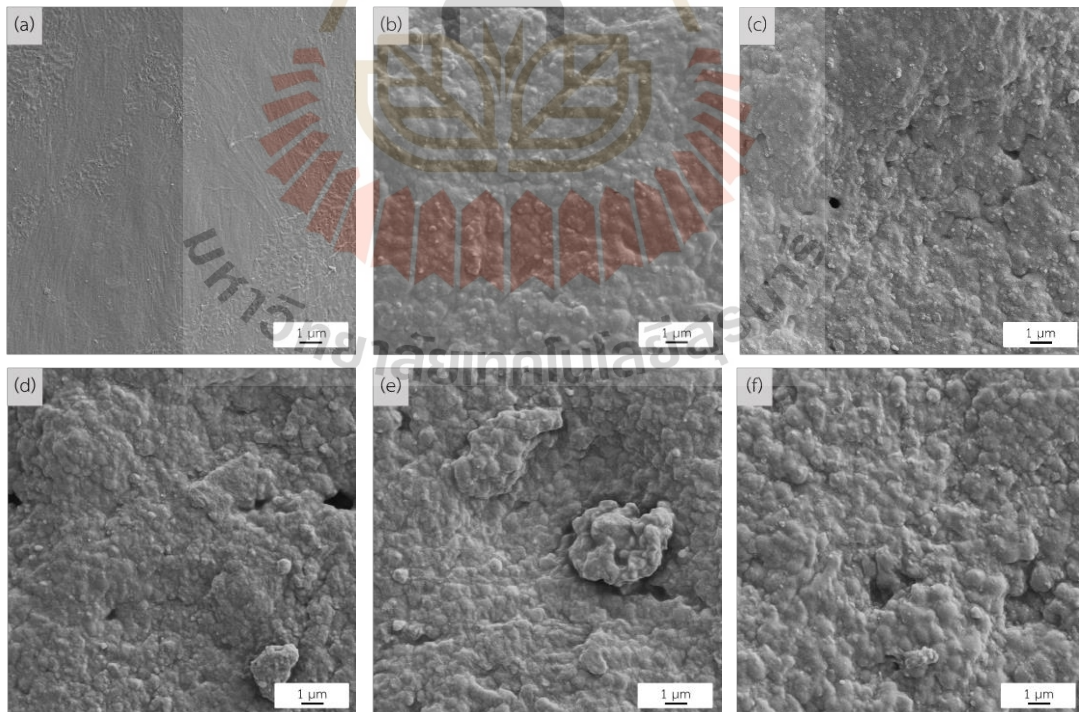


Figure 4.13. NRL foam composites morphology at the top surface of specimens (5k \times magnification): (a) EPE-FN; (b) NRL-FN-BLF0.0; (c) NRL-FN-BLF2.5; (d) NRL-FN-BLF5.0; (e) NRL-FN-BLF7.5; (f) NRL-FN-BLF10.0.

The addition of BLF fiber into NRL-FN resulted in larger foam cells. As the BLF content increased, the cell size of the NRL-FN-BLF composites noticeably increased. On the other hand, the number of foam cells decreased as the BLF content increased. From statistical analysis, the average cell size was insignificant difference between that of the NRL foam at BLF loading at (0.00 and 2.50 phr) and (7.50 and 10.00 phr). The addition of BLF seemed to cause the foam cells to coalesce, resulting in fewer cell counts and larger pore sizes. Similar results were reported by Tomyangkul et al. (2016) and Surya et al. (2019). It is commonly known that NRL foam structure dictates most foam properties. The foam structure could be tailored through various parameters, including foaming agent type and amount (Garrison et al., 2016), fabrication methods, filler type, filler or particle size (Mursalin et al., 2018), filler loading (Hamad et al., 2011), etc.

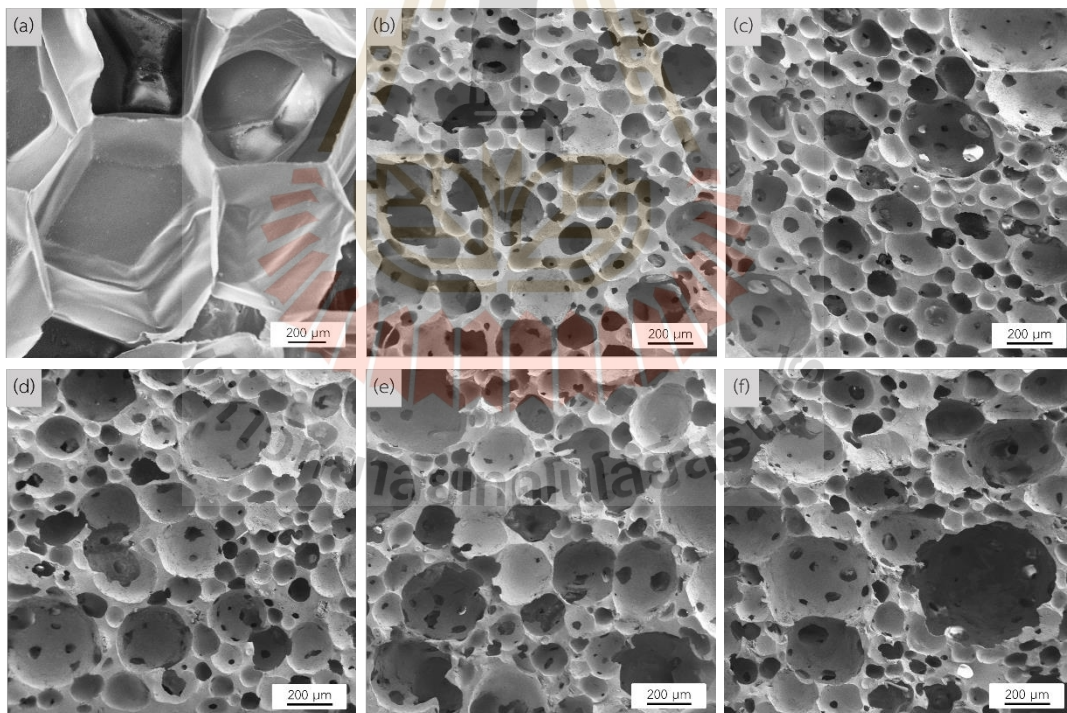


Figure 4.14. Cushion foams morphology at a 50x magnification: (a) EPE-FN; (b) NRL-FN-BLF0.0; (c) NRL-FN-BLF2.5; (d) NRL-FN-BLF5.0; (e) NRL-FN-BLF7.5; (f) NRL-FN-BLF10.0.

4.2.5 Hardness

Hardness is the degree of firmness of a material. It indicates the ability to resist deformation, scratching, or abrasion (Briscoe, Pelillo, & Sinha, 1996). The Shore OO type of durometer hardness was used in this research following ASTM D2240 due to the cushion foam as extremely soft rubber, sponges, and foams. Cushion material with high hardness can cause damage to the soft surface of a fruit. The hardness of the cushion foam samples is shown in Table 4.6. It could be seen that the hardness of EPE-FN and NRL-FN with and without BLF were similar.

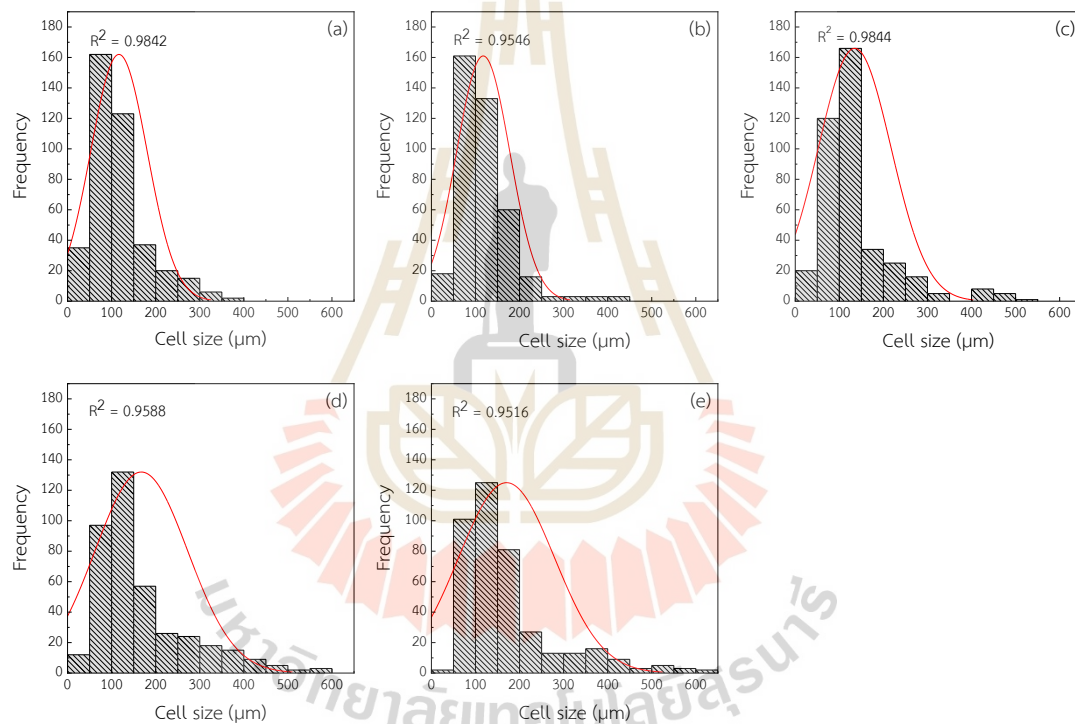


Figure 4.15. Cell size distribution of NRL foam composite with various BLF loadings ($p < 0.05$, $n = 400$): (a) NRL-FN-BLF0.0; (b) NRL-FN-BLF2.5; (c) NRL-FN-BLF5.0; (d) NRL-FN-BLF7.5; (e) NRL-FN-BLF10.0.

The result indicated that the hardness quality of the eco-friendly NRL-FN cushion could be used as an alternative to the EPE-FN fruit cushion. A slight increase in hardness was observed increasing BLF content, but it was statistically insignificant. The finding was unexpected as other researchers had reported an increase in hardness when fillers were added to NRL foams. Bashir et al. added eggshell powder (ESP) at

0.0, 2.5, 5.0, 7.5, and 10.0 phr to the NRL foam. The obtained NRL foam composite possessed higher hardness and stiffness than NRL foam when the ESP content was at least 10 phr. The improvements were because the EPS demobilized the polymer chains of the NRL foam matrix (Bashir, Manusamy, Chew, Ismail, & Ramasamy, 2015). Mahathaninwong, et al. also reported that incorporating Agarwood-waste (ACW) powder led to increased hardness of NRL foam (Mahathaninwong et al., 2021). They also suggested that the change in hardness was due to the change in foam cell morphology, contributing to the filler addition. Sirikulchaikij et al., (2020) fabricated NRL foam using a bubbling process. The hardness of the latex foam increased when the cell size became larger. Thus, the hardness depended on the NRL foam's cell structure or morphology. In our work, as shown in Table 4.6 and Figure 4.14, adding BLF up to 10 phr slightly increased the cell size while the cell wall thickness values remained relatively constant. Therefore, the small change in hardness of the NRL-FN-BLF composites was in good agreement with the insignificant change in the foam morphology.

4.2.6 Compression set

The elastic behavior of elastomeric material is generally determined using a compression set test. A material with a low compression set can restore its thickness close to its original size after removing the compression force, suggesting a high material elasticity. On the other hand, a material with a high compression set may permanently lose its shape due to low elasticity. In general, a smaller permanent compression set leads to higher foam recoverability (Sukkaneewat & Utara, 2022). Figure 4.16 shows the compression set of NRL foams with different BLF loadings. NRL-FN without BLF had a compression set of 12.5%. The addition of 2.5 phr BLF to NRL-FN insignificantly altered the compression set of the foam. The compression set showed an increasing trend as a function of the BLF loading, with a maximum of 16.0% at 10 phr of BLF. A similar trend was observed when rice husk powder (RHP) was added to the NRL foam. The RHP was used to decrease the recovery percentage of the NRL foam. At low RHP loading, the NRL foam composite could be returned to its initial

thickness faster than the foam with higher RHP loading (Ramasamy et al., 2013). Another report showed that better dispersion of a filler (kenaf) and smaller particle size led to a smaller deformation. The filler agglomeration decreased the elasticity behavior of the NRL foam. The agglomerated filler restricted the molecular chains' movements, enhancing the foam's stiffness (Surya et al., 2019). Moreover, foam with larger cells with thinner cell walls might be easily collapsed under the load. Thus, NRL foam with smaller cells and more cell walls, such as what was found in our samples, should be able to withstand compression deformation with good recoverability (Mahathaninwong et al., 2021; Sukkaneewat & Utara, 2022). It should be noted that the compression set percentage reported here (maximum 16%) was significantly lower than those reported by the others (maximum 65%). This might be due to the closed-cell foam structure of our samples, which provided elasticity and resistance to compression deformation. For the target application of fresh produce's cushion material, a lower compression set may be more desirable as the cushion foam with a high compression set may lose its ability to protect the packaged produce after being compressed.

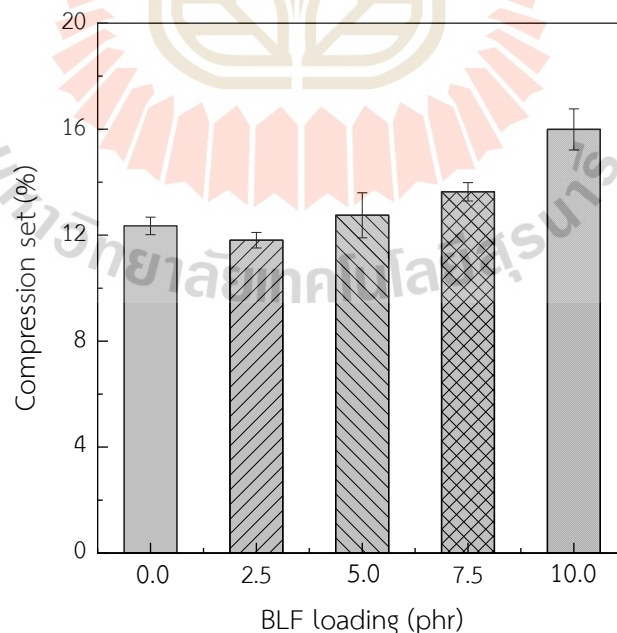


Figure 4.16. Compression set of NRL foam composite various BLF loading. Significant differences at $p < 0.05$ are shown by different letters. The values represent the mean \pm S.E. of five replicates.

4.2.7 Compression test

The relationship between compressive stress and compressive strain of the EPE-FN and the NRL-FN with different BLF loadings is shown in Figure 4.17. Similar behavior was observed in both the commercial EPE-FN and NRL-FN samples, where the compressive stress gradually increased as the compressive strain increased. This behavior was common for a foam with a closed-cell structure.

The compressive stress at 50% strain of EPE-FN was lower than those of NRL-FN at various BLF contents. The results suggested that the commercial EPE-FN was more readily deformed than the NRL-FN and NRL-FN-BLF composites. From the stress–strain curves in Figure 4.17, it could be seen that the NRL-FN and NRL-FN-BLF composites had larger areas under the curves than the EPE-FN. The larger areas under the curves of the eco-friendly foams indicated a greater ability to absorb energy than the EPE-FN commercial cushion materials.

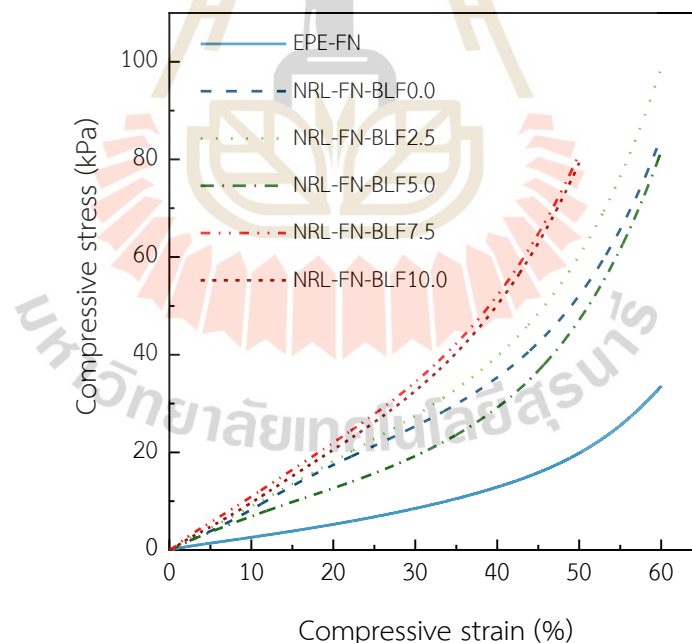


Figure 4.17. Stress–strain curve of the cushion foams.

The presence of BLF in NRL-FN slightly increased the compressive stress at 50% strain. An increasing trend of the compressive stress at 50% strain was observed as the BLF content in NRL-FN increased. The compressive stress at 50% strain of

NRL-FN containing BLF contents of 0.00, 2.50, 5.00, 7.50, and 10.00 phr were 56.58, 58.89, 48.09, 81.14, and 77.85 kPa, respectively.

The maximum stress was obtained when BLF 7.5 phr was added to NRL-FN. Further increasing the BLF content to 10.0 phr showed insignificant change in the compressive stress at 50% compressive strain. The change in the compressive stress of a porous material with a filler depends on the type and content of the filler used as well as its effects on the foam cell structure. Typically, a foam's compression stress and stiffness increased with increasing filler loading. Consequently, the increase in stiffness led to an increment in hardness (Kudori & Ismail, 2019; Ramasamy et al., 2013; Sallehuddin & Ismail, 2020). From our results, adding BLF insignificantly changed the foam morphology. The slight increase in the compressive stress at 50% strain possibly came from the presence of the harder particle of BLF.

In the packaging of fresh produce, the cushion material must absorb energy from external forces during transportation. Consequently, the lowest amount of energy may transfer to the packed fresh produce. The cushion that absorbs more energy is, therefore, better at reducing the bruising damage of fresh produce. The ability of a material to absorb energy could be determined in terms of "cushion coefficient (C)". The cushion coefficient is determined from the compressive stress-strain curve, and the results are shown in Figure 4.18. It could be seen that the cushion coefficient was dependent on the strain percentage. A significant decline in the cushion coefficient was observed initially up to 45% strain before it leveled off. To compare the cushion coefficient of the samples, cushion coefficients at 50% compressive strain were chosen and shown in Table 4.7. It could be seen that the commercial EPE-FN cushion possessed the highest cushion coefficient of 5.24, indicating it had the lowest ability to absorb energy among all samples.

On the other hand, the cushion NRL-FN without BLF possessed the lowest cushion coefficient of 4.62. Increasing content of BLF in the NRL-FN cushion gave rise to the cushion coefficient. The results suggested that NRL-FN was the best material for the cushioning application as it could absorb the highest energy from the

external force. A small amount of BLF added in to the NRL-FN might be beneficial for enhancing the biodegradability of the cushion foam net without sacrificing the cushion performance. A pack test using the eco-friendly cushions with the actual model fruit is required to prove their effectiveness as a cushion material. Based on the available data, the NRL-FN-BLFs might be used instead of EPE-FN for commercial purposes in the future.

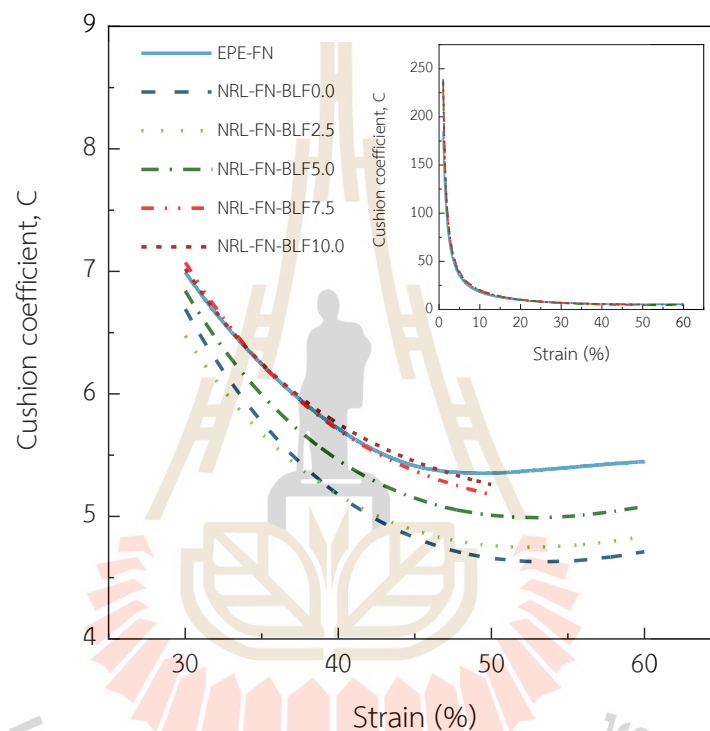


Figure 4.18. Cushion coefficient–compressive strain curves of cushion foams.

4.2.8. Crosslink density

The crosslink density is used to examine the degree of crosslinking. Crosslink density was determined using swelling method and calculated using Flory-Rhener equation. The crosslink density and swelling ratio of the NRL foam composite are shown in Table 4.8. With increasing BLF loading, crosslink density was decreased. but swelling ratio was increased The decrease in crosslink density was dependent on the expansion of gas from the foaming agent in the foaming process, which affected the density because the expansion destroyed the crosslinks (Eyssa, Mogy, & Youssef, 2021). In addition, an increase in gas resulted in decreased the crosslink density,

increased the cell size and reduced the density of the foam (Ariff, Zakaria, Tay, & Lee, 2008). The cell size in this research increased with increasing BLF content in the foam. Accordingly, the BLF loading affected the foam structure and reduced the crosslink density. Additionally, the foam with low crosslink density degraded more readily than foam with a high crosslink density.

Table 4.7. Cushion coefficient at 50% strain of a commercial cushion foam compared to the eco-friendly cushion NRL-FN at various BLF contents.

Cushion Foams	Cushion Coefficient (c) at 50% Strain
EPE-FN	5.24
NRL-FN-BLF0.0	4.62
NRL-FN-BLF2.5	4.81
NRL-FN-BLF5.0	5.01
NRL-FN-BLF7.5	5.19
NRL-FN-BLF10.0	5.21

Table 4.8 Crosslink density and swelling ratio of the NRL foam composite at various BLF contents.

Cushion foams	Crosslink density (mol/cm ³)	Swelling ratio
NRL-FN-BLF0.0	24.344	2.768
NRL-FN-BLF2.5	24.084	2.784
NRL-FN-BLF5.0	22.823	2.867
NRL-FN-BLF7.5	17.599	3.304
NRL-FN-BLF10.0	16.371	3.437

4.2.9 Biodegradation study

In the biodegradation study, the cushion foams of EPE-FN, NRL-FN, and NRL-FN-BLFs were buried in planting soil and placed outdoors for 24 weeks (May–October 2022). The biodegradation of the foams were investigated from the appearance, weight loss percentage, chemical structure, and mechanical properties.

4.2.9.1 Appearance

Table 4.9 shows the appearance (photographs on the left column) and surface microstructure (SEM micrographs on the right column) of the cushion samples before and after soil burial for 24 weeks. Before the soil burial experiment (week 0), the EPE-FN was white and cumulus. The NRL-FN was off-white with a yellowish tint. A greenish color was observed when BLF was incorporated into the NRL-FN. The intensity of the green color increased as a function of BLF content. After 24 weeks of the soil burial test, the EPE-FN became slightly denser, and its color remained white. The NRL-FN and NRL-FN-BLFs, on the other hand, did not show a change in shape, but the color turned slightly brownish. The darker shade of the brownish color was more prominent as the BLF content in the NRL-FN-BLFs increased. The change in color was used as an indicator for the biodegradation of natural fiber/polymer composites. Luthra, Vimal, Goel, V. et al. (2020) suggested that the color appearance was an important parameter used in the assessing the deterioration of the PP/natural fiber composite. The color change was mainly due to the changes in the chemical structure of the lignocellulosic complex of the natural fiber in the composite. A similar result was also reported by Butylina et al. (2012). It was also reported that removing the lignin from the fiber decreased the change in color. In our study, BLF was used without any treatment. Therefore, it could be inferred that the brownish color that appeared on the NRL-FN and NRL-FN-BLFs was a sign of degradation. The greater color changes of the NRL-FN-BLF cushion foams as the BLF content increased were in good agreement with the changes on the cushions' surfaces observed in the SEM micrographs.

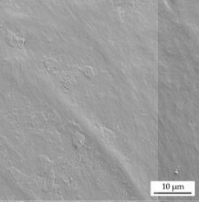
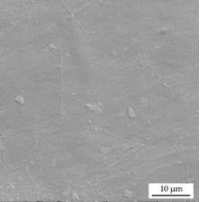
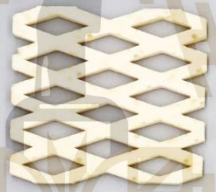
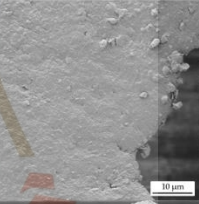
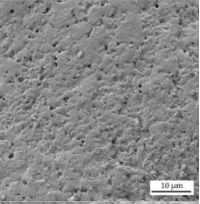
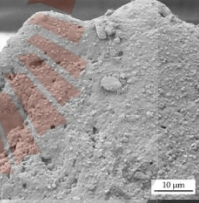
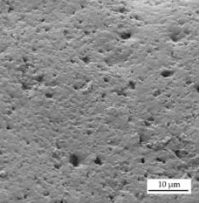
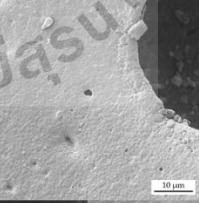
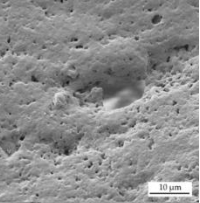
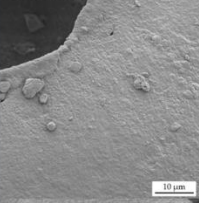
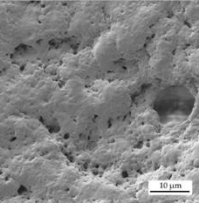
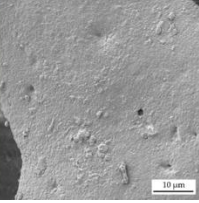
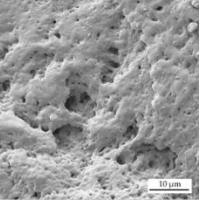
The SEM micrographs of the cushions' foam surfaces showed significant changes in the surface appearance and roughness. The increases in surface roughness coupled with the emergence of microvoids became more pronounced as the BLF content increased. Similar results were reported by Shah, Hasan, Shah et al. (A. A. Shah, Hasan, Shah, Mutiullah, & Hameed, 2012). They showed that a NR latex glove appeared rough with irregular cracks and pits after 2 weeks of exposure to *Bacillus* sp. AF-666. The greater surface erosion suggested higher degradation of NRL-FN with higher BLF contents. Similar increasing trends of degradation as a function of the increasing natural fiber contents were reported by others (Butylina, Hyvärinen, & Kärki, 2012; Luthra, Vimal, Goel, Singh, & Kapur, 2020). To confirm the degradation of the NRF-FN-BLF cushion foam, foam appearance, weight loss, and chemical structure were investigated.

4.2.9.2 Weight loss

The weight loss values of the EPE -FN, NRL-FN, and NRL-FN-BLFs after 24 weeks of soil burial are shown in Figure 4.19. The weight loss percentage is a crucial indicator of the degradation of the samples. From the graph, it could be seen that EPE-FN showed a reduction in the first 4 weeks before the weight loss became constant. The maximum weight loss was approximate 1%. The NRL-FN showed a higher weight loss than the EPE-FN. The fast-increasing weight loss was observed in the first 8 weeks before it leveled off. The maximum weight loss at 24 weeks of soil burial was about 4%. With the presence of BLF in NRL-FN, a greater initial weight loss was observed, and the weight loss continued to increase after week 8. It was noticeable that higher weight loss was observed with higher BLF content in NRL-FN. The degradation rate could be estimated from the slope of the curves in Figure 4.18. The results suggested a fast degradation rate was observed in the initial soil burial time before week 8. After week 8, the NRL-FN samples containing BLF continued to degrade with slower degradation rates. The rate tended to increase with the BLF content. At the end of soil burial at week 24, the weight loss of NRL-FN containing 10 phr of BLF was 1.8 times greater than that of NRL-FN without BLF. The results suggested that the

natural fiber acted as a biodegradation accelerator for the NRL foam composites. The weight reduction was due to the microorganisms' activity during soil burial, which took place on the skin of the samples and appeared as surface erosion and microvoids in the SEM micrographs in Table 4.9.

Table 4.9. Appearance and micrograph of cushion foams before soil burial (0 weeks) and after soil burial (24 weeks).

Cushion Foams	Foams Appearance		Foams Micrograph	
	Before Soil Burial	After Soil Burial	Before Soil Burial	After Soil Burial
EPE-FN				
NRL-FN-BLF0.0				
NRL-FN-BLF2.5				
NRL-FN-BLF5.0				
NRL-FN-BLF7.5				
NRL-FN-BLF10.0				

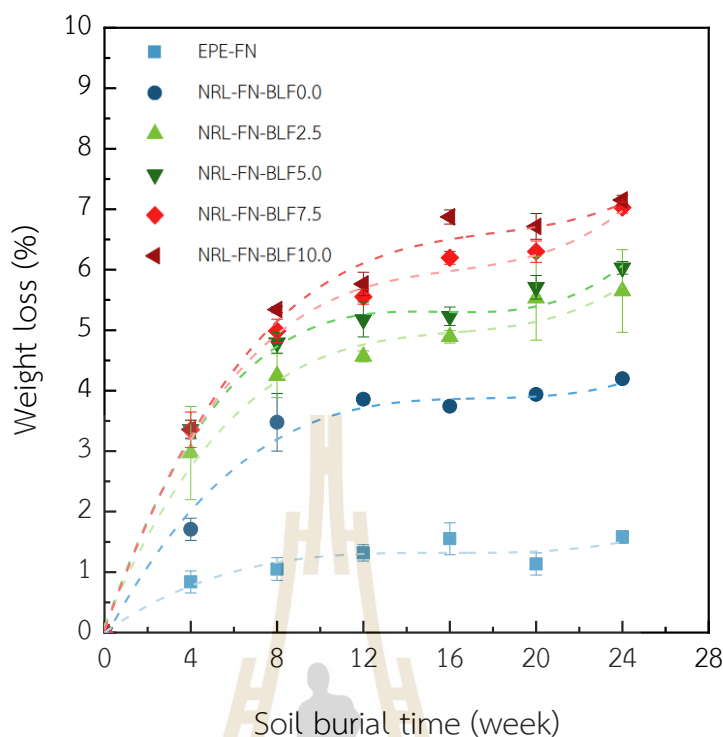


Figure 4.19. Weight loss percentage of EPE-FN, NRL-FN, and NRL-FN-BLFs cushion foams at various BLF contents over 24 weeks of soil burial times.

Tsuchii et al. (1985) reported that a surgical glove was degraded in 20 days in a culture medium. This was probably because their samples were very thin compared to ours, and their controlled environment also played a crucial role in degrading their NR products. Soil burial was used in this study to simulate the normal ecological condition of the landfill method, the most common technique of waste management. The biodegradation rate may be accelerated significantly in a controlled environment with the right microbe (fungi and/or bacteria) strain. Moreover, several reports suggested that some chemicals in the NR compound may enhance or prohibit the biodegradation of rubber products. The use of BLF as a filler in the NRL-FN enhanced biodegradation of the eco-friendly foam cushion. Optimization of the chemicals used in the making of the NRL-F may be done to further increase the biodegradation rate.

Moreover, thickness of the foam affects biodegradability. When compared between NRL-FN-BLF0.0 (Thickness ~ 3 mm) and NRL-FN-BLF0.0 (Thickness

~ 2 mm), the weight loss of NRL-FN-BLF0.0 (Thickness ~ 2 mm) was higher than the NRL-FN-BLF0.0 (Thickness ~ 3 mm). The effect of sample thickness on weight loss of the foam is shown in Figure 4.20. The thin or high surface area foam produce exhibited higher weight loss than that of thick foam. Datta, Samanta et al. (2021) reported that increasing the thickness of a film decreased weight loss because a thicker film spreads less and thus has less surface area exposed to biological media, which has a negative impact on how easily it degrades (Datta, Samanta, & Halder, 2021).

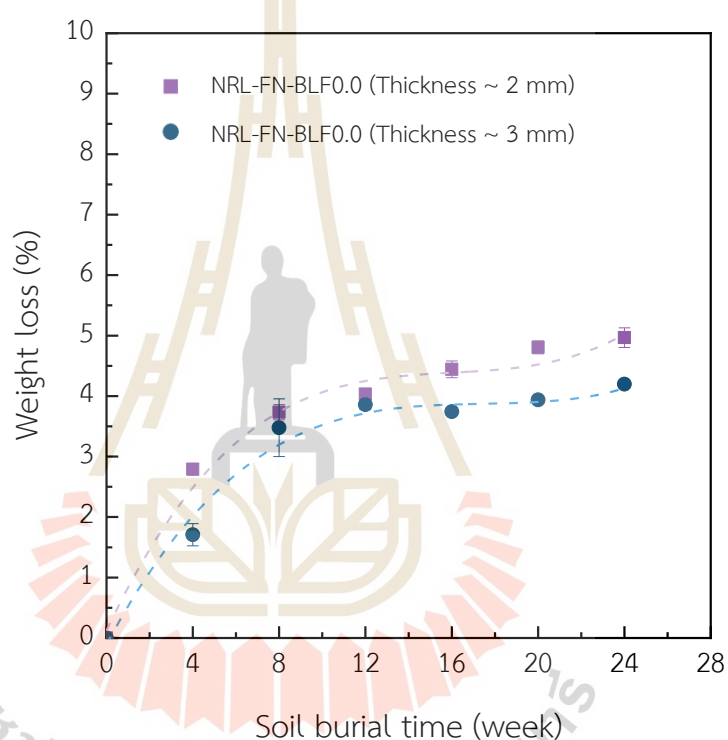


Figure 4.20. Weight loss percentage of NRL-FN-BLF0.0 (thickness ~ 3 mm) and NRL-FN-BLF0.0 (thickness ~ 2 mm) cushion foams at thickness over 24 weeks of soil burial times.

4.2.9.3 Fourier transform infrared (FTIR) analysis

FTIR analysis method is a technique for observing the chemical structure of materials. FTIR spectra of the cushion foam samples before and after 24 weeks of soil burial at various BLF loadings (0.00, 2.50, 5.00, 7.50, and 10.00 phr) are compared, as shown in Figure 4.21. FTIR bands assignment of NRL, BLF, and NRL composites are shown in Table 4.10.

Table 4.10. IR bands assignment of NRL, BLF, and NRL composite.

Wavenumber (cm ⁻¹)	Assignment
3300–3380	–OH stretching vibration (–OH as a result of the degradation by oxidation) (Manaila, Stelescu, & Craciun, 2018)
2958–2960	–CH ₃ asymmetric stretching vibration of natural rubber (Manaila et al., 2018)
2919–2927	–CH ₂ asymmetric stretching vibration of natural rubber (Manaila et al., 2018)
2852–2854	–CH ₂ asymmetric stretching vibration of natural rubber (Manaila et al., 2018)
1710–1740	Carbonyl group (C=O) from ketone or aldehyde results from oxidative degradation (Manaila et al., 2018)
1655–1665	–C=C-stretching vibration in the NR structure or maybe due to absorbed water or carboxylate or conjugated ketone (–C=O) resulted from the degradation (Manaila et al., 2018)
1618	Aromatic skeletal vibration, C=O stretching, absorbed O-H of hemicellulose and lignin (Zhuang, Li, Pu, Ragauskas, & Yoo, 2020) of BLF
1508	C=C-C aromatic ring stretching and vibration of lignin (Zhuang et al., 2020) of BLF
1537, 1270	C=O and –O-R of hemicellulose (Gao, Chen, Yang, Yang, & Han, 2011) of BLF
1032	C-O stretching, aromatic C-H in-plane deformation of cellulose and lignin (Zhuang et al., 2020) of BLF
1020	–C-O-C-stretching of esther group (Daud, Ismail, & Bakar, 2016)
870–830	Isoprene backbone of NR (Jayathilaka, Ariyadasa, & Egodage, 2020)

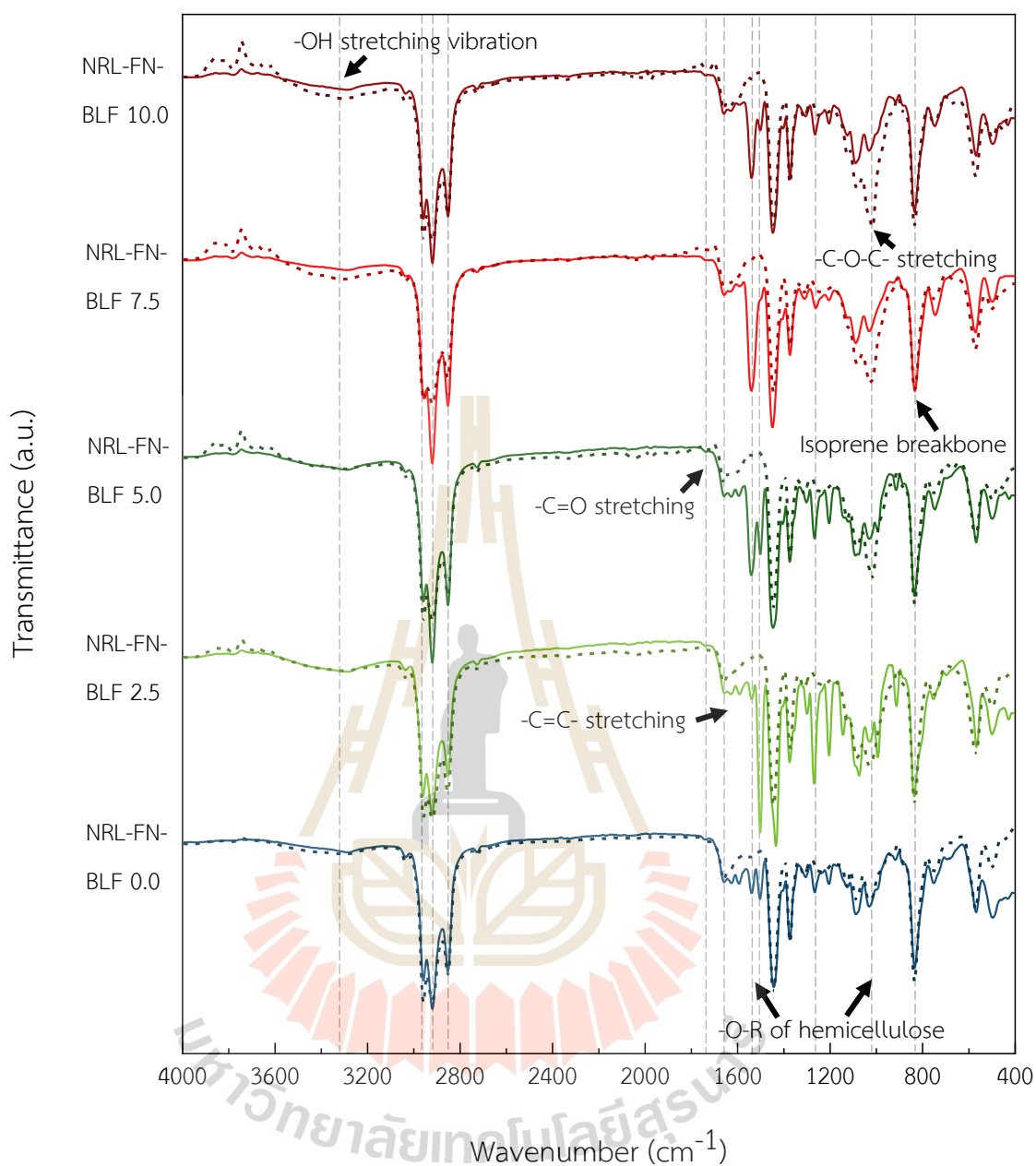


Figure 4.21. FTIR spectra of NRL foam composites before (solid lines) and after (dash lines) soil burial.

FTIR spectra of NRL-FN-BLF0.0 before soil burial showed peaks at $2800\text{--}3000\text{ cm}^{-1}$ (-CH stretching), $1655\text{--}1665\text{ cm}^{-1}$ (-C=C- stretching), and 835 cm^{-1} (=CH bending in isoprene backbone of NR). When compared to NRL foam, NRL foam composites exhibited absorption peaks at 3326 cm^{-1} (-OH stretching vibration of cellulose, hemicellulose, and lignin), 2918 cm^{-1} (C-H stretching of cellulose, hemicellulose, and lignin),

1628 (asymmetric stretching band of the carboxyl group of glucuronic acid in hemicellulose, -C=O stretching in conjugated of a carboxyl group), 1512 (-C=C- aromatic ring stretching and vibration in lignin), and 1033 (-C-O- stretching of cellulose and lignin) cm^{-1} . The absorption peaks of BLF are shown in Figure 4.22.

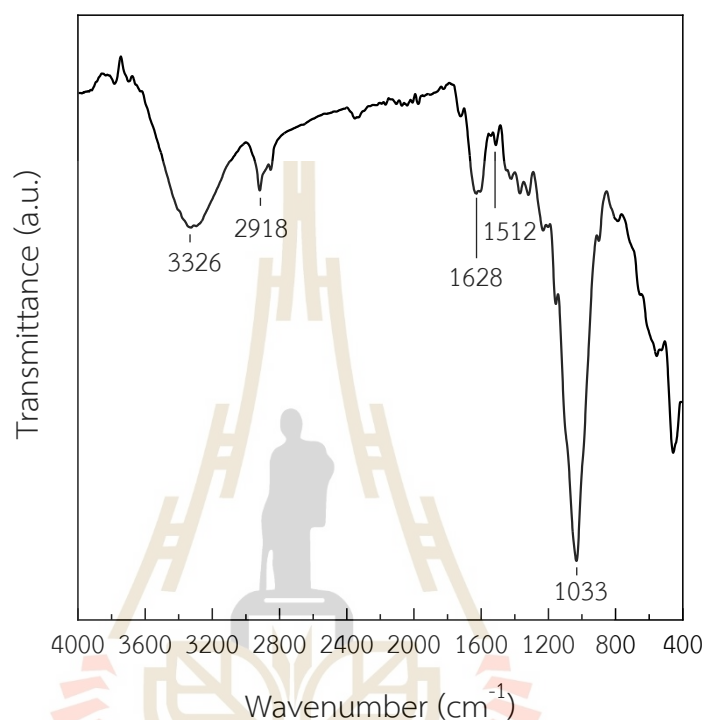


Figure 4.22. FTIR spectra of BLF.

The degradation of the vulcanized natural rubber is caused by direct action from microbes, which results in polymer chain cleavage and affects the functional group of the material (Tsuchii et al., 1985). The cleavage of the poly (cis-1,4-isoprene) backbone occurred first at the double bond via oxidative degradation (Aamer Ali Shah, Hasan, Shah, Kanwal, & Zeb, 2013). After the soil burial, the band intensity of -OH stretching at 3326 cm^{-1} and -C=O stretching at 1739 cm^{-1} of NRL foam slightly increased, as shown in Figure 4.23. The formation of carbonyl and hydroxyl bonds (-C=O and -OH) was due to the oxidative degradation of NR. In addition, the intensity of the band at 1020 cm^{-1} assigned to -C-O-C- stretching was marginally increased.

Moreover, the intensity of the peaks at 1628, 1541, and 1270 cm^{-1} ($-\text{C}=\text{O}$ stretching of hemicellulose and lignin) and 1503 cm^{-1} ($-\text{C}=\text{C}-\text{C}$ -aromatic ring stretching and vibration of lignin) decreased after soil burial due to the degradation of BLF. With increasing BLF content in the NRL foam composites, the increment of the intensity of $-\text{OH}$ stretching, $-\text{C}=\text{O}$ stretching, and $-\text{C}-\text{O}-\text{C}$ -stretching were seen in Figure 4.23. This may be because BLF improved the degradation of the composites. The biodegradability of the NRL foam composites was confirmed by the weight loss percentage and morphology.

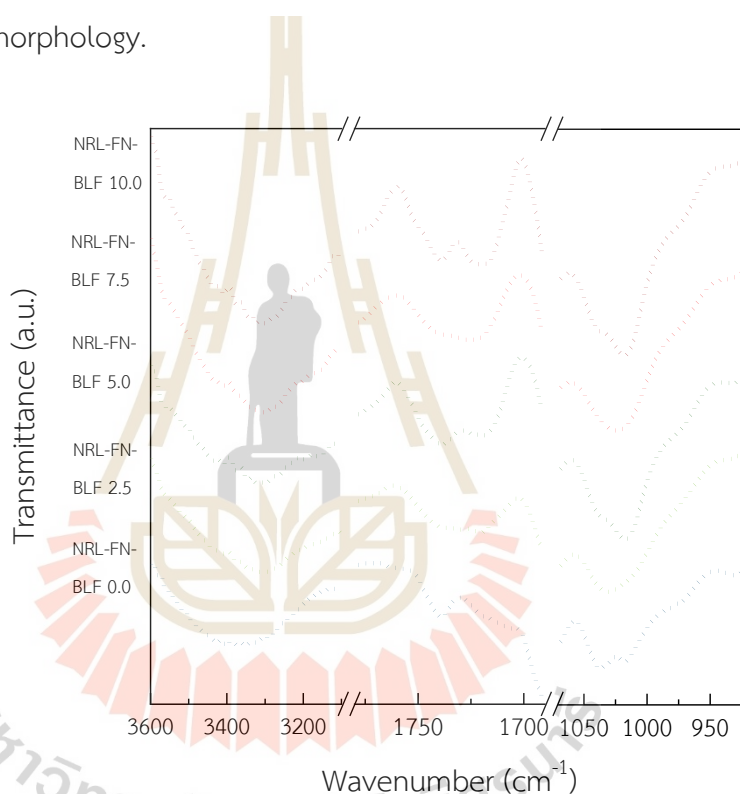


Figure 4.23. FTIR spectra of NRL foam composites at various BLF contents after soil burial for 24 weeks.

4.2.9.4 Compression test

Generally, a decline in physical properties of NR products is expected due to the degradation (Tsuchii et al., 1985). The 50% compressive strength of cushion foams at over 24 weeks of soil burial time is shown in Figure 4.24. The 50% compressive strength of EPE-FN was unchanged over the 24 weeks period. The compressive strength of the NRL-FN without and with BLF showed a decreasing trend

in the 12 weeks but became constant or even increased (such as in the case of 10 phr of BLF in NRL-FN). The slight decreases in compressive strength with increasing soil burial time in the NRL-FN samples were expected as the biodegradation damaged the samples' structure and integrity from microbial. The loss in long hydrocarbon chains also weaken the rubber properties. The increase in 50% compressive strength in some samples in the later weeks was plausibly because the degraded cushion became stiffer, hence more resistance to compressive force. Overall, the degradation of the foam sample took place, and the BLF increased the degradation rate of the NRL-FN. However, the changes in properties were relatively low. This result may be beneficial as it suggested that the eco-friendly NRL cushion could be continuously used or reused for a prolonged period of time. A well-designed logistical strategy must be created for recovering/returning the cushion after use.

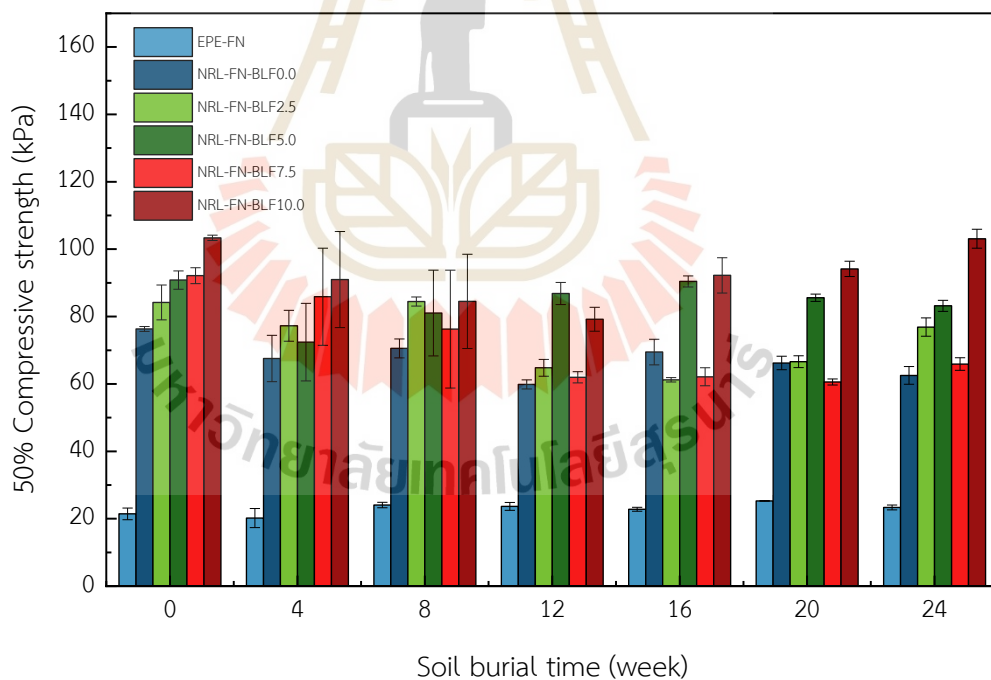


Figure 4.24. Compressive strength of 50% after soil burial for 24 weeks of cushion foam at various soil burial times.

4.3 Evaluation of the cushion performance of eco-friendly NRL foam using a vibration condition in pack test

The NRL foam composite at 0.00, 2.50, and 5.00 phr of BLF were selected to study simulated vibration transportation and compared with EPE-FN (commercial foam net).

4.3.1 Cushioning properties and percentage transmission

Cushioning performance of NRL-FN were compared with the commercially available EPE-FN. The thicknesses of the NRL-FNs was in the range of 3.080–3.196 mm which was thinner than that of the EPE-FN cushion (5.444 mm). The NRL-FN-BLF0.0 and NRL-FN-BLF2.5 treatments gave the highest energy (E) values, followed by NRL-FN-BLF5.0 and EPE-FN treatments (Table 4.12). High E value indicated high potential energy absorption from the vibration force and related to low C values in the NRL-FN-BLF0.0 and NRL-FN-BLF2.5 treatments at 50% strain compared to NRL-FN-BLF5.0 and EPE-FN treatments (Table 4.12 and Figure. 4.18). Song et al. (2018) explained that the best cushioning performance provided the smallest C value in a plot of the static cushion coefficient-strain curve indicating the highest absorbed energy (Song et al., 2018). As shown in Figure 4.18, the lowest C level was recorded at 50% strain. It was found that both NRL-FN-BLF0.0 and NRL-FN-BLF2.5 treatments with thickness of 3 mm exhibited the highest cushioning performance in absorbing vibration energy and preventing vibration bruising of guava fruit, as compared to EPE-FN cushion with a thickness of 5 mm. Adding BLF (2.5 phr) had no effect on cushioning performance. However, further increasing BLF loading in NRL-FN resulted in increased C value. The result may indicated that reduced BLF levels could be applied in NRL-FN cushion as promotion from agricultural waste (Chonhenchob et al., 2010).

The percentage transmissibility (P_T) value of the five treatments was also investigated at 13.5 Hz in the frequency range of 15–20 Hz caused by tires (Singh, Singh, & Joneson, 2006) and commonly found in truck transportation in Thailand (Chonhenchob et al., 2010). For the resonance frequency of fresh produce packaging, the highest P_T was recorded in MK4 and MK6 package designs (corrugated fiberboard boxes) of apple with frequency range 9–12 Hz (Fadji, Coetzee, Chen, Chukwu, & Opara, 2016). The most critical frequencies of apple packaging were between 3 and 15 Hz

determined by transmissibility evaluation of corrugated fiberboard boxes (VURSAVUŞ & Özgüven, 2004). Khodaei et al. (2019) found that the P_T of reusable plastic containers for fresh apricot at a frequency of 17 Hz, indicating that the selected frequency at 13.5 Hz was a representative critical range for guava packaging systems (cushion and OPF box) (Khodaei, Seiiedlou, & Sadeghi, 2019). Results showed that P_T of the control (a bare fruit) (87%) exhibited the highest value compared to NRL-FN with BLF 2.5 and 5.0 phr (74–79%), while NRL-FN-BLF0.0 phr and EPE-FN s had the lowest P_T values at 58% and 69%, respectively (Table 4.12). At higher P_T levels the fruit bounced more inside the package during transportation (Fernando, Fei, Stanley, & Enshaei, 2018). The cushioning material also reduced the free space inside the package (Khodaei et al., 2019) and restricted fruit movement/bounce during the simulated vibration test. The free space (%) of the OPF box was calculated by the length of the box (18.5 cm) and the two fruit horizontal diameters (2×7.5 cm), including four layers of cushioning thickness (Table 4.10). The free space of a bare fruit was highest at 18.9% box length, followed by all NRL-FN treatments (18.2%) and EPE-FN (17.8%). No significant differences in P_T level were found between NRL-FN-BLF0.0 phr and EPE-FN cushioning treatments and were below 100% P_T (Table 4.12). The NRL-FN-BLF0.0 phr and EPE-FN absorbed vibration force that exhibited a lower acceleration than the vibration shaker. However, adding BLF composition in NRL-FN increased P_T level above 100%. From overall cushioning properties and P_T value of NRL-FN-BLF0.0 phr showed high cushioning performance with reduced thickness, lower C and lower P_T levels than the EPE-FN cushion.

4.3.2 Appearance

Browning incidence of guava peel from vibration bruising was observed after storage at 20 °C under 80% RH for 4 days (Table 4.12). The control (a bare fruit) had the highest BA followed by NRL-FN-BLF5.0 phr and the other three cushioning treatments, with no significant difference from EPE-FN cushioning. Adding BLF at 5.0 phr to NRL-FN increased BA due to the higher C value (Table 4.11 and Figure 4.18) and rougher surface (Figure 4.13) as compared to other treatments. Therefore, the

cushioning packaging from the NRL foam (NRL-FN-BLF0.0) had the ability to protect the fresh produce from vibration damage in transportation due to its C value, P_T , and appearance, resulting in an efficacy similar to or greater than that of the commercial foam (EPE-FN).

Table 4.11 Guava appearance on day 0 and day 4 of simulated vibration transportation.

Treatment	Day 0	Day 4
Control (a bare fruit)		
EPE-FN		
NRL-FN-BLF0.0		
NRL-FN-BLF2.5		
NRL-FN-BLF5.0		

Table 4.12 Thickness, energy (E), cushion coefficient (C) and percentage transmissibility (P_T) of five treatments.

Treatment	Thickness (mm)	Energy (E) at 50% strain	C at 50% strain	P_T at 13.5 Hz
Control (a bare fruit)	-	-	-	87.393 ± 3.491 ^a
EPE-FN	5.385 ± 0.057 ^a	0.004 ± 0.000 ^c	5.203 ± 0.052 ^a	69.376 ± 2.576 ^{bc}
NRL-FN-BLF0.0	3.198 ± 0.021 ^b	0.012 ± 0.001 ^a	4.613 ± 0.081 ^c	58.546 ± 2.215 ^c
NRL-FN-BLF2.5	3.163 ± 0.032 ^b	0.012 ± 0.000 ^a	4.839 ± 0.027 ^b	79.851 ± 7.758 ^{ab}
NRL-FN-BLF5.0	3.043 ± 0.039 ^b	0.010 ± 0.000 ^b	5.003 ± 0.033 ^{ab}	74.479 ± 2.579 ^{abc}

Different letters indicate significant differences at $p < 0.05$. Values are mean ± S.E. from four replications.



CHAPTER 5

CONCLUSIONS AND RECOMMENDATIONS

The eco-friendly cushions of NRL foam were developed to be used as an alternative cushioning packaging for fresh produce. The NRL was primarily made of renewable resource material. The Dunlop process and microwave irradiation were optimized and used in the fabrication as they were energy efficient techniques. Optimal microwave irradiation condition were found at 600 W for 6 min.

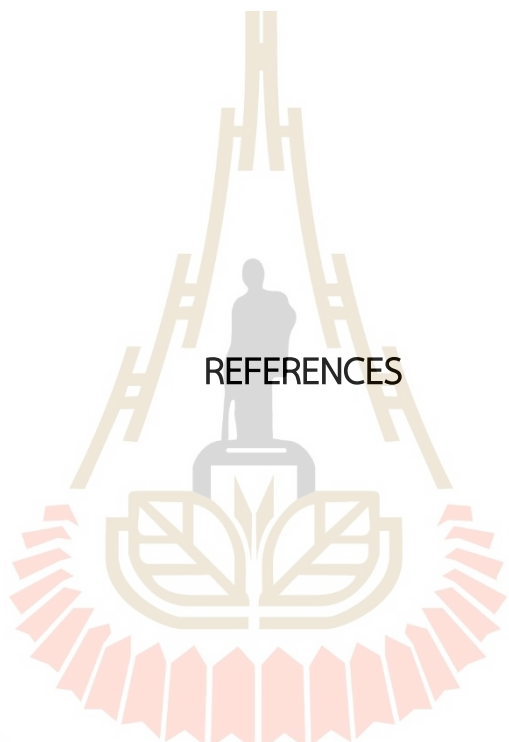
In the foaming step, parameters including stirring time, stirring speed, and foaming agent content were investigated. The relationship between the cell characteristics, bulk density, and compressive strength of NRL foam was established. The final foam product properties and performance strongly depended on the foam structure, generated during the foaming step. The compressive strength depended on both bulk density and cell morphology. The NRL foam with the lowest bulk density (271.88 kg/m^3) and cushion coefficient was selected to fabricate the foam net cushioning packaging for fresh produce and NRL foam composite containing BLF to enhance biodegradation rate.

The addition of BLF to the NRL-FN improved the cushion biodegradability. The presence of BLF also affected of the NRL foams, processability, bulk density, and foam cell structure, mechanical properties and cushion coefficient were also affected. This study illustrated the possibility of improving the packaging cushion to be more sustainable and lessen its negative impact to the environment. The presence of BLF positively enhanced the biodegradation of the cushion up to 1.8 times (weight loss) as compared to the NRL-FN without BLF after 24 weeks of soil burial test. Meanwhile, the EPE commercial cushion foam exhibited insignificant

weight loss during the same period under the same ecological conditions. Other properties, including bulk density, compression set, compressive strength and cushion coefficient, were slightly increased but no statistical significance.

To verify the cushioning performance of the eco-friendly NRL foam, the pack test of the foam with a model fruit (guava) was carried out under the simulated vibration of transportation. The results suggested that the NRL foam can be replaced the commercial EPE foam. Small bruised area was observed on the fruit packed in both eco-friendly NRL foam and the commercial foam. These two foam nets possessed the similar energy transmission quality.

Adding, 10 phr of BLF into the NRL-FN insignificantly altered the cell foam size and structure. The results suggested that the process used in creating the cushioned NRL foam composite was eco-friendly. One might add other different fillers or additives to the cushion foam to create extra functions, such as acting as an ethylene absorber and antibacterial and/or anti-browning agents. Moreover, other natural fibers can also be used to enhance the biodegradability of the NRL cushion foam, including rice husk, banana, hemp, pineapple, bamboo, coconut, etc. Hence, the natural fibers from agricultural waste may become valuable material. Ultimately, an alternative cushion that is both smart and eco-friendly may be obtainable in the near future.



REFERENCES

มหาวิทยาลัยเทคโนโลยีสุรนารี

REFERENCES

- Acıcan, T., Alibaş, K., & Özelkök, I. (2007). Mechanical damage to apples during transport in wooden crates. *Biosystems Engineering*, *96*(2), 239-248.
- Ahmad Zauzi, N. S., Ariff, Z. M., & Khimi, S. R. (2019). Foamability of Natural Rubber via Microwave Assisted Foaming with Azodicarbonamide (ADC) as Blowing Agent. *Materials Today: Proceedings*, *17*, 1001-1007. doi:<https://doi.org/10.1016/j.matpr.2019.06.498>.
- Alvarez, V., Fraga, A., & Vazquez, A. (2004). Effects of the moisture and fiber content on the mechanical properties of biodegradable polymer–sisal fiber biocomposites. *Journal of Applied Polymer Science*, *91*(6), 4007-4016.
- Ameram, N., Afiq Che Agoh, M., Idris, W., & Ali, A. (2018). Chemical characterization of bamboo leaves (*Gigantochloa albociliata* and *Dracaena surculosa*) by sodium hydroxide treatment [version 1; peer review: 1 approved, 1 approved with reservations]. *F1000Research*, *7*(1024). doi:[10.12688/f1000research.15036.1](https://doi.org/10.12688/f1000research.15036.1).
- Ariff, Z. M., Afolabi, L. O., Salmazo, L. O., & Rodriguez-Perez, M. A. (2020). Effectiveness of microwave processing approach and green blowing agents usage in foaming natural rubber. *Journal of Materials Research and Technology*, *9*(5), 9929-9940. doi:<https://doi.org/10.1016/j.jmrt.2020.06.096>.
- Barchi, G., Berardinelli, A., Guarnieri, A., Ragni, L., & Fila, C. T. (2002). PH—postharvest technology: damage to loquats by vibration-simulating intra-state transport. *Biosystems Engineering*, *82*(3), 305-312.
- Bashir, A., Manusamy, Y., Chew, T. L., Ismail, H., & Ramasamy, S. (2015). Mechanical, thermal, and morphological properties of (eggshell powder)-filled natural rubber latex foam. *Journal of Vinyl and Additive Technology*, *23*. doi:[10.1002/vnl.21458](https://doi.org/10.1002/vnl.21458).
- Briscoe, B. J., Pelillo, E., & Sinha, S. K. (1996). Scratch hardness and deformation maps for polycarbonate and polyethylene. *Polymer Engineering & Science*, *36*(24), 2996-3005.

- Butylina, S., Hyvärinen, M., & Kärki, T. (2012). A study of surface changes of wood-polypropylene composites as the result of exterior weathering. *Polymer Degradation and Stability*, 97(3), 337-345. doi:<https://doi.org/10.1016/j.polymdegradstab.2011.12.014>.
- Chaiwong, S., Yoythaisong, P., Arwatchananukul, S., Aunsri, N., Tontiwattanakul, K., Trongsatitkul, T., Saengrayap, R. (2021). Vibration damage in guava during simulated transportation assessed by digital image analysis using response surface methodology. *Postharvest Biology and Technology*, 181, 111641. doi:<https://doi.org/10.1016/j.postharvbio.2021.111641>.
- Chonhenchob, V., Singh, S. P., Singh, J. J., Sittipod, S., Swasdee, D., & Pratheepthinthong, S. (2010). Measurement and analysis of truck and rail vibration levels in Thailand. *Packaging Technology and Science: An International Journal*, 23(2), 91-100.
- Datta, D., Samanta, S., & Halder, G. (2021). Effect of thickness and starch phthalate/starch content on the degradability of LDPE/silane-modified nanosilica films: a comparative parametric optimization. *Polymer Bulletin*, 78(4), 2287-2328. doi:[10.1007/s00289-020-03213-4](https://doi.org/10.1007/s00289-020-03213-4).
- Daud, S., Ismail, H., & Bakar, A. A. (2016). Soil burial study of palm kernel shell-filled natural rubber composites: The effect of filler loading and presence of silane coupling agent. *Bioresources*, 11(4), 8686-8702.
- Dubey, N., & Mishra, V. (2019). cushioning materials for fruits, vegetables and flowers.
- Fadiji, T., Coetzee, C., Chen, L., Chukwu, O., & Opara, U. L. (2016). Susceptibility of apples to bruising inside ventilated corrugated paperboard packages during simulated transport damage. *Postharvest Biology and Technology*, 118, 111-119.
- Faraca, G., & Astrup, T. (2019). Plastic waste from recycling centres: Characterisation and evaluation of plastic recyclability. *Waste Management*, 95, 388-398. doi:[10.1016/j.wasman.2019.06.038](https://doi.org/10.1016/j.wasman.2019.06.038).
- Fernando, I., Fei, J., Stanley, R., & Enshaei, H. (2018). Measurement and evaluation of the effect of vibration on fruits in transit. *Packaging Technology and Science*, 31(11), 723-738.

- Filho, W. L., Salvia, A. L., Bonoli, A., Saari, U. A., Voronova, V., Klõga, M., . . . Barbir, J. (2021). An assessment of attitudes towards plastics and bioplastics in Europe. *Science of The Total Environment*, 755, 142732. doi:<https://doi.org/10.1016/j.scitotenv.2020.142732>.
- Gao, W.-H., Chen, K.-F., Yang, R.-D., Yang, F., & Han, W.-J. (2011). Properties of bacterial cellulose and its influence on the physical properties of paper. *Bioresources*, 6(1), 144-153.
- Garrison, T. F., Murawski, A., & Quirino, R. L. (2016). Bio-based polymers with potential for biodegradability. *Polymers*, 8(7), 262.
- Georges, A., Lacoste, C., & Damien, E. (2018). Effect of formulation and process on the extrudability of starch-based foam cushions. *Industrial Crops and Products*, 115, 306-314.
- Gillen, K. T., & Clough, R. L. (1997). *Prediction of elastomer lifetimes from accelerated thermal-aging experiments*. Retrieved from
- Goodwin, D., & Young, D. (2011). *Protective packaging for distribution: design and development*: DEStech Publications, Inc.
- Hamad, K., Kaseem, M., & Deri, F. (2011). Rheological and mechanical characterization of poly (lactic acid)/polypropylene polymer blends. *Journal of Polymer Research*, 18(6), 1799-1806.
- Harnnarongchai, W., & Chaochanchaikul, K. (2015). Effect of Blowing Agent on Cell Morphology and Acoustic Absorption of Natural Rubber Foam. *Applied Mechanics and Materials*, 804, 25-29. doi:10.4028/www.scientific.net/AMM.804.25.
- Horodytska, O., Valdés, F. J., & Fullana, A. (2018). Plastic flexible films waste management – A state of art review. *Waste Management*, 77, 413-425. doi:<https://doi.org/10.1016/j.wasman.2018.04.023>.
- Hui Mei, E. L., & Singh, M. (2010). The Dunlop Process in Natural Rubber Latex Foam. *Malaysian Rubber Development Technology*, 10, 23-26.
- Ishikawa, Y., Kitazawa, H., & Shiina, T. (2009). Vibration and shock analysis of fruit and vegetables transport cherry transport from Yamagata to Taipei. *Japan Agricultural Research Quarterly: JARQ*, 43(2), 129-135.

- Jayathilaka, L. P., Ariyadasa, T. U., & Egodage, S. M. (2020). Development of biodegradable natural rubber latex composites by employing corn derivative bio-fillers. *Journal of Applied Polymer Science*, *137*(40), 49205.
- Jedruchniewicz, K., Ok, Y. S., & Oleszczuk, P. (2021). COVID-19 discarded disposable gloves as a source and a vector of pollutants in the environment. *Journal of Hazardous Materials*, *417*, 125938.
- Jitkokkrud, K., Jarukumjorn, K., Chaiwong, S., & Trongsatitkul, T. (2021, 6th August 2021). *Effect of Foaming Time and Speed on Morphology and Mechanical Properties of Natural Rubber Latex Foam Vulcanized by Microwave Heating*. Paper presented at the SUT International Virtual Conference on Science and Technology 2021 (IVCST 2021), Nakhon Ratchasima, Thailand.
- Karatepe, B., Karatepe, M., Çakmak, A., Karaer, Z., & Ergün, G. (2009). Investigation of seroprevalence of *Theileria equi* and *Babesia caballi* in horses in Nigde province, Turkey. *Tropical Animal Health and Production*, *41*, 109-113.
- Ke, T., & Sun, X. S. (2003). Starch, poly (lactic acid), and poly (vinyl alcohol) blends. *Journal of Polymers and the Environment*, *11*(1), 7-14.
- Khodaei, M., Seiedlou, S., & Sadeghi, M. (2019). The evaluation of vibration damage in fresh apricots during simulated transport. *Research in Agricultural Engineering*, *65*(4), 112-122.
- Kudori, S. N. I., & Ismail, H. (2019). The effects of filler contents and particle sizes on properties of green kenaf-filled natural rubber latex foam. *Cellular Polymers*, *39*(2), 57-68. doi:10.1177/0262489319890201.
- Lewis Bamboo, I. (2022). Bamboo Leaves. Retrieved from <https://lewisbamboo.com/pages/bamboo-leaves>.
- Li, G. (2021). Development of cold chain logistics transportation system based on 5G network and Internet of things system. *Microprocessors and Microsystems*, *80*, 103565. doi:<https://doi.org/10.1016/j.micpro.2020.103565>.
- Lokesh, P., Kumari, T. S., Gopi, R., & Loganathan, G. B. (2020). A study on mechanical properties of bamboo fiber reinforced polymer composite. *Materials Today: Proceedings*, *22*, 897-903.

- Luthra, P., Vimal, K. K., Goel, V., Singh, R., & Kapur, G. S. (2020). Biodegradation studies of polypropylene/natural fiber composites. *SN Applied Sciences*, 2(3), 1-13.
- Mahathaninwong, N., Chuchee, T., Karrila, S., Songmuang, W., Roodsang, N., & Limhengha, S. (2021). Morphology and Properties of Agarwood-waste-filled Natural Rubber Latex Foam. *Bioresources*, 16, 176-189. doi:10.15376/biores.16.1.176-189.
- Manaila, E., Stelescu, M. D., & Craciun, G. (2018). Degradation studies realized on natural rubber and plasticized potato starch based eco-composites obtained by peroxide cross-linking. *International Journal of Molecular Sciences*, 19(10), 2862.
- Materials, A. S. f. T. a. (2010). ASTM D 1055: Standard Specifications for Flexible Cellular Materials—Latex Foam. In *Annual Book of ASTM Standards* (Vol. 08.01): ASTM.
- Mohd Nazri, M. K. H., & Sapawe, N. (2020). Removal of methyl orange over low-cost silica nanoparticles extracted from bamboo leaves ash. *Materials Today: Proceedings*, 31, A54-A57. doi:https://doi.org/10.1016/j.matpr.2020.10.969.
- Mursalim, R., Islam, M. W., Moniruzzaman, M., Zaman, M. F., & Abdullah, M. A. (2018). *Fabrication and Characterization of Natural Fiber Composite Material*. Paper presented at the 2018 International Conference on Computer, Communication, Chemical, Material and Electronic Engineering (IC4ME2).
- Najib, N., Ariff, Z., Bakar, A., & Sipaut, C. (2011). Correlation between the acoustic and dynamic mechanical properties of natural rubber foam: Effect of foaming temperature. *Materials & Design*, 32(2), 505-511.
- Ncube, L. K., Ude, A. U., Ogunmuyiwa, E. N., Zulkifli, R., & Beas, I. N. (2021). An overview of plastic waste generation and management in food packaging industries. *Recycling*, 6(1), 12.
- Nilsen-Nygaard, J., Fernández, E. N., Radusin, T., Rotabakk, B. T., Sarfraz, J., Sharmin, N., Pettersen, M. K. (2021). Current status of biobased and biodegradable food packaging materials: Impact on food quality and effect of innovative processing technologies. *Comprehensive Reviews in Food Science and Food Safety*, 20(2), 1333-1380.

- Phomrak, S., Nimpaiboon, A., Newby, B.-m. Z., & Phisalaphong, M. (2020). Natural Rubber Latex Foam Reinforced with Micro- and Nanofibrillated Cellulose via Dunlop Method. *Polymers*, *12*(9). doi:10.3390/polym12091959.
- Prasopdee, T., & Smitthipong, W. (2020). Effect of Fillers on the Recovery of Rubber Foam: From Theory to Applications. *Polymers*, *12*(11), 2745. Retrieved from <https://www.mdpi.com/2073-4360/12/11/2745>.
- Programme, U. N. E. (2018). Banning Single-Use Plastics: Lessons and Experiences from Countries.
- Ramasamy, S., Ismail, H., & Manusamy, Y. (2013). Effect of Rice Husk Powder on Compression Behavior and Thermal Stability of Natural Rubber Latex Foam. *Bioresources*, *8*, 4258-4269. doi:10.15376/biores.8.3.4258-4269.
- Ramasamy, S., Ismail, H., & Munusamy, Y. (2015). Soil burial, tensile properties, morphology, and biodegradability of (rice husk powder)-filled natural rubber latex foam. *Journal of Vinyl and Additive Technology*, *21*(2), 128-133.
- Roithner, C., Cencic, O., & Rechberger, H. (2022). Product design and recyclability: How statistical entropy can form a bridge between these concepts - A case study of a smartphone. *Journal of Cleaner Production*, *331*, 129971. doi:<https://doi.org/10.1016/j.jclepro.2021.129971>.
- Sallehuddin, N. J., & Ismail, H. (2020). Treatment's effect on mechanical properties of kenaf bast/natural rubber latex foam. *Bioresources*, *15*, 9507-9522.
- Shah, A. A., Hasan, F., Shah, Z., Kanwal, N., & Zeb, S. (2013). Biodegradation of natural and synthetic rubbers: A review. *International Biodeterioration & Biodegradation*, *83*, 145-157.
- Shah, A. A., Hasan, F., Shah, Z., Mutiullah, & Hameed, A. (2012). Degradation of polyisoprene rubber by newly isolated bacillus sp. AF-666 from soil. *Applied Biochemistry and Microbiology*, *48*(1), 37-42. doi:10.1134/S0003683812010140.
- Singh, J., Singh, S. P., & Joneson, E. (2006). Measurement and analysis of US truck vibration for leaf spring and air ride suspensions, and development of tests to simulate these conditions. *Packaging Technology and Science: An International Journal*, *19*(6), 309-323.

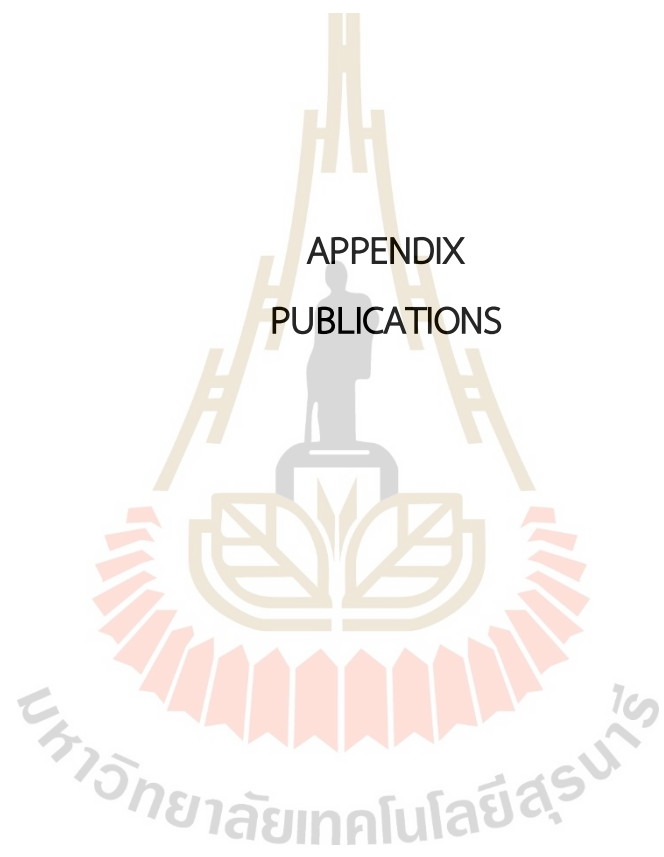
- Sirikulchaikij, S., Kokoo, R., & Khangkhamano, M. (2020). Natural rubber latex foam production using air microbubbles: Microstructure and physical properties. *Materials Letters*, 260, 126916. doi:<https://doi.org/10.1016/j.matlet.2019.126916>.
- Sohn, J. S., Kim, H. K., Kim, S. W., Ryu, Y., & Cha, S. W. (2019). Biodegradable foam cushions as ecofriendly packaging materials. *Sustainability*, 11(6), 1731.
- Song, X., Zhang, G., Lu, J., Zhang, L., & Zhang, S. (2018, 2018//). *Study on the Cushion Performance of the Cushion Material Composed of EPE and Corrugated Paperboard*. Paper presented at the Applied Sciences in Graphic Communication and Packaging, Singapore.
- Srisuwan, L., Jarukumjorn, K., & Suppakarn, N. (2018). Effect of silane treatment methods on physical properties of rice husk flour/natural rubber composites. *Advances in Materials Science and Engineering*, 2018.
- Suethao, S., Phongphanphanee, S., Wong-Ekkabut, J., & Smitthipong, W. (2021). The relationship between the morphology and elasticity of natural rubber foam based on the concentration of the chemical blowing agent. *Polymers*, 13(7), 1091.
- Sukkaneewat, B., & Utara, S. (2022). Ultrasonic-assisted Dunlop method for natural rubber latex foam production: Effects of irradiation time on morphology and physico-mechanical properties of the foam. *Ultrasonics Sonochemistry*, 82, 105873. doi:<https://doi.org/10.1016/j.ultsonch.2021.105873>.
- Suksup, R., Sun, Y., Sukatta, U., & Smitthipong, W. (2019). Foam rubber from centrifuged and creamed latex. *Journal of Polymer Engineering*, 39(4), 336-342. doi:[doi:10.1515/polyeng-2018-0219](https://doi.org/10.1515/polyeng-2018-0219).
- Surip, S., Khalil, H. A., Wan Othman, W., & Jawaid, M. (2013). Bamboo Based Biocomposites Material, Design and Applications. In (pp. 489-517).
- Surya, I., Kudori, S. N. I., & Ismail, H. (2019). Effect of Partial Replacement of Kenaf by Empty Fruit Bunch (EFB) on the Properties of Natural Rubber Latex Foam (NRLF). *Bioresources*, 14, 9375-9391.

- Syahrin, S., Zunaida, Z., Hakimah, O., & Nuraqmar, S. (2020). *Effect of blowing agent on compression and morphological properties of natural rubber latex foam*. Paper presented at the AIP Conference Proceedings.
- Tang, J., & Resurreccion Jr, F. (2009). Electromagnetic basis of microwave heating. In *Development of packaging and products for use in microwave ovens* (pp. 3-38e): Elsevier.
- Tomyangkul, S., Pongmuksuwan, P., Harnnarongchai, W., & Chaochanchaikul, K. (2016). Enhancing sound absorption properties of open-cell natural rubber foams with treated bagasse and oil palm fibers. *Journal of Reinforced Plastics and Composites*, 35(8), 688-697.
- Torres-Huerta, A., Domínguez-Crespo, M., Palma-Ramírez, D., Flores-Vela, A., Castellanos-Alvarez, E., & Del Angel-López, D. (2019). Preparation and degradation study of HDPE/PLA polymer blends for packaging applications. *Revista Mexicana de Ingeniería Química*, 18(1), 251-271.
- Trongsatitkul, T., & Chaiwong, S. (2017). In situ fibre-reinforced composite films of poly (lactic acid)/low-density polyethylene blends: effects of composition on morphology, transport and mechanical properties. *Polymer International*, 66(11), 1456-1462.
- Tsuchii, A., Suzuki, T., & Takeda, K. (1985). Microbial degradation of natural rubber vulcanizates. *Applied and Environmental Microbiology*, 50(4), 965-970.
- Vroman, I., & Tighzert, L. (2009). Biodegradable polymers. *Materials*, 2(2), 307-344.
- VURSAVUŞ, K. K., & Özgüven, F. (2004). Determining the effects of vibration parameters and packaging method on mechanical damage in golden delicious apples. *Turkish Journal of Agriculture and Forestry*, 28(5), 311-320.
- Yuan, J., Zhu, Y., Wang, J., Liu, Z., Wu, J., Zhang, T., Qiu, F. (2021). Agricultural bamboo leaf waste as carbon precursor for the preparation of Cu-Al/biomass fiber adsorption and its application in the removal of ammonia nitrogen pollutants from domestic wastewater. *Journal of Wood Chemistry and Technology*, 41(4), 137-149. doi:10.1080/02773813.2021.1914110.
- Zhang, N., & Cao, H. (2020). Enhancement of the antibacterial activity of natural rubber latex foam by blending it with chitin. *Materials*, 13(5), 1039.

Zhuang, J., Li, M., Pu, Y., Ragauskas, A. J., & Yoo, C. G. (2020). Observation of potential contaminants in processed biomass using fourier transform infrared spectroscopy. *Applied Sciences*, 10(12), 4345.



APPENDIX
PUBLICATIONS



List of Publications

Parts of this conferences work were published and presented in the following journal;

Jitkokkruad, K., Jarukumjorn, K., Chaiwong, S., and Trongsatitkul, T. (2021). Effect of foaming time and speed on morphology and mechanical properties of natural rubber latex foam vulcanized by microwave heating. In Proceedings of the SUT International Virtual Conference on Science and Technology 2021 (IVCST 2021), Nakhon-Ratchasima, Thailand. 245-251.

Jitkokkruad, K., Jarukumjorn, K., Raksakulpiwat, C., Chaiwong, S., Rattanakaran, J., and Trongsatitkul, T. (2023). Effects of bamboo leaf fiber content on cushion performance and biodegradability of natural rubber latex foam composites. *Polymers*, 15(3), 654.

Chaiwong, S., Saengrayap, R., Rattanakaran, J., Chaithanarueang, A., Arwatchananukul, S., Aunsri, N., Tontiwattanakul K., Jitkokkruad, K., Kitazawa, H., and Trongsatitkul, T. (2022). Natural rubber latex cushioning packaging to reduce vibration damage in guava during simulated transportation. *Postharvest Biol. Technol.* 199: 112273.

EAT0044

Effect of Foaming Time and Speed on Morphology and Mechanical Properties of Natural Rubber Latex Foam Vulcanized by Microwave Heating

K Jitkokkrud^{1,2}, K Jarukumjorn^{1,2,3}, S Chaiwong⁴, and T Trongsatitkul^{1,2,3,*}

¹School of Polymer Engineering, Institute of Engineering, Suranaree University of Technology, Nakhon Ratchasima, 30000, Thailand

²Center of Excellence on Petrochemical and Materials Technology, Chulalongkorn University, Bangkok, 10330, Thailand

³Research Center for Biocomposite Materials for Medical Industry and Agricultural and Food Industry, Suranaree University of Technology, Nakhon Ratchasima, 30000, Thailand

⁴School of Agro-Industry, Mae Fah Luang University, Chiang Rai, 57100, Thailand

* Corresponding Author: tatiya@sut.ac.th

Abstract. Natural rubber latex foam (NRLF) was prepared using Dunlop process and vulcanized by microwave heating using optimized condition with irradiation power and time of 600 W and 6 min, respectively. Effects of foaming time (2, 4, 6, 8, and 10 min) and speed (650, 950, 1250, 1550, and 1850 rpm) on cell structure, density, and compressive properties of NRLF were investigated. Cell size of NRLF decreased whereas number of cells increased with increasing foaming time and speed. The increasing foaming time and speed led to a reduction of bulk density of NRLF but an improvement of compressive strength at 50% strain.

Keywords: Natural rubber latex foam, Dunlop process, Microwave heating, Morphology

1. Introduction

Natural rubber latex foam (NRLF) product has been used in several applications such as mattresses, pillow, and cushion [1-4]. Unique properties of the natural rubber foam are lightweight, good thermal insulation, good sound absorption, excellent elasticity, and tunable cushioning performance [4].

Generally, two main methods used in the production of NRLF are Dunlop and Talalay processes. Both methods hold the basic common steps which are firstly air incorporation and secondly vulcanization. Dunlop process is widely used to produce NRLF because of its simpler processing and lower production cost as compared to Talalay process [2]. NRLF properties depend on cell characteristics controlled by many parameters such as kind of blowing agent, content of chemicals in NRL compound and foaming temperature [5].

Microwave heating technique is one of heating methods used in rubber processing, including drying and de-vulcanization steps. However, there is a limited number reported the use of this technique in vulcanizing process of NRLF. Microwave heating is considered to be a green method as it consumes

significantly lower energy, time, and in some case, chemicals used, as compared to a conventional heating. Microwave irradiation heating mechanism greatly differs from conventional heating that it generates heat from inside to outside [6]. The prominent points of this technique for vulcanization of NRLF are faster heat rate, lower processing time and energy, and better uniformity of generated heat over the conventional heating technique [7].

The use of microwave assisted vulcanization is limited and has not been widely studied. The change in heating mechanism when use microwave irradiation may affect the delicate balance of the latex foam before it fully set. Systematic study is needed in order to understand the relationships of processing parameters in each step and the foam structure as well as its properties. The objectives of this work were, firstly to determine the microwave irradiation processing window and secondly to investigate the effects of foaming time (2, 4, 6, 8, and 10 min at foaming speed of 1250 rpm) and foaming speed (650, 950, 1250, 1550, and 1850 rpm at foaming time of 8 min) on cell structure and mechanical properties. This study was expected to provide the improved, environmentally friendly process for fabricating NRLF by combining Dunlop process and microwave heating technique.

2. Experimental

2.1. Materials

Chemicals and their contents used in the formulation of natural rubber latex foam compound are listed in table 1. Natural rubber latex (60% high ammonium latex) and chemicals including potassium oleate (K-oleate; foaming agent), sulfur (vulcanizing agent), zinc diethylthiocarbonate (ZDEC; primary accelerator), zinc 2-mercaptobenzothiazone (ZMBT; secondary accelerator), Wingstay L (antioxidant), zinc oxide (ZnO; activator), sodium silicofluoride (SSF; primary gelling agent), and diphenyl guanidine (DPG; secondary gelling agent) were supplied by Chemical and Materials Co., Ltd.

Table 1. Formulation of NRLF compound.

Ingredients	Content (phr)	Ingredients	Content (phr)	Ingredients	Content (phr)
60% HA Latex	100	50% ZDEC	2	50% ZnO	5
10% K-oleate	0.15	50% ZDMT	2	33% DPG	1.4
50% Sulfur	2	50% Wingstay L	2	12.5% SSF	0.25

2.2. Preparation of natural rubber latex foam

The preparation of NRLF can be divided into 5 steps (reduction ammonia, foaming, gelling, vulcanizing, and drying process). Natural rubber latex (60% high ammonium latex) was stirred by a mechanical stirrer at speed of 300 rpm for 30 min to reduce amount of ammonia in the latex. Chemical ingredients for foaming process i.e. K-oleate, ZDEC, ZMBT, and Wingstay L were incorporated into the reduced ammonia latex. In this foaming step, foaming times were varied from 2, 4, 6, 8, and 10 min at a constant stirrer speed of 1250 rpm. Then ZnO, DPG, and SSF were added into the NRL compound at speed of 700 rpm for 1 min. After that, NRL compound was gelled by SSF. The gelled foam was poured into a silicone mold (5.5 cm x 5.5 cm x 2.5 cm) at room temperature for 1 h. The foam was vulcanized using a commercial microwave oven (Samsung, MS23K3513AW) at constant power of 600 W and time of 6 min. Finally, the NRLF was washed and dried in a hot air oven at 70°C for 24 h.

Similar process was used to study the effects of stirrer speed during the foaming step. The speed was varied from 650, 950, 1250, 1550, and 1850 rpm at a constant foaming time of 8 min. Other parameters in other steps were kept constant.

2.3. Characterizations

2.3.1. Bulk density

Bulk foam density was carried out by measuring the weight and volume the samples. The bulk density of natural rubber latex foam can be determined using the following Equation (1)

$$\text{Bulk density} = \frac{M}{V} \quad (1)$$

Where; M is mass of specimen (kg)
V is volume of specimen (m³)

2.3.2. Morphology

Cell morphology of NRLF was observed using a scanning electron microscope (SEM, JEOL/JSM6010LV) with an accelerating voltage of 10 kV. The cross-sectional surfaces of the samples were prepared using a sharp blade and then sputtered coated with gold for 3 min.

2.3.3. Compressive strength

Compressive strength of NRLF was tested according to ASTM D3574 using a universal testing machine (UTM, INSTRON/5565) with a load cell of 5 kN. The foam specimen was compressed to 50% of each foam original thickness at a crosshead speed of 50 mm/min. At least three specimens were tested and the averaged values were reported.

3. Results and discussion

In this work, we used Dunlop process together with microwave-assisted curing for NRLF fabrication. We first optimized microwave irradiation conditions (power and time). The foaming time and speed using the optimal microwave irradiation condition were investigated.

Microwave irradiation optimization for curing NRLF was performed using different power (450, 600, and 800 W) and time (4, 6, and 8 min). The curing results and their physical appearance are shown in table 2. It can be seen that too low in heating energy (low power or time) could lead to unsuccessful curing. Overheating also caused browning at the core of the sample, indicating the degradation of the rubber foam samples. The core of the rubber foam became brown first was well agreed with the heat characteristic of microwave irradiation that heated from inside out. This study provided the processing window for curing of the NRLF. The results indicated that the optimum microwave curing condition of NRLF was at power of 600 W and time of 6 min where the foams with good foam structure and no degradation were obtained.

This work also aimed to investigate the two important parameters in Dunlop process for making rubber foam from rubber latex using microwave assisted vulcanization. The two parameters were foaming time and stirring speed. In the foaming step, air was whipped into the latex creating air-in-liquid colloidal dispersion. The stability of the colloid depended on various factors and crucial for controlling the foam structure in the final product. The volume of the air incorporated into the latex was expected to affect the foam structure. Longer foaming time may increase the air volume in the foam but can also destabilize the colloid and, as a consequence, alters the final foam product's properties. The results reported here discussed the effects of foaming time and speed on foaming density, structure, and compressive strength.

3.1. Effect of foaming time

3.1.1. Bulk density

The effect of foaming time on the bulk density of NRLF is shown in figure 1(a). It can be seen that the bulk density decreased as the foaming time increased. This was due to the longer whipping time (foaming time) allowed greater amount of air to be incorporated into the compound [8]. As a result, the

foams prepared using longer foaming time expanded to a greater degree/volume while the weight of the samples were relatively constant.

Table 2. Physical appearance of NRLF at various processing conditions.

Power (W)	Time (min)		
	4	6	8
450	N/A	N/A	Partially cured 
600	Partially cured 	Fully cured 	Fully cured 
		Cross section 	Cross section 
800	Fully cured 	Fully cured 	Fully cured/degrade 
	Cross section 	Cross section 	Cross section 

3.1.2. Morphology

SEM micrographs of a cross-sectional surface of NRLF at various foaming times are displayed in figure 2. From these images, it could be seen that as the foaming time increased, the cell size of NRLF decreased, at the same time the number of cells increased as a function foaming time. These images gave the insight detail of the foam structure and how they changed as the foaming time increased. Longer foaming time allowed more air to be incorporated with the rubber latex and the mechanical mixing action also generated greater number of foam cell. It could be hypothesized that the large foam cells were initially formed and then disrupted into smaller ones as the mixing continued. The smaller foam cell also resulted in shorter cell wall which was less likely to collapse. On the other hand, the greater number of cells meant that the cell wall may become thinner and less stable. When the cell foam become smaller but being greater in number, the final properties of the foam depended on the balance of these two characters.

3.1.3. Compressive strength

Compressive strength at 50% compressive stain of NRLF prepared with different foaming times is listed in table 3. Compressive strength of NRLF decreased with increasing foaming time. This was likely due to the change in the structure of the foams and their density. As previously shown, both higher volume of air, greater number of foam cell can contribute to the lower of the compressive strength. This finding

was also recognized by others. Samsudin et al. reported that there was relationship between density and compressive properties of NRF. Higher density resulted in increased compressive strength of NRF [9].

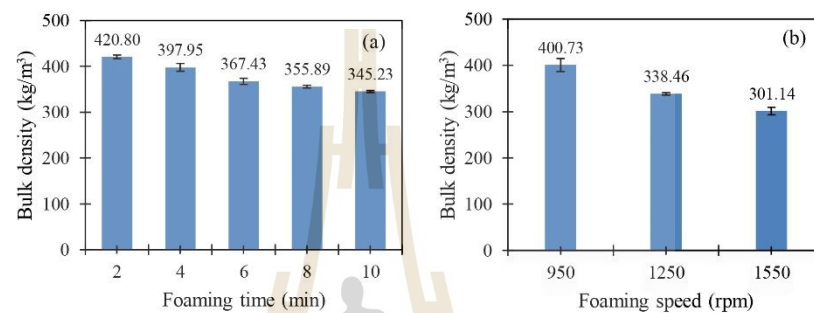


Figure 1. Bulk density of NRLF prepared using different (a) foaming time and (b) foaming speed.

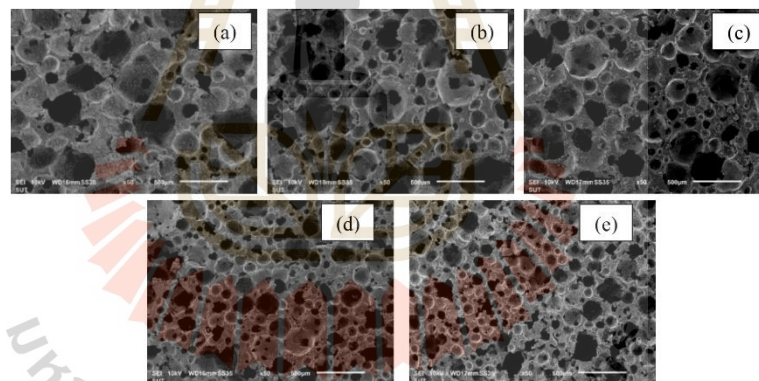


Figure 2. SEM images of NRLF at foaming speed of 1250 rpm and various foaming times (a) 2 min, (b) 4 min, (c) 6 min, (d) 8 min, and (e) 10 min.

Table 3. Compressive strength at 50% compressive strain of NRLF.

Foaming time (min) @1250 rpm	Compressive strength (kPa)	Foaming speed (rpm) @ 8 min	Compressive strength (kPa)
2	263.30 ± 9.60	650	-
4	198.66 ± 9.73	950	251.16 ± 7.62
6	171.76 ± 9.89	1250	137.94 ± 3.17
8	156.01 ± 4.12	1550	117.03 ± 5.08
10	154.69 ± 1.67	1850	-

3.2. Effect of foaming speed

3.2.1. Bulk density

In Dunlop process, stirring speed during the foaming process is one of the most important parameters to develop character of a cell foam of NRLF. Effect of stirring speed in foaming step on bulk density is reported in figure 1(b). Five different foaming speeds were used in the NRLF preparation (650-1850 rpm). However, only 3 speeds were successfully used in the NRLF production. Too low and too high of the foaming speed created unstable foam bubbles which broke down before the foam can be settled as shown in figure 3. Too low of the foaming speed of 650 rpm, the air was not enough to create foam cells throughout the sample. The top surface of the foam was dense and burst during vulcanization as moisture vapour in the foam trying to escape from the inside. Foam sample at foaming speed 1850 rpm after adding SSF in gelling process was presented in figure 3(b). Too high of the foaming speed probably destabilized the latex rubber and gooey-rubber paste was obtained. We could establish processing window for the foaming speed for our system from this results.

In figure 1(b), it can be seen that higher speed during foaming step caused the lower in the bulk density of NRLF. The lower in the bulk density could be due to that the higher speed was more efficient in term of aeration of the latex rubber. The lower bulk density indicated that greater volume of the air was incorporated into the latex at the higher foaming speed but the same amount of time.

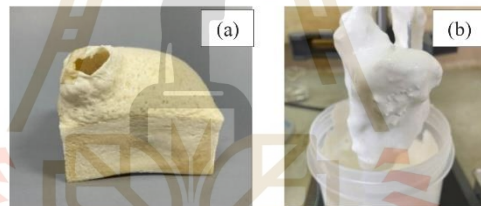


Figure 3. Physical appearance of NRLF during foam production at (a) 650 rpm and (b) 1850 rpm.

3.2.2. Morphology

SEM results in figure 4 revealed that cell size of the foams tended to decrease as the foaming speed increased. Again higher number of foam cell occurred simultaneously with the lower in cell size. It should be noted that at 1550 rpm foaming speed, the cell structure seemed to open with the presence of smaller cells inside the cell wall itself. This structure could lead to a lowering in the mechanical properties of this NRLF.

3.2.3. Compressive strength

Compressive strength of NRLFs prepared using different foaming speeds of 950, 1250, and 1550 rpm are presented in table 3. At low foaming speed 950 rpm, the foam possessed the highest compressive strength at 50% compressive strain. As the foaming speeds increased to 1250 and 1550 rpm, the compressive strength of the foams decreased, respectively. The results may be caused by the lowered bulk density as well as the changes in the foam structure as described earlier [9].

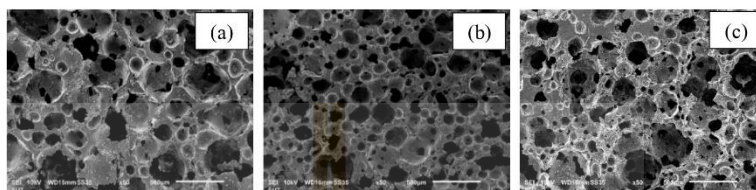


Figure 4. SEM micrographs of NRLF at foaming time of 8 min and various foaming speed (a) 950 rpm, (b) 1250 rpm, and (c) 1550 rpm.

4. Conclusions

This study reported the result of the investigation of two important parameters i.e. time and speed used in foaming step in Dunlop process. The relationship between the cell characteristics, bulk density, and compressive strength of NRLF was established. The final foam product properties and performance strongly depended on the foam structure, generated during the foaming step. The compressive strength depended on both bulk density and cell morphology. Understanding the parameters affecting the foam structure and properties could lead to the better control and design the foam product to give desired properties suitable for specific applications. Microwave heating is one of the techniques that should be adopted in the near future as it could save significant amount of time and energy during vulcanization process.

Acknowledgments

The authors greatly acknowledge the financial supports from Center of Excellence on Petrochemical and Materials Technology (PETROMAT) and Suranaree University of Technology for equipment, facilities, and technical staff supports.

References

- [1] Salmazo L O, Lopez-Gil A, Ariff Z M, Job A E, and Rodriguez-Perez M A 2016 *Ind. Crops. Prod.* **89** 339-349
- [2] Sirikulchaikij S, Kokoo R, and Khanghamano M 2020 *Mater. Lett.* **260** 126916
- [3] Oliveira-Salmazo L, Lopez-Gil A, Silva-Bellucci F, Job A E, and Rodriguez-Perez M A 2016, *Ind. Crops. Prod.* **80** 26-35
- [4] Suksup R, Sun Y, Sukatta U, and Smithipong W 2019 *J. Polym. Eng.* **39(4)** 336-342
- [5] Hammarongchai W, and Chaochanchaikul K 2015 *Appl. Mech. Mater.* **804** 25-29
- [6] Ariff Z M, Afolabi L O, Salmazo L O, and Rodriguez-Perez M A 2020 *J. Mater. Res. Technol.* **9(5)** 9929-9940
- [7] Ahmad Zauzi N S, Ariff Z M, and Khimi S R 2019 *Int. Conf. on Advances in Materials, Mineral and Environment (Penang)* **17** (Amsterdam: Elsevier) p 1001-1007
- [8] Hui Mei E L, and Singh M 2010 *Malaysian Rubber Development Technology* **10** 23-26
- [9] Samsudin M S F, Ariff Z M, and Ariffin A 2019 *Int. Conf. on Advances in Materials, Mineral and Environment (Penang)* **17** (Amsterdam: Elsevier) p 1133-1142

Article

Effects of Bamboo Leaf Fiber Content on Cushion Performance and Biodegradability of Natural Rubber Latex Foam Composites

Keavalin Jitkokkrud^{1,2}, Kasama Jarukumjorn^{1,2,3}, Chaiwat Raksakulpiwat^{1,2,3}, Saowapa Chaiwong^{4,5,*}, Jutarat Rattanakaran^{4,5} and Tatiya Trongsatitkul^{1,2,3,4}

¹ School of Polymer Engineering, Institute of Engineering, Suranaree University of Technology, Nakhon Ratchasima 30000, Thailand

² Center of Excellence on Petrochemical and Materials Technology, Chulalongkorn University, Bangkok 10330, Thailand

³ Research Center for Biocomposite Materials for Medical Industry and Agricultural and Food Industry, Suranaree University of Technology, Nakhon Ratchasima 30000, Thailand

⁴ School of Agro-Industry, Mae Fah Luang University, Chiang Rai 57100, Thailand

⁵ Integrated AgriTech Ecosystem Research Group, Mae Fah Luang University, Chiang Rai 57100, Thailand

* Correspondence: saowapa@mfu.ac.th (S.C.); tatiya@sut.ac.th (T.T.);

Tel.: +66-5391-6766 (S.C.); +66-044-224685 (T.T.)



Citation: Jitkokkrud, K.; Jarukumjorn, K.; Raksakulpiwat, C.; Chaiwong, S.; Rattanakaran, J.; Trongsatitkul, T. Effects of Bamboo Leaf Fiber Content on Cushion Performance and Biodegradability of Natural Rubber Latex Foam Composites. *Polymers* **2023**, *15*, 654. <https://doi.org/10.3390/polym15030654>

Academic Editor: Amitesh Maiti

Received: 31 December 2022

Revised: 20 January 2023

Accepted: 25 January 2023

Published: 27 January 2023



Copyright: © 2023 by the authors. Licensee MDPI, Basel, Switzerland. This article is an open access article distributed under the terms and conditions of the Creative Commons Attribution (CC BY) license (<https://creativecommons.org/licenses/by/4.0/>).

Abstract: Bamboo leaf fiber (BLF) was incorporated into an eco-friendly foam cushion made from natural rubber latex (NRL) to enhance the biodegradation rate. The objective of this work was to investigate the effects of BLF content on the foam structure, mechanical properties, cushion performance, and biodegradability. The NRL foam cushion nets with and without BLF were prepared using the Dunlop method along with microwave-assisted vulcanization. BLF (90–106 µm in length) at various loadings (0.00, 2.50, 5.00, 7.50, and 10.00 phr) were introduced to the latex compounds before gelling and vulcanizing steps. Scanning electron microscopy (SEM) showed that the BLF in a NRL foam caused an increase in cell size and a decrease in the number of cells. The changes in the cell structure and number of cells resulted in increases in the bulk density, hardness, compression set, compressive strength, and cushion coefficient. A soil burial test of 24 weeks revealed faster weight loss of 1.8 times when the BLF content was 10.00 phr as compared to the NRL foam without BLF. The findings of this work suggest the possibility of developing an eco-friendly cushion with a faster degradation rate while maintaining cushion performance, which could be a better alternative for sustainable packaging in the future.

Keywords: natural rubber latex foam; bamboo leaf fiber; foam composite; foam net; Dunlop process; microwave-assisted vulcanization; cushion coefficient; biodegradability

1. Introduction

Plastic waste is one of the most problematic among various materials. The beneficial qualities such as its light weight, durability, inertness, ease of the process, and versatility of plastics have served humans well for several decades. On the other hand, these qualities also lead to an enormous amount of plastic waste accumulation due to the high consumption volume and poor decomposability/degradability. The UN environment program (UNEP) anticipates that plastic will increase by 1100 million tons in 2050 from 400 million tons in the present year. Because most plastics are fossil-based materials, the widespread use of these materials adds other concerns to environmental issues, such as the exhaustion of natural resources and global warming [1]. Several key aspects must be considered to effectively address these problems, including product design and material selection to enhance recyclability [2], strict regulation enforcement [3], and proper education of the public [4] are examples of how to remedy the situation sustainably.

Because plastics are versatile materials, they are used in several industries, such as automotive, construction, home appliances, electronics, and packaging [5]. The proper management of plastic product waste requires an understanding of their natures, including the type of materials used, how they are made, how they are used, service life, and post-consumer disposal. Among all plastic products, approximately 36% is used in packaging. Single-use items such as food and drink containers are made up of the most share of waste. Although rigid plastic packaging, such as bottles, boxes, trays, and cups, has been successfully recycled [6], 85% of plastic packaging waste is discarded as uncontrolled waste or in landfills [7]. These problematic wastes are mainly flexible packaging, such as plastic films and bags, as well as cushioning materials. These types of packaging are difficult to collect as they are very thin or/and low in bulk density. They are also difficult to separate (multi-layer film) and once contaminated, they are also difficult to clean. Recycling these plastics waste is often logistically and economically unfeasible. For example, cushion foam nets for fresh produce protect the goods during transportation. Once the produce arrives customers, the cushion is discarded even though it could have been reused or recycled. The cost to retrieve, collect, and transport back to the packaging location is cumbersome and requires combined efforts from several parties.

Plastics used to fabricate cushion foam nets for fresh produce are mainly made from expanded polystyrene foam (EPS) and expanded polyethylene foam (EPE). With the foam structure, they are exceptionally light and able to absorb mechanical shock, vibration, and impact forces that occur during transportation. Fresh fruit covered with proper cushion materials are therefore protected from mechanical damage. Together with good cold-chain management, the fruit's appearance, quality, and nutrients can be preserved [8]. Cushioning is thus a crucial part of a packaging system. However, to reduce the negative impact of the synthetic foams [9,10], many countries have placed restrictions on their use. This includes laws imposed by local and state governments on single-use packaging at the end of its life cycle. Consequently, an alternative cushion that is eco-friendly and possesses a good cushion performance is in great demand.

To substitute the current nondegradable polystyrene and polyethylene packaging materials, researchers have focused on using biodegradable polymers, such as polylactic acid (PLA), poly(lactic-co-glycolic acid) (PLGA), polybutylene adipate terephthalate, (PBAT), and poly(3-hydroxybutyrate-co-3-hydroxyvalerate) (PHBV) [11]. However, these polymers are substantially more expensive compared to conventional petroleum-based polymers [12], such as high-density polyethylene (HDPE), low-density polyethylene (LDPE), and polypropylene (PP), etc. The lack of processability and, even less so, their cushioning performance information lead to the unsuccessful use of these biodegradable polymers. Blends of biodegradable polymers and conventional polymers, such as HDPE/PLA [13], PLA/PP [14] and PLA/LDPE [15], etc., have also been investigated. Their practicality and implementation, as well as environmental impacts, are yet to be evaluated.

Another interesting alternative for cushioning materials is natural rubber (NR). NR is harvested from the rubber tree (*Hevea brasiliensis*) in latex [16,17]. NR is, therefore, bio-based material that comes from a renewable resource and is inherently biodegradable [18]. In fact, a NR product may undergo degradation via one or a combination of several degradation modes, including mechanical degradation, oxidation, photodegradation, thermal degradation, and/or biodegradation [19]. Previous works have been done to prevent the degradation of a NR product to extend its service life. Now degradation of NR is appreciatively viewed as a solution for environmental pollution. Foam products of NR have been used as mattresses, pillows [16,20], cushions [17], padding foam [21], etc. The NRL foam possesses unique properties such as lightweight, good thermal insulation, good sound absorption, excellent elasticity, good cushioning performance, and biodegradability [20,22,23]. Our research team is interested in using NRL foam as cushion material for fresh produce.

Generally, the NRL foam can be fabricated using a Dunlop or Talalay process. The Dunlop process has been widely used as it is a simpler process with a lower production

cost and is more energy efficient than those of the Talalay process [24]. The Dunlop process steps include incorporation of the air and some chemicals into the latex via a mechanical method to create and stabilize the foam structure before vulcanization. Heating in the vulcanization step may use either a conventional hot air oven and a microwave oven [25]. The recent trend of replacing conventional heating with microwave irradiation is due to the advantages of the later process. For the microwave heating, the heat generated in the product results from the conversion of electromagnetic energy to thermal energy [26]. Because of the direct interaction between the microwave and the heated article, energy transfer occurs more efficiently. Thus, microwave heating provides a significantly faster heating rate, resulting in shorter vulcanization time, higher production rate, and less time and energy consumption compared to conventional heating [25,27]. We have successfully optimized the microwave irradiation condition for making the NRL foam [28]. The study showed the promising and important finding that the use of microwave heating could reduce vulcanization time by 15-fold (from 90 min [24] to 6 min [28]). Using microwave irradiation for NRL foam fabrication is, therefore, fundamentally making the foam product more eco-friendly.

To further improve the eco-friendly attributes of NRL foam, enhancing its biodegradation rate is considered. Even though NR is fully degraded, the degradation time of rubber products could be up to several decades. The relatively long degradation time may lead to environmental pollution as landfill sites become too limited [19,29]. A biodegradable filler may be added to the NRL to reduce such issues. Natural fillers, such as rice husk [30,31], fiber of banana, coir, bagasse [32], oil palm fiber [33], sisal [34], bamboo [35], and kenaf [36,37] have been added to polymer matrixes. Several research groups have reported that the addition of natural fibers contributed to the enhancement of biodegradability for the polymer products [30].

Bamboo is one of the most common plants available in Asian countries. It is one of the fastest-growing plants, is widely accessible, considered a sustainable resource [38,39], and is strong and lightweight [40]. Bamboo leaf is the by-product of growing bamboo trees. It is high in fiber, protein, and silica content and can be used for bamboo tea, bamboo beer, livestock feed, medicinal aids, aromatherapy, and essential oils [41]. Research and development have found bamboo leaves to be a good carbon source. They can be made into aerogel, silica nanoparticles, adsorbents, and composites. Adding BLF into NRL foam should positively affect the environment, society, and the economy [42]. However, limited information is available regarding how the BLF affects the cushion performance of NRL foam, especially for fresh produce packaging applications.

Therefore, the aim of this study is to develop eco-friendly cushioning packaging from NRL foam composites. The main focus is to investigate the effect of BLF content on mechanical properties, cushion performance, and biodegradability. The NRL foam composites containing different BLF contents (0.00, 2.50, 5.00, 7.50, and 10.00 phr) were prepared into a similar shape to the commercial foam net cushion using the Dunlop process and vulcanization via microwave heating. The NRL foam composites were compared to a commercial EPE cushion net in terms of foam density, hardness, morphology, cushion coefficient (C), and biodegradability. Additionally, the composites' mold shrinkage, compression set, number of cells per unit volume, and average cell size were studied. A soil burial test of the samples was carried out for a duration of 24 weeks (6 months). The degradation of the NRL foam composites were analyzed via weight loss, Fourier transform infrared (FTIR) analysis, foam appearance, morphology, and compressive properties.

2. Materials and Methods

Chemical ingredients and their contents used in the formulation of the NRL foam composites are listed in Table 1. The ingredients were supplied by Chemical and Materials Co., Ltd., Bangkok, Thailand. Dried bamboo leaf was purchased from local farmers in Nakhon Ratchasima, Thailand. The BLF preparation is described below.

Table 1. Formulation of NRL foam composite at various BLF loadings.

Ingredients	Content (phr ¹)	Functions
60% High ammonia natural rubber latex (HA Latex)	100.00	Matrix
10% Potassium oleate (K-oleate)	4.50	Foaming agent
50% Sulfur	2.00	Vulcanizing agent
50% Zinc diethylthiocarbonate (ZDEC)	2.00	1st accelerator
50% Zinc 2-mercaptobenzothiazone (ZDMT)	2.00	2nd accelerator
50% Wingstay L	2.00	Antioxidant
50% Zinc oxide (ZnO)	5.00	Activator
12.5% Sodium silicofluoride (SSF)	1.00	1st gelling agent
33% Diphenyl guanidine (DPG)	1.40	2nd gelling agent
Bamboo leaf fiber (90 ≤ x ≤ 106 μm)	0.00, 2.50, 5.00, 7.50, 10.00	Natural fiber

¹ Parts per hundred rubber.

2.1. Preparation of Bamboo Leaf Fiber

Dried bamboo leaf was ground in a fine wood crusher machine (WSC-20, CT, Samut Prakan, Thailand) for 1 h. The ground BLF was then sieved using a vibratory sieve shaker (Analysette 3 Pro, Fritsch, Idar-Oberstein, Germany). Fibers with lengths in the range of 90–106 μm were obtained. The appearance of the BLF fiber is shown in Figure 1a. The BLF appeared as greenish particles, and SEM micrograph in Figure 1b reveals the irregular shape of the BLF particles. To use the BLF in the formular, the prepared fibers were soaked in deionized (DI) water with a 1:1 ratio of fiber to water.

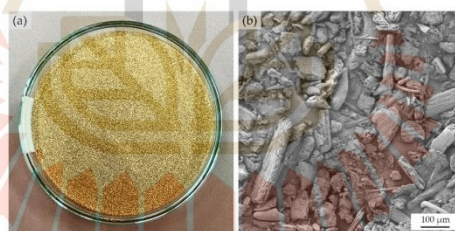


Figure 1. The appearance and shape of bamboo leaf fibers: (a) photograph; (b) SEM micrograph at a 100× magnification.

2.2. Preparation of Rapid Silicone Mold

In this work, 3D printing was used to prepare a master with the desired shape of a cushion net, which was then used for making a negative cavity silicone mold. 3D printing has many benefits. The technique gives flexibility in designing molds and products. The process is fast and cost-effective compared to that of a conventional metal mold. The resulting silicone mold is also lightweight with good heat resistance and, most importantly, is suitable to be used in a microwave oven. First, the SolidWorks program (Dassault Systèmes, Vélizy-Villacoublay, France) was used to create a 3D model of the cushion net (Figure 2a). Then a CAD file was generated and converted to G-code using the PrusaSlicer program (Prusa Research, Prague, Czech Republic) (Figure 2b) before printing (Figure 2c). PLA filament (Prusament Prusa Galaxy Black, Prusa Research, Prague, Czech Republic) was used to print the inverted mold via a 3D printer (Original Prusa i3 MK3S, Prusa Research, Prague, Czech Republic). Silicone rubber and hardener, supplied by Infinite Crafts Co., Ltd., Bangkok, Thailand were mixed before pouring into the inverted mold. The silicone mold was left at room temperature until fully set. The working mold was

obtained after the inverted mold was removed. The inverted and silicone molds are shown in Figure 2d and Figure 2e, respectively.

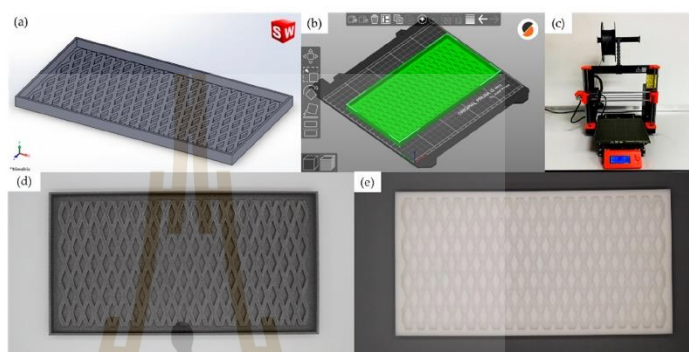


Figure 2. Schematic for fabricating a rapid silicone mold using 3D printing: (a) 3D model; (b) converting to G-code; (c) 3D printing; (d) inverted mold; and (e) silicone mold.

2.3. Fabrication of NRL Foam Composites via the Dunlop Process Together with Microwave-Assisted Vulcanization Technique

The NRL foam composites were prepared using the Dunlop process to generate a foam structure before curing via microwave irradiation. The process used here is similar to that reported previously [28] with the additional step of adding BLF. In short, the NRL was first stirred using a mechanical stirrer (Eurostar 20 digital, IKA Works, Wilmington, NC, USA). The stirring speed of the first step was 300 rpm for 30 min to reduce the ammonia content in the latex. Secondly, chemical ingredients required for the foaming process, i.e., K-oleate, Sulfur, ZDEC, ZMBT, and Wingstay L were incorporated, and the latex mixture was whipped at a speed of 1250 rpm for 6 min. Thirdly, a soaked bamboo leaf fiber was added to the whipped latex mixture at a speed of 500 rpm for 2 min. The BLF to DI water ratio was 1:1. Finally, ZnO, DPC, and SSF were added to the whipped latex for foam gelation at a speed of 700 rpm for 1 min. The gelled foam was poured into a silicone mold and set at room temperature for 1 h. The foams were vulcanized using a commercially available domestic microwave oven (MS23K3513AW/TC, Samsung, Kuala Lumpur, Malaysia). The optimum vulcanization condition was used, i.e., microwave irradiation power and time of 600 watts and 6 min, respectively [28]. Finally, the NRL foam product was washed with water and dried in a hot air oven at 70 °C for 4 h.

2.4. Characterization

2.4.1. Bulk Density

The bulk density of NRL foam and its composites were calculated using the following Equation (1) [20]:

$$\text{Bulk density} = \frac{M}{V} \quad (1)$$

where: M is the mass of specimen (kg), V is the volume of the specimen (m^3).

2.4.2. Hardness

The hardness values of the NRL foam composites were determined using a durometer hardness (Durometer LX-OO Shore OO, X.F, Graigar, Guangdong, China) according to ASTM D2240 [43]. The hardness of the cushion foam net was measured on the sample surface. Five measurements on five different locations on each specimen were measured. The values reported were averaged from at least five replicates.

2.4.3. Mold Shrinkage

The shrinkage of the NRL foam composites can be determined using the following Equation (2). The shrinkage is compared in three dimensions (width, length, and height). The reported values were averaged from at least five replicates.

$$\text{Shrinkage}(\%) = \frac{(X_0 - X_1)}{X_0} \times 100 \quad (2)$$

where X_0 are the dimensions of mold (mm), X_1 is the dimension of NRL foam composite after vulcanization (mm).

2.4.4. Morphology

The cellular morphology of the cushion foams was analyzed using a scanning electron microscope (SEM) (AURIGA, Zeiss, Germany). Surface and cross-section of the foam samples were investigated. A foam sample was prepared from a small piece using a sharp blade. The surface and cross-section were sputter-coated with gold at 5.7 nm (Leica EM ACE600, Vienna, Austria). The SEM micrographs were taken at an accelerating voltage of 3 kV and working distance of 6.7–9.8 mm.

ImageJ image analyzer software was used to determine the foam's cell size and cell count. For each cell, four lines were drawn across the cell, and the length of each line was measured. For each location or image, at least 100 cells were measured and recorded. Then, cell size distribution and average cell size were determined using a nonlinear curve fit (Gaussian) in the Origin program (OriginLab Corporation, Northampton, MA, USA). Additionally, the cell wall thickness of the cushion foams was measured using ImageJ software (NIH, Bethesda, MD, USA) and reported using average data from five locations of cell wall thickness.

The number of cells per unit volume (N) was evaluated by the averaged cell size data from ImageJ software and the foam density. Equation (3) was used to calculate the number of cells per unit volume of the NRL foam composite, as shown below [24]:

$$N = \left(\frac{6}{\pi d^3} \right) \left(\frac{\rho_{rubber}}{\rho_{foam}} - 1 \right) \quad (3)$$

where N is the number of cells per unit volume, d is the average cell diameter (cm), ρ_{rubber} is a density of the solid rubber (1.09 g/cm³), and ρ_{foam} is the density of the rubber foam (g/cm³) or the bulk density.

2.4.5. Compression Test

A compression test of the cushion foam nets was performed using a universal testing machine (UTM) (Instron 5565, Norwood, MA, USA). The test was carried out using the load cell of 1 kN at a crosshead speed of 12 mm/min. The NRL composite foam net was cut into a rectangular shape with the dimensions of (width × length × thickness) 100 mm × 100 mm × 3 mm. The compression test was adapted from the static compression method for packaging buffer material (GB/T 8168-2008) to determine the cushion performance of cushion materials [44]. The relationship between stress and strain was obtained. The raw data of the compressive stress–strain curve was used to calculate the cushion coefficient. Moreover, 50% compressive strength was reported in the mechanical properties of the biodegradation study. The reported results were the averaged values from testing at least five replicates.

2.4.6. Cushion Coefficient (C)

The cushion coefficient (C) is an ability of a cushion material to absorb the applied energy. The calculation was carried out using the data from the compression test mentioned earlier. The cushion coefficient equation is as follows [45]:

$$C = \frac{\sigma}{e} \quad (4)$$

where σ is the compressive stress (N/mm²), e is the energy absorption of the material (N·mm/mm³), which is estimated from the compressive stress–strain curve using Equation (5) [45]:

$$e = \int_0^{\epsilon} \sigma d\epsilon \quad (5)$$

where ϵ is the compressive strain (mm/mm).

2.4.7. Compression Set

Compression set measurements were performed as per ASTM D1055 [46]. A cylindrical specimen with a diameter of 29 mm and a height of 19 mm was prepared using the same processing condition as the NRL composite foam net. Using a compression set apparatus, the specimen was compressed to 50% of its original thickness. The specimen was then placed in a hot air oven at 70 °C for 22 h. Afterward, the specimen was removed from the oven, and the compression set apparatus was removed from the specimen before being left to cool at room temperature for 30 min. The final thickness of the specimen was measured within 10 min after the cooling step. The compression set was calculated according to Equation (6) [46]:

$$C_h = \frac{(t_0 - t_1)}{t_0} \times 100 \quad (6)$$

where C_h is the compression set, t_0 is the original thickness of the specimen (mm), t_1 is the thickness of the specimen after 30 min of removal from the compression set apparatus (mm).

2.4.8. Biodegradation Study

The soil burial method was used to investigate the effect of BLF content in NRL foam composites on their biodegradability. Square specimens with the size of 50 mm × 50 mm × 3 mm (width × length × thickness) of each NRL composite foam net sample were placed in a box containing planting soil at the dept of 12–15 cm. The 100 L plastic box (500 mm × 770 mm × 43 mm) used was covered with a plastic lid, and small holes of 5 mm in diameter were uniformly drilled on all sides of the box for ventilation (see Figure 3). The soil used was planting soil from Suranaree farm, Suranaree University of Technology, Nakhon Ratchasima, Thailand. The plastic boxes filled with soil were placed outdoors beside equipment building 4 (F4) at Suranaree University of Technology, Nakhon Ratchasima, Thailand. The soil's moisture content was maintained at 60–80% (water as needed). The commercial cushion EPE foam net (EPE-FN) was also buried in the soil with the same protocol and condition. The degradation study was carried out over a period of 24 weeks (May–October 2022). Every 4 weeks, five specimens of each sample were taken out from the soil and then washed with water and dried in a hot-air oven at 70 °C for 4 h. These specimens were tested for changes in the foam appearance, morphology, compression property (at 50% strain), and weight loss. The compression property and weight loss values were reported as averaged values calculated from at least three replicates. The weight loss formula [30] is given as Equation (7). An analytical balance with four digits (ML240, Mettler Toledo, Greifensee, Switzerland) was used for the weight loss determination.

$$\text{Weight loss (\%)} = \frac{(W_0 - W_1)}{W_0} \times 100 \quad (7)$$

where W_0 is the sample weight before the test (g) and W_1 is the sample weight after the test (g).



Figure 3. Biodegradation experiment of cushion foams: (a) plastic box used for soil burial; (b) cushion foam placement.

2.4.9. Fourier Transform Infrared (FTIR) Analysis

A FTIR spectrometer (Vertex 70-RamII, Bruker, Billerica, MA, USA) was used in attenuated total reflection (ATR) mode to study the change in the chemical structure of the samples after soil burial for 24 weeks. A small piece of the cushion foam sample was recorded at $400\text{--}4000\text{ cm}^{-1}$, and 64 scans were averaged at a resolution of 4 cm^{-1} .

2.4.10. Statistical Analysis

The SPSS software for Windows version 20 (SPSS Inc., Chicago, IL, USA) was implemented to conduct the statistical analysis of the cushion foam properties. Tukey's HSD post-hoc test was used to compare the means of five replicates of bulk density, hardness, mold shrinkage, and compression set, and 400 measurements of average cell size for each cushion foam sample at the 0.05 significance level.

3. Results and Discussion

An eco-friendly cushion foam net was developed by the NRL. The aim of this development was to create an alternative cushion for the nonbiodegradable commercial EPE foam net used in fresh produce packaging. The NRL foam net was made from a sustainable resource using an energy-efficient process. Though natural rubber is generally considered inherently biodegradable, an increase in its biodegradation rate is desirable. The addition of BLF to the NRL foam net was mainly to enhance biodegradability. However, adding BLF to NRL may affect several other aspects, including processability, mechanical properties, appearance, and cushion performance. This work is focused on the investigation of the effects of the addition of BLF and its content into NRL foam cushion based on these aspects.

The NRL foam net was fabricated using the Dunlop process with microwave vulcanization. In the Dunlop process, the air was incorporated into the NRL and stabilized with chemicals. The appearance of the resulting NRL foam at this stage was similar to that of whipped cream, which was relatively delicate. Adding dried BLF directly to the compound caused the NRL foam to destabilize and collapse instantly. This could be attributed to the dried BLF absorbing significant amounts of moisture from the foam compound, destroying the delicate balance of the foamed rubber. Adding the moisture to the BLF, therefore, solved the problem and the NRL composite foams with different BLF contents were successfully fabricated.

The following sections are the results and discussion of the effects of the BLF addition into NRL foam based on their appearance and properties related to the fruit cushion packaging application.

3.1. Appearance and Design of the NRL Foam Cushion

The NRL foam cushion was made so that it could be tested and compared with a conventional EPE foam cushion. A flat net sheet was first made (see Figure 4a), and it was rolled to form a tube shape before fastening with rubber glue (see Figure 4b). The final shape of the NRL foam net (NRL-FN) cushion resembled that of the fruit foam net used commercially (EPE-FN) (Figure 5a). It should be noted that the flat net sheet of NRL-FN

was comprised of one layer of square-cross-section filaments (see Figure 4d). This design was used to simplify the process of making the prototype cushion foam net. On the other hand, the commercial EPE-FN comprised round-cross-section filaments crossing over one another (see Figure 4c).

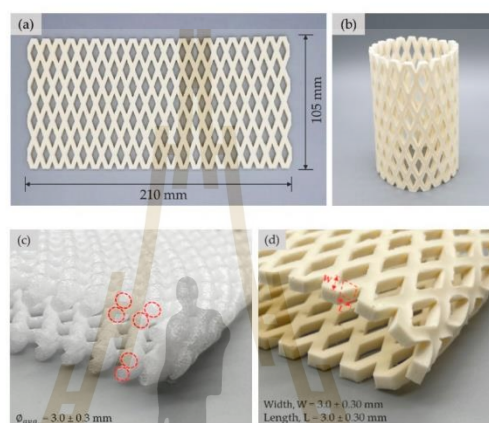


Figure 4. Fabrication and design of NRL-FN: (a) foam net sheet; (b) foam net cylindrical tube; (c) cross-section of EPE-FN; and (d) cross-section of NRL-FN.

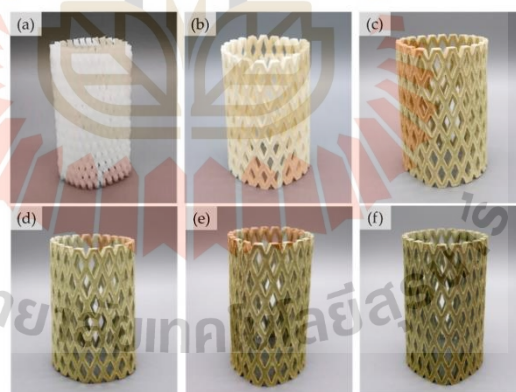


Figure 5. Cushion foam net: (a) EPE-FN; (b) NRL-FN-BLF0.0; (c) NRL-FN-BLF2.5; (d) NRL-FN-BLF5.0; (e) NRL-FN-BLF7.5; (f) NRL-FN-BLF10.0.

The NRL-FN with and without BLF are shown in Figure 5b–f. The NRL-FN without BLF was off-white with a slight yellow tint. Adding BLF to the NRL-FN resulted in a green color and its intensity increased with the BLF content. The green color was the natural color of BLF, as shown previously in Figure 1a.

3.1.1. Mold Shrinkage

The shrinkage of cushion foam is an important parameter for cushion packaging design and fabrication. The shrinkage of NR products after vulcanization may have an

impact on the final density and performance. The understanding of this shrinkage behavior can also be used to design the mold so the desired shape and dimension of the cushion can be obtained. The shrinkage of NRL-FN at different BLF contents is displayed in Figure 6. It could be generally seen that the height of all samples showed the highest shrinkage rates compared to the width and length. The height shrinkage further increased with the presence of BLF and with the increasing content.

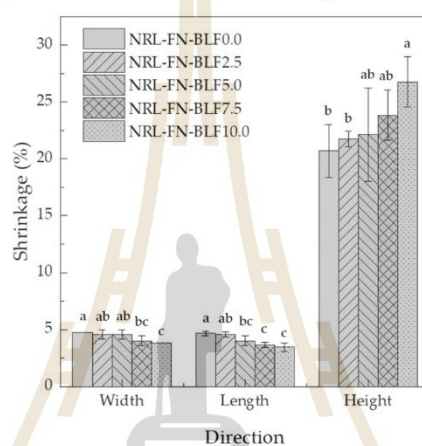


Figure 6. Shrinkage percentage of NRL foam composite at various BLF loading at different shrinkage directions compared with silicone mold size. Significant differences at $p < 0.05$ are shown by different letters. The values represent the mean \pm S.E. of five replicates.

On the other hand, the width and length slightly decreased with increasing BLF loading. The different shrinkages in height from the width and length were plausibly due to freedom of shrinkage from the top, the free surface of the molding foam during fabrication. Adding the higher-density ingredient of BLF into the foamed NR increased the weight that was pulled on the free surface of the molding NR foam. The side walls prohibited the changes in the width and length from molding the NR foam and prevented shrinkage in these directions.

The higher shrinkage rate observed when higher filler contents were incorporated into the foam was also reported by Ramli, R. et al. [47]. Moreover, the addition of filler was most likely to corrupt the foam's cell structure [17]. Consequently, the density of the composite foam increased. The effect of BLF incorporation into the NRL-FN and its contents on the bulk density and cell structures are discussed in the following section.

3.1.2. Bulk Density

In packaging, low bulk density material is preferred due to the lower fuel consumption and, thus, a lower cost of transportation. Table 2 shows the bulk density of EPE-FN compared to NRL-FN and NRL-FN-BLFs. It was clear that the density of EPE-FN commercial foam was greatly lower than that of the NRL-FN-BLFs (≥ 10 folds). This was expected as polyethylene (PE) possessed a lower density than NR. In addition, PE had a good melt strength, which was required to fabricate a foam structure with high porosity (large cell and thin wall). The SEM micrographs in the following section were in good agreement with the bulk density result.

Table 2. Foam properties of EPE-FN and NRL-FN-BLFs.

Cushion Foams	Bulk Density (kg/m ³)	Hardness (Shore OO)	Number of Cells per Unit Volume (Cells/cm ³)	Average Cell Size (μm)
EPE-FN	18.869 [44]	29.56 ± 0.65 ^a	-	-
NRL-FN-BLF0.0	264.59 ± 4.64 ^b	28.88 ± 0.61 ^{ab}	63,726.67	93.54 ± 2.64 ^c
NRL-FN-BLF2.5	272.56 ± 5.35 ^{ab}	28.64 ± 0.67 ^b	56,892.56	100.73 ± 4.76 ^c
NRL-FN-BLF5.0	276.99 ± 7.22 ^{ab}	29.08 ± 0.78 ^{ab}	50,968.49	108.06 ± 2.06 ^b
NRL-FN-BLF7.5	281.53 ± 11.60 ^a	29.28 ± 0.67 ^{ab}	51,381.86	115.05 ± 3.66 ^a
NRL-FN-BLF10.0	288.47 ± 12.51 ^a	29.48 ± 0.48 ^b	45,758.51	122.58 ± 4.52 ^a

Note: Significant differences at $p < 0.05$ are shown by different letters. The values represent the mean ± S.E. of five replicates.

The bulk density of NRL-FN was approximately 265 kg/m³. The density was higher than those values reported by Prasopdee, T. and W. Smithipong (~65 kg/m³) [13] and Mahathaninwong, N. et al. (~161.6 kg/m³) [14]. Generally, the low density of NRL foam was achieved by the incorporation of the air into the NR latex or whipping in the Dunlop process [48]. Foaming time, foaming speed [28], and blowing agent content [22,49] were used to adjust the bulk density of the NRL foam. The differences in the density of the NR forms reported here as compared to others may be due to the different methods and/or equipment used during the aeration process. The addition of the BLF, which possessed higher density than the NRL foam, gave rise to the bulk density of NRL-FN-BLF composites. The presence of BLF also induced a higher degree of shrinkage (Figure 6), resulting in an increase in bulk density. A similar result was also found by Zhang, N. and H. Cao when chitin was used to enhance the antibacterial activity in NRL foam. The volume of the air in the NRL foam was decreased because chitin particles agglomerated and destroyed the original cellular structure of the foam cells, resulting in the collapse of the foam and thus increasing the foam bulk density [50].

3.1.3. Morphology and Cell Structure Analysis

The foam surface and the foam cell characteristics of the EPE-FN and NRL-FN with and without BLF cushions were studied using SEM. The surfaces of the foam samples are shown in Figure 7. The EPE-FN surface shown in Figure 7a was dense and smooth without any holes or protrusions on the surface. On the other hand, the surface of the NRL-FN and NRL-FN-BLFs (Figure 7b–f) appeared to be dense and rough, with some holes and lumps present on the surface of some samples. The addition of BLF to the NRL-FN slightly caused the change in the surface roughness. The roughness increased slightly as a function of BLF content. No obvious fiber was found protruding from the surface. The roughness of the foam surface may implicate its use as cushioning for fresh produce. As the cushion foam surface is usually directly in contact with the fresh produce's surface, the rough surface may cause bruising damage due to the rubbing that can occur during transportation. However, several other parameters can also contribute to accrued bruise damage on some fruit, including the foam's hardness, cushion efficiency, fruit firmness, etc. The pack test of the target fruit using cushions with different BLF contents must be done to elucidate the effect of surface roughness of the NRL-FN on fruit surface bruising.

SEM micrographs of the cross-sectioned samples are shown in Figure 8. For EPE-FN (Figure 8a), the foam appeared to be a closed-cell structure with a very large cell size of 600–900 μm. The cell wall was relatively thin, with a thickness of 2–5 μm. The shape of the foam cell was a polygon with interconnecting thin walls similar to that of the honeycomb structure. A SEM micrograph of the NRL-FN foam structure in Figure 8b–f also revealed a more or less closed-cell structure of a spherical shape cell morphology with opens on some cell walls. Spherical foam cells were scattered throughout the sample. The spherical foam cells with different sizes were relatively small as compared to that of the EPE-FN. Cell size was analyzed using the ImageJ program and shown as a cell size distribution curve in

Figure 9. The average cell size of the samples was calculated and shown in Table 2. The difference in cell size in a sample indicated that the air bubbles generated during the Dunlop process were nonuniform. This is a common result of a mechanical foaming technique, such as in the Dunlop process, where poor pore formation regulation is observed [19]. The cell wall was relatively thick, with a thickness in the range of 10–70 μm . The structures of the obtained NRL foams agreed with the high bulk density results discussed earlier. The lower bulk density of the NRL foam reported by [18,46] was due to the open cell structure of NRL they obtained. The polymeric foam can be made into either open or closed-cell foam, depending on the stabilizing agent used [18]. The results suggested that our NRL foam could be further optimized to obtain a lower bulk density to make it suitable for packaging applications. However, such a structure may need to prove its ability to withstand the incorporation of BLF.

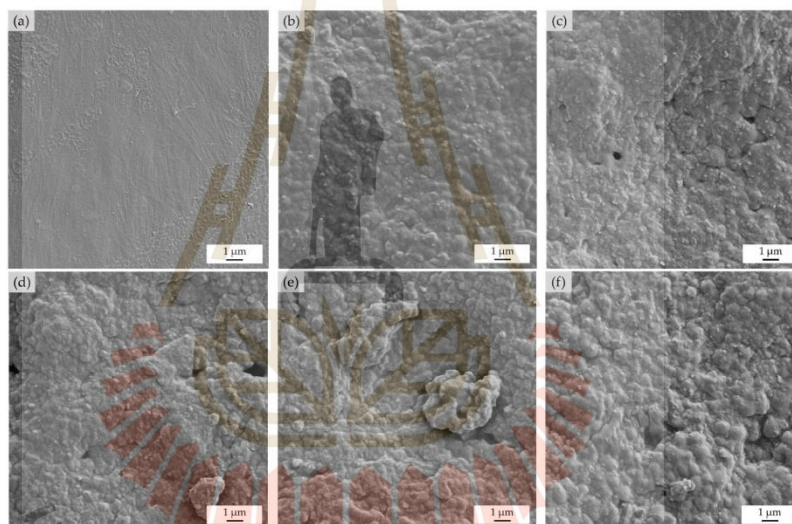


Figure 7. NRL foam composites morphology at the top surface of specimens (5k \times magnification): (a) EPE-FN; (b) NRL-FN-BLF0.0; (c) NRL-FN-BLF2.5; (d) NRL-FN-BLF5.0; (e) NRL-FN-BLF7.5; (f) NRL-FN-BLF10.0.

The addition of BLF fiber into NRL-FN resulted in larger foam cells. As the BLF content increased, the cell size of the NRL-FN-BLF composites noticeably increased. On the other hand, the number of foam cells decreased as the BLF content increased. From statistical analysis, the average cell size displayed insignificantly different between that of the NRL foam at BLF loading at (0.00 and 2.50 phr) and (7.50 and 10.00 phr). The addition of BLF seemed to cause the foam cells to coalesce, resulting in fewer cell counts and larger pore sizes. Similar results were reported by Tomyangkul, S. et al. [33] and Surya, I. et al. [51]. It is commonly known that NRL foam structure dictates most foam properties. The foam structure could be tailored through various parameters, including foaming agent type and amount [18], fabrication methods, filler type, filler or particle size [32], filler loading [14], etc.

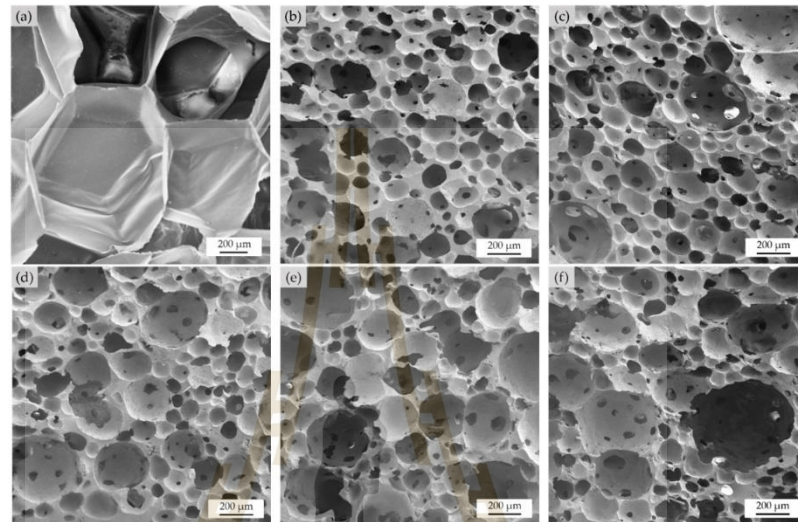


Figure 8. Cushion foams morphology at a 50× magnification: (a) EPE-FN; (b) NRL-FN-BLF0.0; (c) NRL-FN-BLF2.5; (d) NRL-FN-BLF5.0; (e) NRL-FN-BLF7.5; (f) NRL-FN-BLF10.0.

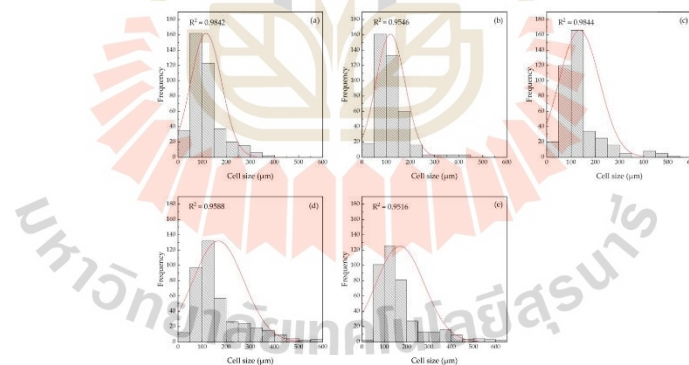


Figure 9. NRL foam composites distribution curve with various BLF loadings ($p < 0.05$, $n = 400$): (a) NRL-FN-BLF0.0; (b) NRL-FN-BLF2.5; (c) NRL-FN-BLF5.0; (d) NRL-FN-BLF7.5; (e) NRL-FN-BLF10.0.

3.1.4. Hardness

Hardness is the degree of firmness of a material—it is the ability to resist deformation, scratching, or abrasion [52]. The Shore OO type of durometer hardness was used in this research following ASTM D2240 due to the cushion foam as extremely soft rubber, sponges, and foams [43]. Cushion material with too much hardness can cause damage to the soft surface of a fruit. The hardness of the cushion foam samples is shown in Table 2. It could be seen that the hardness of EPE-FN and NRL-FN with and without BLF were similar. The result indicated that the hardness quality of the eco-friendly NRL-FN cushion could be used as an alternative to the EPE-FN fruit cushion. A slight increase in hardness was observed as

the BLF content increased, but it was statistically insignificant. The finding was unexpected as other researchers had reported increases in hardness when fillers were added to NRL foams. Bashir, A. et al. added eggshell powder (ESP) to the NRL foam. The obtained NRL foam composite possessed improved harness and stiffness when the ESP content was at least 10 phr. The improvements were due to the EPS demobilizing the polymer chains of the NRL foam matrix [53]. Mahathaninwong, N. et al. also reported a similar finding of the increased hardness of NRL foam due to the incorporation of Agarwood-waste (ACW) powder [17]. They also suggested that the change in hardness was due to the change in foam cell morphology, contributing to the filler addition. Sirikulchaikij, S. et al. also reported the fabrication of NRL foam using a bubbling process. The hardness of the latex increased when the cell size became larger. Thus, it could be inferred that the hardness depended on the NRL foam's cell structure or morphology [24]. In our work, as shown in Table 2 and Figure 8, adding BLF up to 10 phr slightly increased the cell size while the cell wall thickness values remained relatively constant. Therefore, the small change in hardness of the NRL-FN-BLF composites was in good agreement with the insignificant change in the foam morphology.

3.1.5. Compression Set

The elastic behavior of elastomeric material is generally determined using a compression set test. A material with a low compression set can restore its thickness close to its original size after removing the compression force, suggesting a high material elasticity. On the other hand, a material with a high compression set may permanently lose its shape due to low elasticity. In general, a smaller permanent compression set leads to higher foam recoverability [54]. Figure 10 shows the compression set percentage of NRL foams with different BLF loadings. NRL-FN without BLF had a compression set of 12.5%. The addition of 2.5 phr BLF to NRL-FN insignificantly altered the compression set of the foam. The compression set percentage showed an increasing trend as a function of the BLF loading, with a maximum of 16.0% at 10 phr of BLF. A similar trend was observed when rice husk powder (RHP) was added to the NRL foam. The RHP was used to decrease the recovery percentage of the NRL foam. At low RHP loading, the NRL foam composite could be returned to its initial thickness faster than the foam with higher RHP loading [31]. Another report showed that better dispersion of a filler (kenaf) and smaller particle size led to a smaller deformation. The filler agglomeration decreased the elasticity behavior of the NRL foam. The agglomerated filler restricted the molecular chains' movements, enhancing the foam's stiffness [51]. Moreover, foam with larger cells with thinner cell walls might be easily collapsed under the load. Thus, NRL foam with smaller cells and more cell walls, such as what was found in our samples, should be able to withstand compression deformation with good recoverability [17,54]. It should be noted that the compression set percentage reported here (maximum 16%) was significantly lower than those reported by the others (maximum 65%). This might be due to the closed-cell foam structure of our samples, which provided elasticity and resistance to compression deformation. For the target application of fresh produce's cushion material, a lower compression set may be more desirable as the cushion foam with a high compression set may lose its ability to protect the packaged produce after being compressed.

3.1.6. Compressive Test

The relationship between compressive stress and compressive strain of the EPE-FN and the NRL-FN with different BLF loadings is shown in Figure 11. Similar behavior was observed for both the commercial EPE-FN and NRL-FN samples, where the compressive stress gradually increased as the compressive strain increased. This behavior was common for a foam with a closed-cell structure. The compressive stress at 50% strain of EPE-FN was lower than those of NRL-FN at various BLF contents. The results suggested that the commercial EPE-FN was more readily deformed than the NRL-FN and NRL-FN-BLF composites. From the stress-strain curve in Figure 11, it could be seen that the NRL-FN and

NRL-FN-BLF composites had larger areas under the curves than the EPE-FN. The larger areas under the curves of the eco-friendly foams indicated a greater ability to absorb energy over the EPE-FN commercial cushion materials.

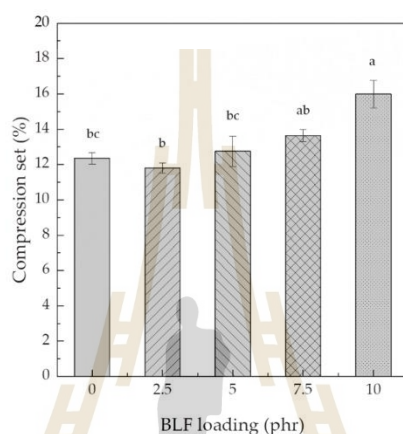


Figure 10. Compression set of NRL foam composite various BLF loading. Significant differences at $p < 0.05$ are shown by different letters. The values represent the mean \pm S.E. of five replicates.

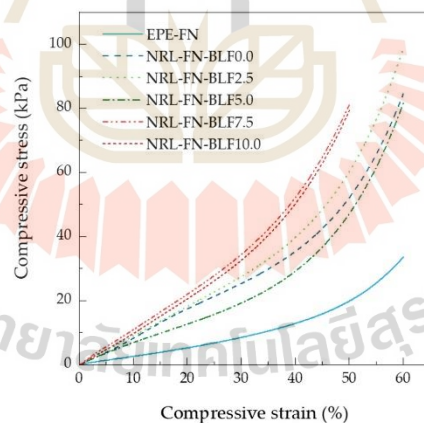


Figure 11. Stress–strain curve of the cushion foams.

The presence of BLF in NRL-FN slightly increased the compressive stress at 50% strain. An increasing trend of the compressive stress at 50% strain was observed as the BLF content in NRL-FN increased. The compressive stress at 50% strain of NRL-FN containing BLF contents of 0.00, 2.50, 5.00, 7.50, and 10.00 phr were 56.58, 58.89, 48.09, 81.14, and 77.85 kPa, respectively. The maximum stress was obtained when BLF 7.5 phr was added to NRL-FN. Further increased the BLF content to 10.0 phr showed insignificant change in the compressive stress at 50% compressive strain. The change in the compressive stress of a porous material with a filler depends on the type and content of the filler used as well as its effects on the foam cell structure. Typically, a foam's compression stress and stiffness

increase with increasing filler loading. Consequently, the increase in stiffness leads to an increment in hardness [31,36,55]. From our results, adding BLF insignificantly changed the foam morphology; the slight increase in the compressive stress at 50% strain possibly came from the presence of the harder particle of BLF.

In the packaging of fresh produce, the cushion material must absorb energy from external forces during transportation. Consequently, the lowest amount of energy may transfer to the packed fresh produce, thus preventing damage from occurring. The cushion that absorbs more energy is, therefore, better at reducing the bruising damage of fresh produce. The ability of a material to absorb energy could be determined in terms of “cushion coefficient (C)”. The cushion coefficient is determined from the compressive stress–strain curve, and the results are shown in Figure 12. It could be seen that the cushion coefficient was dependent on the strain percentage. A significant decline in the cushion coefficient was observed initially up to 45% strain before it leveled off. To compare the cushion coefficient of the samples, cushion coefficients at 50% compressive strain were chosen and shown in Table 3. It could be seen that the commercial EPE-FN cushion possessed the highest cushion coefficient of 5.24, indicating it had the lowest ability to absorb energy among all samples.

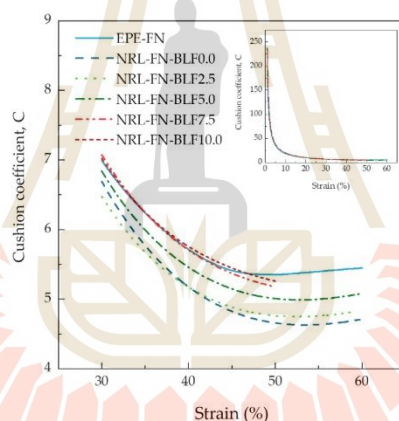


Figure 12. Cushion coefficient–compressive strain curves of cushion foams.

Table 3. Cushion coefficient at 50% strain of a commercial cushion foam compared to the eco-friendly cushion NRL-FN at various BLF contents.

Cushion Foams	Cushion Coefficient (c) at 50% Strain
EPE-FN	5.24
NRL-FN-BLF0.0	4.62
NRL-FN-BLF2.5	4.81
NRL-FN-BLF5.0	5.01
NRL-FN-BLF7.5	5.19
NRL-FN-BLF10.0	5.21

On the other hand, the cushion NRL-FN without BLF possessed the lowest cushion coefficient of 4.62. The presence of BLF and its increasing content in the NRL-FN cushion gave rise to the cushion coefficient. The results suggested that NRL-FN was the best material for the cushioning application as it could absorb the highest energy from the external force, which, in turn, was the most successful in minimizing the energy that otherwise might damage the packed fruit. A small amount of BLF used in the NRL-FN might be beneficial for enhancing the biodegradability of the cushion foam net without

sacrificing the cushion performance. A pack test using the eco-friendly cushions with the actual model fruit is required to prove their effectiveness as a cushion material. Based on the available data, the encouraging results implied that the NRL-FN-BLFs might be used instead of EPE-FN for commercial purposes in the future.

3.2. Biodegradation Study

In the biodegradation study, the cushion foams of EPE-FN, NRL-FN, and NRL-FN-BLFs were buried in planting soil and placed outdoors for 24 weeks (May–October 2022). The biodegradation evaluations include the visual inspection of the appearance and their microstructure (SEM), weight loss percentage, chemical structure, and mechanical properties.

3.2.1. Appearance

Table 4 shows the appearance (photographs on the left column) and surface microstructure (SEM micrographs on the right column) of the cushion samples before and after soil burial for 24 weeks. Before the soil burial experiment (week 0), the EPE-FN was white and cumulus. The NRL-FN was off-white with a yellowish tint. A greenish color was observed when BLF was incorporated into the NRL-FN, with the intensity of the green color increased as a function of the increasing BLF content. After 24 weeks of the soil burial test, the EPE-FN became slightly denser, and its color remained white. The NRL-FN and NRL-FN-BLFs, on the other hand, did not show a change in shape, but the color turned slightly brownish. The darker shade of the brownish color was more prominent as the BLF content in the NRL-FN-BLFs increased. The change in color was used as an indicator for the biodegradation of natural fiber/polymer composites. Luthra, P., Vimal, K.K., Goel, V. et al. [56] suggested that the color appearance was an important parameter used in the assessing the deterioration of the PP/natural fiber composite. The color change was mainly due to the changes in the chemical structure of the lignocellulosic complex of the natural fiber in the composite. A similar result was also reported by Butylina et al. [57]. It was also reported that removing the lignin from the fiber decreased the change in color. In our study, BLF was used without any treatment. Therefore, it could be inferred that the brownish color that appeared on the NRL-FN and NRL-FN-BLFs was a sign of degradation. The greater color changes of the NRL-FN-BLF cushion foams as the BLF content increased were in good agreement with the changes on the cushions' surfaces observed in the SEM micrographs.

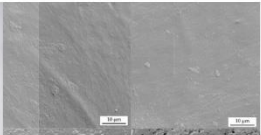
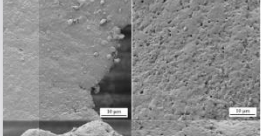
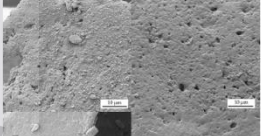
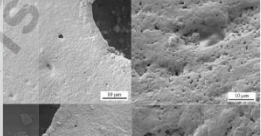
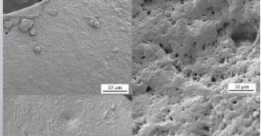
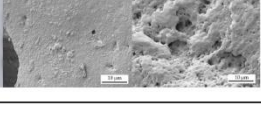
The SEM micrographs of the cushions' foam surfaces showed significant changes in the surface appearance and roughness. The increases in surface roughness coupled with the emergence of microvoids became more pronounced as the BLF content increased. Similar results were reported by Shah, A.A., Hasan, F., Shah, Z. et al. [58]. They showed that a NR latex glove appeared rough with irregular cracks and pits after 2 weeks of exposure to *Bacillus sp. AF-666*. The greater surface erosion suggested higher degradation of NRL-FN with higher BLF contents. Similar increasing trends of degradation as a function of the increasing natural fiber contents were reported by others [56,57]. To confirm the degradation of the NRF-FN-BLF cushion foam, physical properties, weight loss, and chemical structure were investigated.

3.2.2. Weight Loss

The weight loss values of the EPE-FN, NRL-FN, and NRL-FN-BLFs over 24 weeks of soil burial are shown in Figure 13. The weight loss percentage is a crucial indicator of the degradation of the samples. From the graph, it could be seen that EPE-FN showed a slight weight loss initially in the first 4 weeks before the weight loss became constant. The maximum weight loss was approximately 1%. The NRL-FN showed a greater degree of degradation than the EPE-FN. The fast-increasing weight loss was observed in the first 8 weeks before it leveled off. The maximum weight loss at 24 weeks of soil burial was about 4%. With the presence of BLF in NRL-FN, a greater initial weight loss was observed, and the weight loss continued to increase after week 8. It was noticeable that higher weight loss

was observed with higher BLF content in NRL-FN. The degradation rate could be estimated from the slope of the curves in Figure 13. The results suggested a fast degradation rate was observed in the initial soil burial time before week 8. After week 8, the NRL-FN samples containing BLF continued to degrade with slower degradation rates. The rate tended to increase with the BLF content. At the end of soil burial at week 24, the weight loss of NRL-FN containing 10 phr of BLF was 1.8 times greater than that of NRL-FN without BLF. The results suggested that the natural fiber acted as a biodegradation accelerator for the NRL foam composites. The weight reduction was due to the microorganisms' activity during soil burial, which took place on the skin of the samples and appeared as surface erosion and microvoids in the SEM micrographs in Table 4.

Table 4. Appearance and micrograph of cushion foams before soil burial (0 weeks) and after soil burial (24 weeks).

Cushion Foams	Foams Appearance		Foams Micrograph	
	Before Soil Burial	After Soil Burial	Before Soil Burial	After Soil Burial
EPE-FN				
NRL-FN-BLF0.0				
NRL-FN-BLF2.5				
NRL-FN-BLF5.0				
NRL-FN-BLF7.5				
NRL-FN-BLF10.0				

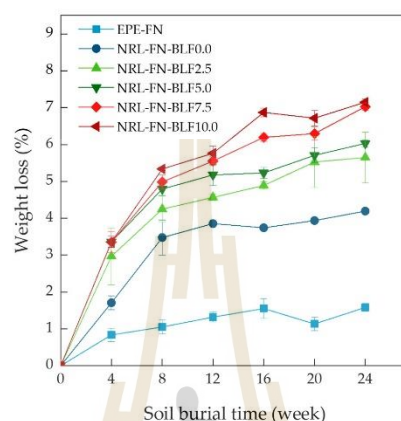


Figure 13. Weight loss percentage of EPE-FN, NRL-FN, and NRL-FN-BLFs cushion foams at various BLF contents over 24 weeks of soil burial times.

Tsuchii reported that a surgical glove was degraded in 20 days in a culture medium. This was probably because their samples were very thin compared to ours, and their controlled environment also played a crucial role in degrading their NR products. Soil burial was used in this study to simulate the normal ecological condition of the landfill method, the most common technique of waste management. The biodegradation rate may be accelerated significantly in a controlled environment with the right microbe (fungi and/or bacteria) strain [59]. Moreover, several reports suggested that some chemicals in the NR compound may enhance or prohibit the biodegradation of rubber products [60]. The use of BLF as a filler in the NRL-FN enhanced biodegradation of the eco-friendly foam cushion. Optimization of the chemicals used in the making of the NRL-F may be done to further increase the biodegradation rate.

3.2.3. Fourier Transform Infrared (FTIR) Analysis

FTIR analysis method is a technique for observing the chemical structure of materials. FTIR spectra of the cushion foam samples before and after 24 weeks of soil burial at various BLF loadings (0.00, 2.50, 5.00, 7.50, and 10.00 phr) are compared, as shown in Figure 14. FTIR bands assignment of NRL, BLE, and NRL composites are shown in Table 5.

Table 5. IR bands assignment of NRL, BLE, and NRL composite.

Wavenumber (cm ⁻¹)	Assignment
3300–3380	–OH stretching vibration (–OH as a result of the degradation by oxidation) [59]
2958–2960	–CH ₃ asymmetric stretching vibration of natural rubber [59]
2919–2927	–CH ₂ asymmetric stretching vibration of natural rubber [59]
2852–2854	–CH ₂ asymmetric stretching vibration of natural rubber [59]
1710–1740	Carbonyl group (C=O) from ketone or aldehyde results from oxidative degradation [59]
1655–1665	–C=C-stretching vibration in the NR structure or maybe due to absorbed water or carboxylate or conjugated ketone (–C=O) resulted from the degradation [59]

Table 5. Cont.

Wavenumber (cm ⁻¹)	Assignment
1618	Aromatic skeletal vibration, C=O stretching, absorbed O-H of hemicellulose and lignin [60] of BLF
1508	C=C-C aromatic ring stretching and vibration of lignin [60] of BLF
1537, 1270	C=O and –O-R of hemicellulose [61] of BLF
1032	C-O stretching, aromatic C-H in-plane deformation of cellulose and lignin [60] of BLF
1020	–C-O-C-stretching of ester group [62]
870–830	Isoprene backbone of NR [63]

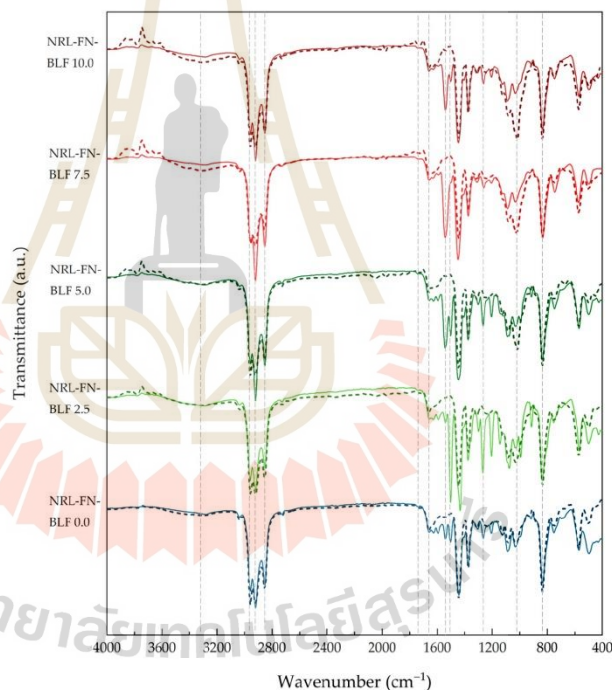


Figure 14. FTIR spectra of NRL foam composites before (solid lines) and after (dash lines) soil burial.

FTIR spectra of NRL-FN-BLF0.0 before soil burial showed peaks at 2800–3000 cm⁻¹ (–CH stretching), 1655–1665 cm⁻¹ (–C=C-stretching), and 835 cm⁻¹ (=CH bending in isoprene backbone of NR). When compared to NRL foam, NRL foam composites exhibited absorption peaks at 3326 (–OH stretching vibration of cellulose, hemicellulose, and lignin), 2918 (C-H stretching of cellulose, hemicellulose, and lignin), 1628 (asymmetric stretching band of the carboxyl group of glucuronic acid in hemicellulose, –C=O stretching in conjugated of a carboxyl group), 1512 (–C=C-C-aromatic ring stretching and vibration in lignin), and 1033 (–C-O-stretching of cellulose and lignin) cm⁻¹. The absorption peaks of BLF are shown in Figure 15.

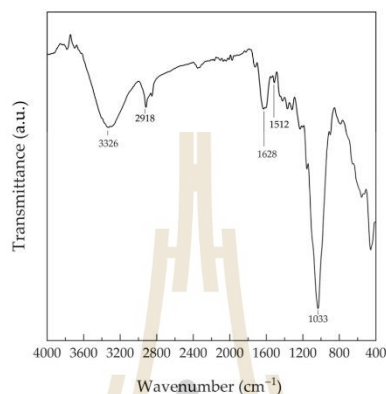


Figure 15. FTIR spectra of BLF.

The degradation of the vulcanized natural rubber is caused by direct action from microbes, which results in polymer chain cleavage and affects the functional group of the material [64]. The cleavage of the poly (cis-1,4-isoprene) backbone occurred first at the double bond via oxidative degradation [65]. After the soil burial, the band intensity of -OH stretching at 3326 cm^{-1} and -C=O stretching at 1739 cm^{-1} of NRL foam slightly increased, as shown in Figure 14. The formation of carbonyl and hydroxyl bonds (-C=O and -OH) was due to the oxidative degradation of NR [59]. In addition, the intensity of the band at 1020 cm^{-1} assigned to -C-O-C -stretching was marginally increased [62].

Moreover, the intensity of the peaks at 1628 , 1541 , and 1270 cm^{-1} (-C=O stretching of hemicellulose and lignin) and 1503 cm^{-1} (-C=C-C -aromatic ring stretching and vibration of lignin) decreased after soil burial due to the degradation of BLF. With increasing BLF content in the NRL foam composites, the increment of the intensity of -OH stretching, -C=O stretching, and -C-O-C -stretching were seen in Figure 16. This may be because BLF improved the degradation of the composites. The biodegradability of the NRL foam composites was confirmed by the weight loss percentage and morphology.

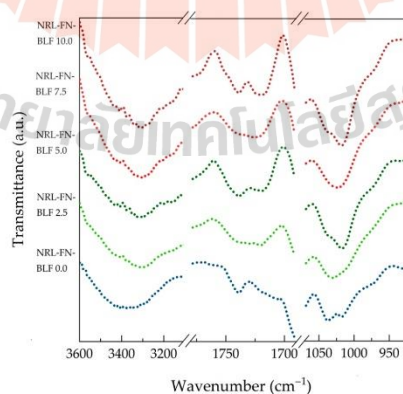


Figure 16. FTIR spectra of NRL foam composite at various BLF contents after soil burial for 24 weeks.

3.2.4. Compressive Test

Generally, a decline in physical properties is expected as NR products are degraded [64]. The 50% compressive strength of cushion foams at over 24 weeks of soil burial time is shown in Figure 17. The 50% compressive strength of EPE-FN was unchanged over the 24-week period. The compressive strength of the NRL-FN without and with BLF showed a decreasing trend in the first 12 weeks but became constant or even increased (such as in the case of 10 phr of BLF in NRL-FN). The slight decreases in compressive strength in the NRL-FN samples were expected as the biodegradation damaged the samples' structure and integrity. The loss in long hydrocarbon chains also weakens the rubber properties. The increase in 50% compressive strength in some samples in the later weeks was plausibly because the degraded cushion became stiffer, hence more resistance to compressive force. Overall, the degradation of the foam sample took place, and the BLF increased the degradation rate of the NRL-FN. However, the changes in properties were relatively low. This result may be beneficial as it suggests that the eco-friendly NRL cushion could be continuously used or reused for a prolonged period of time. A well-designed logistical strategy must be created for recovering/returning the cushion after use.

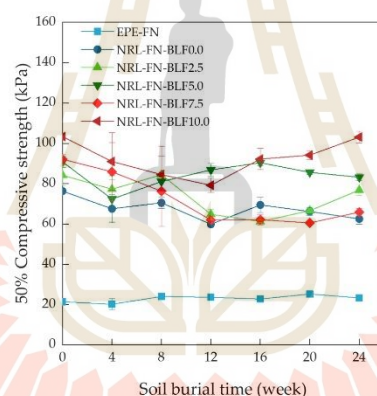


Figure 17. Compressive strength of 50% of cushion foam at various soil burial times.

4. Conclusions

The eco-friendly cushions of NRL foam were developed as an alternative for cushion packaging for fresh produce. The NRL was a primary material from a renewable resource. The Dunlop process and microwave irradiation used in the vulcanization step were energy efficient. The addition of BLF to the NRL-FN improved the cushion biodegradability. The presence of BLF also affected other properties of the NRL foams, including processability, bulk density, and foam cell structure. Thus, the mechanical properties and cushion coefficient were also affected.

This study illustrated the possibility of improving the packaging cushion to be more sustainable and lessen its negative environmental impact. The presence of BLF positively enhanced the biodegradation of the cushion up to 1.8 times (weight loss) compared to the NRL-FN without BLF in 24 weeks. Meanwhile, the EPE commercial cushion foam was indifferent in weight during the same period under the same ecological conditions. Other properties, including bulk density, compression set, compressive strength and cushion coefficient, were slightly increased but statistically insignificant. To verify the cushioning performance of the eco-friendly NRL foam, the pack test of the foam with a model fruit (guava) has been carried out. The results, reported elsewhere [66], are encouraging and provide insight into further improving the cushioning packaging.

In this study, 10 phr of BLF added to the NRL-FN did not significantly alter the cell foam size and structure. The results suggested that the process used in creating the eco-cushion foam net was very forgiving. One might add other different fillers or additives to the cushion foam to create extra functions, such as acting as an ethylene absorber and antibacterial and/or anti-browning agents. Moreover, other natural fibers can also be used to enhance the biodegradability of the NRL cushion foam, including rice husk, banana, hemp, pineapple, bamboo, coconut, etc. Hence, the natural fibers from agricultural waste may become valuable material. Ultimately, an alternative cushion that is both smart and eco-friendly may be obtainable in the near future.

Author Contributions: Conceptualization, T.T. and S.C.; methodology, K.J. (Keavalin Jitkokkrud), K.J. (Kasama Jarukumjorn) and T.T.; software, K.J. (Keavalin Jitkokkrud), J.R. and T.T.; validation, K.J. (Keavalin Jitkokkrud), K.J. (Kasama Jarukumjorn), C.R., S.C. and T.T.; formal analysis, K.J. (Keavalin Jitkokkrud), K.J. (Kasama Jarukumjorn), C.R., S.C., J.R. and T.T.; investigation, K.J. (Keavalin Jitkokkrud) and T.T.; data curation, K.J. (Keavalin Jitkokkrud) and T.T.; writing—original draft preparation, K.J. (Keavalin Jitkokkrud) and T.T.; writing—review and editing, K.J. (Kasama Jarukumjorn), C.R., S.C. and T.T.; supervision, K.J. (Kasama Jarukumjorn) and T.T.; project administration, T.T.; funding acquisition, S.C. and T.T. All authors have read and agreed to the published version of the manuscript.

Funding: This work was funded by Suranaree University of Technology (SUT), the Center of Excellence on Petrochemical and Materials Technology (PETROMAT), High Performance and Smart Materials (HPSM) program, 2019 and Mae Fah Luang University under the National Science, Research, and Innovation Fund (NSRF) 2022: grant 652A04011.

Institutional Review Board Statement: Not applicable.

Data Availability Statement: The data presented in this study are available upon request from the corresponding author.

Acknowledgments: The authors thank the Suranaree University of Technology and Mae Fah Luang University for providing equipment and facilities.

Conflicts of Interest: The authors declare no conflict of interest.

References

- Nilsen-Nygaard, J.; Fernández, E.N.; Radusin, T.; Rotabakk, B.T.; Sarfraz, J.; Sharmin, N.; Pettersen, M.K. Current status of biobased and biodegradable food packaging materials: Impact on food quality and effect of innovative processing technologies. *Compr. Rev. Food Sci. Food Saf.* **2021**, *20*, 1333–1380. [CrossRef] [PubMed]
- Roithner, C.; Cencic, O.; Rechberger, H. Product design and recyclability: How statistical entropy can form a bridge between these concepts—A case study of a smartphone. *J. Clean. Prod.* **2022**, *331*, 129971. [CrossRef]
- Ncube, L.K.; Ude, A.U.; Ogunmuyiwa, E.N.; Zulkifli, R.; Beas, I.N. An overview of plastic waste generation and management in food packaging industries. *Recycling* **2021**, *6*, 12. [CrossRef]
- Leal Filho, W.; Salvia, A.L.; Bonoli, A.; Saari, U.A.; Voronova, V.; Klóga, M.; Barbit, J. An assessment of attitudes towards plastics and bioplastics in Europe. *Sci. Total Environ.* **2021**, *755*, 142732. [CrossRef] [PubMed]
- Faraca, G.; Astrup, T. Plastic waste from recycling centres: Characterisation and evaluation of plastic recyclability. *J. Waste Manag.* **2019**, *95*, 388–398. [CrossRef]
- Horodytska, O.; Valdés, F.J.; Fullana, A. Plastic flexible films waste management—A state of art review. *J. Waste Manag.* **2018**, *77*, 413–425. [CrossRef]
- UN Environment Report “Banning Single-Use Plastic: Lessons and Experiences from Countries” UN Environment Program. 2018. Available online: <https://www.unep.org/interactive/beat-plastic-pollution/> (accessed on 15 November 2022).
- Li, G. Development of cold chain logistics transportation system based on 5G network and Internet of things system. *Microprocess. Microsyst.* **2021**, *80*, 103565. [CrossRef]
- Sohn, J.S.; Kim, H.K.; Kim, S.W.; Ryu, Y.; Cha, S.W. Biodegradable foam cushions as ecofriendly packaging materials. *Sustainability* **2019**, *11*, 1731. [CrossRef]
- Georges, A.; Lacoste, C.; Damien, E. Effect of formulation and process on the extrudability of starch-based foam cushions. *Ind Crops Prod.* **2018**, *115*, 306–314. [CrossRef]
- Vroman, I.; Tighzert, L. Biodegradable polymers. *J. Mater.* **2009**, *2*, 307–344. [CrossRef]
- Ke, T.; Sun, X.S. Starch, poly (lactic acid), and poly (vinyl alcohol) blends. *J. Polym Environ.* **2003**, *11*, 7–14. [CrossRef]

13. Torres-Huerta, A.M.; Domínguez-Crespo, M.A.; Palma-Ramírez, D.; Flores-Vela, A.I.; Castellanos-Alvarez, E.; Del Angel-López, D. Preparation and degradation study of HDPE/PLA polymer blends for packaging applications. *Rev. Mex. Ing. Quim.* **2019**, *18*, 251–271. [[CrossRef](#)]
14. Hamad, K.; Kaseem, M.; Deri, F. Rheological and mechanical characterization of poly (lactic acid)/polypropylene polymer blends. *J. Polym. Res.* **2011**, *18*, 1799–1806. [[CrossRef](#)]
15. Trongsatitkul, T.; Chaiwong, S. In situ fibre-reinforced composite films of poly (lactic acid)/low-density polyethylene blends: Effects of composition on morphology, transport and mechanical properties. *Polym. Int.* **2017**, *66*, 1456–1462. [[CrossRef](#)]
16. Prasopdee, T.; Smitthipong, W. Effect of fillers on the recovery of rubber foam: From theory to applications. *Polymers* **2020**, *12*, 2745. [[CrossRef](#)] [[PubMed](#)]
17. Mahathaninwong, N.; Chuchee, T.; Karrila, S.; Songmuang, W.; Rodsang, N.; Limhengha, S. Morphology and properties of agarwood-waste-filled natural rubber latex foam. *Bioresources* **2021**, *16*, 176. [[CrossRef](#)]
18. Garrison, T.F.; Murawski, A.; Quirino, R.L. Bio-based polymers with potential for biodegradability. *Polymers* **2016**, *8*, 262. [[CrossRef](#)]
19. Jędruchiewicz, K.; Ok, Y.S.; Oleszczuk, P. COVID-19 discarded disposable gloves as a source and a vector of pollutants in the environment. *J. Hazard. Mater.* **2021**, *417*, 125938. [[CrossRef](#)]
20. Suksup, R.; Sun, Y.; Sukatta, U.; Smitthipong, W. Foam rubber from centrifuged and creamed latex. *J. Polym. Eng.* **2019**, *39*, 336–342. [[CrossRef](#)]
21. Syahrin, S.M.; Zunaida, Z.; Hakimah, O.; Nuraqmar, S.M.S. Effect of blowing agent on compression and morphological properties of natural rubber latex foam. *AIP Conf. Proc.* **2020**, *2267*, 020037.
22. Suethao, S.; Phongphanphane, S.; Wong-Ekkabut, J.; Smitthipong, W. The relationship between the morphology and elasticity of natural rubber foam based on the concentration of the chemical blowing agent. *Polymers* **2021**, *13*, 1091. [[CrossRef](#)] [[PubMed](#)]
23. Phomrak, S.; Nimpai boon, A.; Newby, B.M.Z.; Phisalaphong, M. Natural rubber latex foam reinforced with micro-and nanofibrillated cellulose via Dunlop method. *Polymers* **2020**, *12*, 1959. [[CrossRef](#)] [[PubMed](#)]
24. Sirikulchaikij, S.; Kokoo, R.; Khangkhamano, M. Natural rubber latex foam production using air microbubbles: Microstructure and physical properties. *Mater. Lett.* **2020**, *260*, 126916. [[CrossRef](#)]
25. Ariff, Z.M.; Afolabi, L.O.; Salmazo, L.O.; Rodriguez-Perez, M.A. Effectiveness of microwave processing approach and green blowing agents usage in foaming natural rubber. *J. Mater. Res. Technol.* **2020**, *9*, 9929–9940. [[CrossRef](#)]
26. Tang, J.; Resurreccion, F.P., Jr. Electromagnetic basis of microwave heating. In *Development of Packaging and Products for Use in Microwave Ovens*; Pesheck, P., Lorence, M., Eds.; Elsevier: Amsterdam, The Netherlands, 2009; pp. 3–37.
27. Zauzi, N.A.; Ariff, Z.M.; Khimi, S.R. Foamability of Natural Rubber via Microwave Assisted Foaming with Azodicarbonamide (ADC) as Blowing Agent. *Mater. Today Proc.* **2019**, *17*, 1001–1007.
28. Jitkokkruad, K.; Jarukumjorn, K.; Paksakulpiwat, C.; Chaiwong, S.; Trongsatitkul, T. Effect of Foaming Time and Speed on Morphology and Mechanical Properties of Natural Rubber Latex Foam Vulcanized by Microwave Heating. In Proceedings of the SUT International Virtual Conference on Science and Technology 2021 (IVCST 2021), Virtual Event on Zoom Web Conferencing Platform, Nakhon-Ratchasima, Thailand, 6 August 2021.
29. Gillen, K.T.; Clough, R.L. Prediction of elastomer lifetimes from accelerated thermal-aging experiments. In Proceedings of the Elastomer-service life prediction symposium '97, University of Akron, Akron, Ohio, 14–15 August 1997.
30. Ramasamy, S.; Ismail, H.; Munusamy, Y. Soil burial, tensile properties, morphology, and biodegradability of (rice husk powder)-filled natural rubber latex foam. *J. Vinyl Addit. Technol.* **2015**, *21*, 128–133. [[CrossRef](#)]
31. Ramasamy, S.; Ismail, H.; Munusamy, Y. Effect of Rice Husk Powder on Compression Behavior and Thermal Stability of Natural Rubber Latex Foam. *Bioresources* **2013**, *8*, 4258–4269. [[CrossRef](#)]
32. Mursalin, R.; Islam, M.W.; Moniruzzaman, M.; Zaman, M.F.; Abdullah, M.A. Fabrication and Characterization of Natural Fiber Composite Material. In Proceedings of the International Conference on Computer, Communication, Chemical, Material and Electronic Engineering (IC4ME2-2018), University of Rajshahi in Bangladesh, Rajshahi, Bangladesh, 8–9 February 2018.
33. Tomyangkul, S.; Pongmuksuwan, P.; Harnnarongchai, W.; Chaochanchaikul, K. Enhancing sound absorption properties of open-cell natural rubber foams with treated bagasse and oil palm fibers. *J. Reinf. Plast. Compos.* **2016**, *35*, 688–697. [[CrossRef](#)]
34. Alvarez, V.A.; Fraga, A.N.; Vazquez, A. Effects of the moisture and fiber content on the mechanical properties of biodegradable polymer-sisal fiber biocomposites. *J. Appl. Polym. Sci.* **2004**, *91*, 4007–4016. [[CrossRef](#)]
35. Lokesh, P.; Kumari, T.S.; Gopi, R.; Loganathan, G.B. A study on mechanical properties of bamboo fiber reinforced polymer composite. *Mater. Today Proc.* **2020**, *22*, 897–903. [[CrossRef](#)]
36. Kudori, S.N.L.; Ismail, H. The effects of filler contents and particle sizes on properties of green kenaf-filled natural rubber latex foam. *Cell. Polym.* **2020**, *39*, 57–68. [[CrossRef](#)]
37. Srisuwan, L.; Jarukumjorn, K.; Suppakarn, N. Effect of silane treatment methods on physical properties of rice husk flour/natural rubber composites. *Adv. Mater. Sci. Eng.* **2018**, *2018*. [[CrossRef](#)]
38. Nazri, M.K.H.M.; Sapawe, N. Removal of methyl orange over low-cost silica nanoparticles extracted from bamboo leaves ash. *Mater. Today Proc.* **2020**, *31*, A54–A57. [[CrossRef](#)]
39. Ameram, N.; Agoh, M.A.C.; Idris, W.F.W.; Ali, A. Chemical characterization of bamboo leaves (*Gigantochloa albociliata* and *dracaena surculosa*) by sodium hydroxide treatment. *F1000Research* **2018**, *7*, 1024. [[CrossRef](#)]

40. Suhaily, S.S.; Khalil, H.A.; Nadirah, W.W.; Jawaid, M. Bamboo based biocomposites material, design and applications. In *Materials Science-Advanced Topics*; Mastai, Y., Ed.; IntechOpen: London, UK, 2013; pp. 489–517.
41. Lewis Bamboo. Bamboo Leaves. Available online: <https://lewisbamboo.com/pages/bamboo-leaves> (accessed on 18 September 2022).
42. Yuan, J.; Zhu, Y.; Wang, J.; Liu, Z.; Wu, J.; Zhang, T.; Li, P.; Qiu, F. Agricultural bamboo leaf waste as carbon precursor for the preparation of Cu-Al/biomass fiber adsorption and its application in the removal of ammonia nitrogen pollutants from domestic wastewater. *J. Wood Chem. Technol.* **2021**, *41*, 137–149. [[CrossRef](#)]
43. *ASTM D 2240-15*; Standard Test Method for Rubber Property—Durometer Hardness. ASTM International: West Conshohocken, PA, USA, 2021.
44. Song, X.; Zhang, G.; Lu, J.; Zhang, L.; Zhang, S. Study on the Cushion Performance of the Cushion Material Composed of EPE and Corrugated Paperboard. In *Applied Sciences in Graphic Communication and Packaging*; Zhao, P., Ouyang, Y., Xu, M., Yang, L., Ren, Y., Eds.; GatewayEast: Singapore, 2018; Volume 447, pp. 467–474.
45. Luo, Y.; Xiao, S.; Li, S. Effect of Initial Water Content on Foaming Quality and Mechanical Properties of Plant Fiber Porous Cushioning Materials. *BioResources* **2017**, *12*, 4259–4269. [[CrossRef](#)]
46. *ASTM D 1055-04*; Standard Specifications for Flexible Cellular Materials—Latex Foam. ASTM International: West Conshohocken, PA, USA, 2010.
47. Ramli, R.; Chai, A.B.; Ho, J.H.; Kamaruddin, S.; Rasdi, F.R.M.; De Focatiis, D.S. Specialty natural rubber latex foam: Foamability study and fabrication process. *Rubber Chem. Technol.* **2022**, *95*, 492–513. [[CrossRef](#)]
48. Hui Mei, E.L.; Singh, M. The Dunlop Process in Natural Rubber Latex Foam. *Malays. Rubber Dev. Technol.* **2010**, *10*, 23–26.
49. Hamnarongchai, W.; Chaochanchaikul, K. Effect of Blowing Agent on Cell Morphology and Acoustic Absorption of Natural Rubber Foam. *Appl. Mech. Mater.* **2015**, *804*, 25–29. [[CrossRef](#)]
50. Zhang, N.; Cao, H. Enhancement of the antibacterial activity of natural rubber latex foam by blending it with chitin. *J. Mater.* **2020**, *13*, 1039. [[CrossRef](#)]
51. Surya, I.; Kudori, S.N.I.; Ismail, H. Effect of partial replacement of kenaf by empty fruit bunch (EFB) on the properties of natural rubber latex foam (NRLF). *Bioresources* **2019**, *14*, 9375–9391. [[CrossRef](#)]
52. Briscoe, B.J.; Pelillo, E.; Sinha, S.K. Scratch hardness and deformation maps for polycarbonate and polyethylene. *Polym Eng Sci.* **1996**, *36*, 2996–3005. [[CrossRef](#)]
53. Bashir, A.S.; Manusamy, Y.; Chew, T.L.; Ismail, H.; Kamasamy, S. Mechanical, thermal, and morphological properties of (eggshell powder)-filled natural rubber latex foam. *J. Vinyl Addit. Technol.* **2015**, *23*, 3–12. [[CrossRef](#)]
54. Sukkaneewat, B.; Utara, S. Ultrasonic-assisted Dunlop method for natural rubber latex foam production: Effects of irradiation time on morphology and physico-mechanical properties of the foam. *Ultrason. Sonochem.* **2022**, *82*, 105873. [[CrossRef](#)] [[PubMed](#)]
55. Sallehuddin, N.J.; Ismail, H. Treatment's effect on mechanical properties of kenaf bast/natural rubber latex foam. *Bioresources* **2020**, *15*, 9507–9522. [[CrossRef](#)]
56. Luthra, P.; Vimal, K.K.; Goel, V.; Singh, R.; Kapur, G.S. Biodegradation studies of polypropylene/natural fiber composites. *SN Appl. Sci.* **2020**, *2*, 512. [[CrossRef](#)]
57. Butylina, S.; Hyvärinen, M.; Kärki, T. A study of surface changes of wood-polypropylene composites as the result of exterior weathering. *Polym. Degrad. Stab.* **2012**, *97*, 337–345. [[CrossRef](#)]
58. Shah, A.A.; Hasan, F.; Shah, Z.; Hameed, A. Degradation of polyisoprene rubber by newly isolated *Bacillus* sp. AF-666 from soil. *Appl. Biochem. Microbiol.* **2012**, *48*, 37–42. [[CrossRef](#)]
59. Manaila, E.; Stelescu, M.D.; Craciun, G. Degradation studies realized on natural rubber and plasticized potato starch based eco-composites obtained by peroxide cross-linking. *Int. J. Mol. Sci.* **2018**, *19*, 2862. [[CrossRef](#)] [[PubMed](#)]
60. Zhuang, J.; Li, M.; Pu, Y.; Ragauskas, A.J.; Yoo, C.G. Observation of potential contaminants in processed biomass using fourier transform infrared spectroscopy. *Appl. Sci.* **2020**, *10*, 4345. [[CrossRef](#)]
61. Gao, W.H.; Chen, K.F.; Yang, R.D.; Yang, F.; Han, W.J. Properties of bacterial cellulose and its influence on the physical properties of paper. *BioResources* **2011**, *6*, 144–153. [[CrossRef](#)]
62. Shuhairiah, D.; Hanafi, I.; Azhar, A.B. Soil burial study of palm kernel shell-filled natural rubber composites: The effect of filler loading and presence of silane coupling agent. *BioResources* **2016**, *11*, 8686–8702.
63. Jayathilaka, L.P.; Ariyadasa, T.U.; Egodage, S.M. Development of biodegradable natural rubber latex composites by employing corn derivative bio-fillers. *J. Appl. Polym.* **2020**, *137*, 49205. [[CrossRef](#)]
64. Tsuchii, A.; Suzuki, T.; Takeda, K. Microbial degradation of natural rubber vulcanizates. *Appl. Environ. Microbiol.* **1985**, *50*, 965–970. [[CrossRef](#)] [[PubMed](#)]
65. Shah, A.A.; Hasan, F.; Shah, Z.; Kanwal, N.; Zeb, S. Biodegradation of natural and synthetic rubbers: A review. *Int. Biodeterior. Biodegrad.* **2013**, *83*, 145–157. [[CrossRef](#)]
66. Chaiwong, S.; Saengrayap, R.; Rattanakaran, J.; Chaitanarueang, A.; Arwathananukul, S.; Aunsri, N.; Tontiwattanakul, K.; Jitkokkrud, K.; Kitazawa, H.; Trongsatitkul, T. Natural rubber latex cushioning packaging to reduce vibration damage in guava during simulated transportation. *Postharvest Biol. Technol.* **2013**; accepted.

Disclaimer/Publisher's Note: The statements, opinions and data contained in all publications are solely those of the individual author(s) and contributor(s) and not of MDPI and/or the editor(s). MDPI and/or the editor(s) disclaim responsibility for any injury to people or property resulting from any ideas, methods, instructions or products referred to in the content.



Contents lists available at ScienceDirect

Postharvest Biology and Technology

journal homepage: www.elsevier.com/locate/postharvbio

Natural rubber latex cushioning packaging to reduce vibration damage in guava during simulated transportation

Saowapa Chaiwong^{a,b}, Rattapon Saengrayap^{a,b}, Jutarat Rattanakaran^a,
 Arraya Chaithanarueang^a, Sujitra Arwathananukul^{b,c}, Nattapol Aunsri^{b,c},
 Khemapat Tontiwattanukul^d, Keavalin Jitkokkrud^{e,g}, Hiroaki Kitazawa^f,
 Tatiya Trongsatitkul^{e,g,*}

^a School of Agro-Industry, Mae Fah Luang University, Chiang Rai, Thailand

^b Integrated AgriTech Ecosystem Research Group, Mae Fah Luang University, Chiang Rai, Thailand

^c School of Information Technology, Mae Fah Luang University, Chiang Rai, Thailand

^d Department of Mechanical and Aerospace Engineering, King Mongkut's University of Technology North Bangkok, Bangkok, Thailand

^e School of Polymer Engineering, Suranaree University of Technology, Nakhon Ratchasima, Thailand

^f Institute of Food Research, National Agriculture and Food Research Organization, Ibaraki, Japan

^g Center of Excellence on Petrochemical and Materials Technology, Chulalongkorn University, Bangkok 10330, Thailand

ARTICLE INFO

Keywords:

Foam net
 Image analysis
 Mechanical damage
 Natural rubber latex
 Polyethylene

ABSTRACT

A conventional foam net is commercially applied to protect or reduce mechanical damage of guava fruit during transportation. This study investigated the utilization of natural rubber latex foam net (NRL-FN) cushioning material to protect Guava fruit against vibration damage. NRL-FN is an eco-friendly cushioning material which was designed to enhance its biodegradability by adding bamboo leaf fiber (BLF). Different loadings of the BLF were added into the NRL-FN (0.0, 2.5 and 5.0 phr). Cushioning performance of the NRLFNs were compared with a commercial polyethylene foam net (EPE-FN) using a bare fruit as the control. The cushioning test investigated thickness, energy (E), cushion coefficient (C) and percentage transmissibility (P_T) using Glom Sali guava under simulated vibration at acceleration (G_{rms}) (8.826 m s^{-2}), frequency (13.5 Hz), and vibration duration (40 min). Guava fruit was stored at 20 °C under 80% RH for 4 d to assess vibration bruising on guava peel by digital image analysis as bruise area (BA), gray scale, normalized fractal dimension difference ($\Delta FD/FD_0$), browning index (BI) and total color difference (TCD). Results showed that NRL-FN+BLF0.0 phr and NRL-FN+BLF2.5 phr (thickness of 3.2 mm) gave lower C and higher E values than that of NRL-FN+BLF5.0 phr (thickness of 3.1 mm) and EPE-FN (thickness of 5.4 mm), while NRL-FN+BL0.0 phr and EPE-FN had the lowest P_T value. The NRL-FN+BLF0.0 phr, NRL-FN+BL2.5 phr and EPE produced the lowest BA (<2.5%) on guava peel followed by NRL-FN+BL0.0 phr (6–7%) and a bare fruit (control) (30–45%). No significant differences in $\Delta FD/FD_0$, BI and TCD were found among the four cushioning treatments. The NRL-FN with lower BLF composition provided greater cushioning performance against vibration bruising on guava peel with reduced thickness and lower C and P_T values. Results demonstrated that NRL-FN possessed a potential for application in distribution packaging as a new cushioning material to protect against fruit mechanical vibration damages.

1. Introduction

Guava (*Psidium guajava* L.) is economically cultivated in many tropical and subtropical countries throughout the world including India, Pakistan, China, Brazil, Thailand, Malaysia, Vietnam and the Philippines (Altendorf, 2018). In 2020, total export value of guava was 3.88 billion

USD, Thailand is ranked as the number one global guava exporter at 18.91% of the total exported value followed by Mexico (11.82%) and the Netherlands (10.72%) (Food and Agriculture Organization, 2021). Guava is a climacteric fruit and often damaged by its high respiration rate (Ismail et al., 2010). The guava fruit is delicate and susceptible to mechanical damages such as cuts, punctures, bruises and compression

* Corresponding author at: School of Polymer Engineering, Suranaree University of Technology, Nakhon Ratchasima, Thailand.
 E-mail address: tatiya@sut.ac.th (T. Trongsatitkul).

<https://doi.org/10.1016/j.postharvbio.2023.112273>

Received 20 September 2022; Received in revised form 19 January 2023; Accepted 23 January 2023

Available online 31 January 2023

0925-5214/© 2023 Elsevier B.V. All rights reserved.

(Singh, 2011). Guava mechanical damages caused by rough handling result in bruising and wounding appearing as browning incidence on skin and flesh that are susceptible to microbial spoilage (Singh, 2011; Kamsiati, 2013). Overall postharvest losses of guava throughout postharvest handling accounted for 10–24% with high mechanical damages (Mendes et al., 2019; Katumbi et al., 2021). These losses can be minimized by the application of emerging postharvest technologies that extend the shelf life of guava fruit while also retaining other quality attributes (Yadav et al., 2022).

Vibration damage occurs when fruit moves inside the package during transportation. Fruit incurs bruising by bumping against other fruit or the package, causing impact injury or by rubbing against another surface resulting in abrasion (Dubey, and Mishra, 2019). Simulated vibration testing was extensively reviewed for the three major factors affecting vibration bruising as acceleration, frequency, and shaking duration (Chaiwong, 2016; Fernando et al., 2018). A recent report of simulated vibration testing in guava found that increased vibration bruising depended mainly on acceleration level, particularly at 8.826 m s^{-2} , while frequency and shaking duration were minor factors (Chaiwong et al., 2021). Fruit packaging consists of two components which are exterior and interior packaging. Previous research examined, the protective properties of packaging with particular attention given to exterior packaging including cartons and plastic containers and interior packaging including paper-based and foam materials (Lin et al., 2022). However, additional factors such as the influence of fill status, packaging type, fruit location inside the package, and cushioning on the severity of fruit vibration damage have not been intensely investigated (Fernando et al., 2018). For example, apple fruit on the top tray inside full telescope design style container (FTD) exhibited the largest bruising area as compared to the other three layers at a frequency of 15 Hz (Padji et al., 2016). Packaging is known to play a crucial role in protective the fruit against vibrational damage.

Cushioning packaging of fresh produce plays a significant role in controlling vibration/impact damage. The process of designing cushioning packaging prototypes is carried out under severe vibration conditions to save time when determining cushioning performance (Kitazawa, 2018). Vibration/impact protection of fresh produce is the main aim of packaging but other properties of cushioning materials such as flexibility, environmental compatibility and consumer safety aspects should also be considered. Cushioning materials can be categorized as natural or synthetic based on their origin (Dubey and Mishra, 2019). Synthetic material as foam net is made from expanded polystyrene (EPS), polypropylene (EPP), polyethylene (EPE) and polyurethane (EPU). Foam net characteristics are soft, light weight and offer sufficient ventilation (Dubey and Mishra, 2019). Currently, conventional foam net is one of the available choices for commercial cushioning packaging but is considered to be non-biodegradable in a landfill (Chonhenchob and Singh, 2004; Jarimopas et al., 2004). Recently, consumer demand for environmentally friendly packaging has increased. Stricter environmental regulations have been enforced including taxes for non-degradable packaging and environmental improvement charges. Bio-based composite materials have been extensively employed as eco-friendly lightweight alternatives for electrical and packaging materials (Sohn et al., 2019).

Natural rubber can be made from either liquid latex or rigid rubber. The natural rubber latex can be easily made into a foam structure via Dunlop or Talalay processes. The Dunlop process is generally preferable when the economical concern is crucial. The shape of the natural rubber latex can be in a sheet, pellet, net, and role forms. Natural rubber latex foam net (NRL-FN) possesses the desirable properties and performance required for cushioning material. Moreover, NRL-FN is inherently biodegradable and because it is made from a sustainable resource, therefore NRL-FN is a promising alternative cushion material eco-friendly packaging for fresh produce. Optimizations including process tailoring and compound formulation were performed to further enhance the foam performance of NRL-FN and improve its ecofriendly attributes

while maintaining economical aspects. In our previous work, bamboo leaf fiber (BLF) was incorporated into the NRL-FN and found to enhance its biodegradation rate in soil burial test (Jitkokkrud et al., 2023). Kitazawa et al. (2015) applied rubber foam sheet layers in stacked packaging or outside the bottom of the boxes for drop shock testing in strawberry. However, there are no reports utilizing NRL-FN as a foam net design and primary packaging to cover individual fruit for protection against mechanical damages, particularly vibration damage.

Few studies have addressed cushioning material design to mitigate vibration bruising in fresh produce. Conventional foam net was compared with paper cushioning material under simulated vibration testing for single wall (flute C) corrugated fiberboard in pineapple (Chonhenchob et al., 2008) and paper-wrap packaging in pear (Zhou et al., 2008) and apple (Eissa et al., 2012). Previous studies applied conventional foam net on individual fruit to avoid fruit-to-fruit contact. Results showed that foam net significantly reduced vibration bruising (Chonhenchob et al., 2008; Zhou et al., 2008; Eissa et al., 2012). In peach, cushion design as a 3-compartment tray with a total of 36 cells was recently investigated in different materials such as polyurethane (PU)+ corrugated fiberboard boxes (CFB), expandable polyethylene (EPE)+CFB and CFB. Results showed that PU+CFB exhibited better cushioning performance than EPE+CFB and CFB formats against vibration damage of peach (Lin et al., 2020). Lin et al. (2022) reviewed interior packaging including paper-wrapped, pulp tray, sharded paper, plastic tray, foam net, foam ball, liner and air column bags. Numerous studies of cushioning materials for fresh produce have focused on liners, trays and partition designs as cushioning forms but excluded conventional foam net patterns.

Until recently, little research has addressed packaging cushioning in guava. Extruded polystyrene (XPS) or Styrofoam net exhibited lower damage (39.59%) than without filler material (84.03%) in a cardboard box (Rolle, 2008). While different natural cushioning materials or wrappings were investigated in guava fruit, no significant differences were found in total soluble solids, total acidity and ascorbic acid contents among neem leaves, rice straw, bamboo leaves and the control (unwrapped fruit) (Chandra and Kumar, 2012). No cushioning research has been conducted specifically on mechanical damage to guava using simulated vibration testing, and no studies have investigated eco-friendly NRL-FN as a cushioning material against mechanical damage to fruit, particularly vibration bruising. In addition, cushioning material design and formation using NRL-FN as a conventional foam net applied on individual fruit is lacking. Therefore, this is the first research to present a comparison of the cushioning performance between NRL-FN and a commercial expanded polyethylene foam net (EPE-FN).

This study had two objectives which are 1) compare properties and performances of NRL-FN and EPE-FN for protection of vibration bruising in guava cv. Glom Sali, and 2) investigate the effect of bamboo leaf fiber (BLF) loading on reducing vibration bruising in Glom Sali guava under simulated transportation. The ultimate aim of this work is to develop an eco-friendly cushioning material for fresh produce. The understating of compound formulation, structure, properties, and cushioning performance can lead to optimal designs for different produces.

2. Materials and methods

2.1. Raw material and sample preparation

Guava fruit (*Psidium guajava* L.) cv. Glom Sali was obtained from the Pangha Homestay Orchard, Chiang Rai Province, Thailand (latitude $20^{\circ} 24' 22.7''\text{N}$ longitude $100^{\circ} 00' 23.9''\text{E}$) in March 2022 at the mature green stage (about 100 days after fruit set). The fruit was handled carefully and packed in plastic crates with EPE-FN to prevent mechanical damages throughout the three-hour journey to the Agriculture and Biochemistry Laboratory (S7) at Mae Fah Luang University. The guava fruit was sorted into uniform weight (between 250 and 300 g) and without color defects for simulated vibration testing. Quality attributes

of random Glom Sali guava fruit were examined for uniformity, maturity, weight (volume), density (density), diameter (firmness) and fruit radius. Average guava weight, horizontal width, vertical length, fruit firmness and fruit density were 239.1 g, 7.5 cm, 8.0 cm, 4.68 N and 1.0 g/mL, respectively, while average radius of curvature values at bottom, middle and top positions were 50.024°, 50.532° and 53.890°, respectively. A one-piece folder (OPF) with dimensions (10.5 × 18.5 × 5.0 cm³) was used to pack two guava fruit (500 g) (Fig. 1).

2.2. Cushioning materials and testing

2.2.1. Fabrication of natural rubber latex foam net (NRL-FN)

With environmental concern in mind, the Dunlop process together with microwave irradiation were employed to fabricate natural rubber latex foam (NRL-FN) cushion. Optimization of the fabrication process has been reported elsewhere (Jitkokkrud et al., 2021). In short, a slurry of natural rubber latex was first aerated to generate a foam structure. Ammonia in the latex was reduced by mechanical stirring and air was incorporated into the slurry. Chemical ingredients including foaming agent and gelling agent were introduced into the aerated latex to stabilize the foamed structure. Crosslinker, accelerator, activator and antioxidant were mixed well into the slurry before pouring the resulting compound into a net-shape silicon mold. Chemical ingredients and amounts used were reported in our previous study (Jitkokkrud et al., 2023). The filled mold was then placed in a commercial household microwave oven (Samsung, MS2K3513AW) and vulcanized using irradiation power of 600 W for 6 min. After the vulcanization was completed, the NRL-FN was washed with water to remove any unreacted chemical residues and then dried in hot air before use.

2.2.2. Cushion testing and performance evaluation

The thickness of an NRL-FN specimen reported here was the average value from measuring five different points on a specimen using a vernier caliper (Mitutoyo 530-118, Mitutoyo, Kawasaki, Japan). Compressive properties of the cushion foam net were determined using a Universal testing machine (INSTRON/5565, Norwood, MA, USA). The load cell used was 1 kN with a crosshead speed of 12 mm/min. Foam specimens 3 mm thick were cut into square shapes of 100 mm × 100 mm. The compressive strength was reported at 50% strain.

The cushion coefficient (*C*) is an indicator of cushioning performance as the ability of a material to absorb energy under stress (Song et al., 2018). The cushion coefficient was determined from the compressive stress-strain curve using the following equation:

$$C = \frac{\sigma}{e} \quad (1)$$

where σ is the compressive stress and e is the energy absorption of the material which can be estimated from the area under the compressive stress-strain curve as shown in Eq. (2).

$$e = \int_0^{\epsilon} \sigma d\epsilon \quad (2)$$

In this study, the two main concepts of NRL-FN design were presented as 1) create NRL-FN foaming with a net pattern as a conventional EPE-FN, and 2) reduce the thickness of NRL-FN by around 50% of EPE-FN thickness due to the heavier weight of NRL-FN. As shown in Fig. 1, five treatments were investigated as 1) a bare fruit as the control, 2) EPE-FN as a conventional cushion and NRL-FN with three bamboo leaf (BLF) loadings (parts per hundred rubber: phr) including 3) 0.0 phr, 4) 2.5 phr and 5) 5.0 phr. Increase in green color was related to the increase of BLF composition in the NRL-FN material. Five cushioning treatments with four replications were investigated to determine cushioning properties and cushioning performance against vibration bruising of guava fruit.

2.3. Simulated vibration transportation

Vibration testing and setting followed the method of Chaiwong et al. (2021). Briefly, the simulated frequency level (Hz) of vibration transportation for Glom Sali guava fruit was generated using Audacity® recording and editing software (version 3.1.3, The Audacity Team). A power amplifier was used to drive an electrodynamic vibration exciter to enhance the signals and control the level of acceleration. The sampling signal was processed by a three-channel data acquisition system, and the resulting samples were converted using Fast Fourier Transform (FFT) to produce the frequency spectrum of the signals. A reference accelerometer was attached to the framework, while another two accelerometers were installed inside the OPF box and at the center of a guava fruit. In this study, the vibration condition was examined at acceleration (G_{ms}) (8.826 m s⁻²), frequency (13.5 Hz) and vibration duration (40 min). Based on previous simulated vibration testing in guava fruit (Chaiwong et al., 2021), this research addressed peak frequency and high acceleration levels that were representative of severe vibration conditions of simulated transportation. Low intensity vibration at frequency ranges of 10–20 Hz is generally found in actual truck transportation in Thailand (Chonhenchob et al., 2010). Moreover, this vibration condition was a similar range of vibration conditions from an actual truck transportation in other countries such as Japan, Taiwan (Ishikawa et al., 2009), Turkey (Çakmak et al., 2009), Spain, France and Italy (Barchi et al., 2002). While vibration lengths of 40 min were assumed to correspond to road transportation distances of 1500 km (Acican et al., 2007). This was the estimated distance from the north to the south of Thailand to reach domestic markets.

2.4. Percentage transmissibility (%)

The percentage transmissibility (%) of the cushioning material was calculated using Eq. (3) at frequency 13.5 Hz (Vursavus and Ozguven, 2004; Idah et al., 2012).



Fig. 1. The control (a bare fruit) and four cushioning treatments as a foam net style with EPE-FN and NRL-FN materials combined with BLF at 0.0, 2.5 and 5.0 phr.

$$\text{Percentage Transmission}(P_T)(\%) = \frac{a_b}{a_i} \times 100 \quad (3)$$

where P_T is the packaging transmissibility (%), a_b is the measured acceleration on the package (cushion) (m s^{-2}) and a_i is the applied acceleration from the framework (m s^{-2}).

2.5. Image analysis setting

The vibrated fruit was stored at 20 °C under 80% RH for 4 d and photographed every day. The image condition setting followed Chaiwong et al. (2021). Vibration bruising damage of guava was photographed as 4 shots (left, right, top and bottom sides) for each fruit under a square light box from the top of the box with a uniform light intensity $9.6 \times 10^3 \text{ lm m}^{-2}$ using a light meter (Tenmars TM-204, Taipei, Taiwan, China). A mirrorless camera (EOS M50, 15-45 mm Canon, Tokyo, Japan) was used to capture the vibration bruising images of guava peel.

2.5.1. Vibration bruising area (BA) (%), gray scale and fractal dimension (FD)

ImageJ (version 1.51j8, NIH, USA) was used to investigate the vibration bruises on guava peel. Before analysis, the original image files (6000×3368 pixels) were resized to remove background threshold values. A diagram of the image analysis method is shown in Fig. 2. The RGB color parameters were converted using the procedure and equations explained in Section 2.5.2. The calculated CIELAB values were then used to determine the browning index (BI) and total color difference (TCD) according to section 2.3.5. The grayscale value was obtained after converting RGB images to 8-bit grayscale, and a color histogram was used to determine the mean values of grayscale. The threshold for all images was Otsu's method. The bruising area was determined from the binary image of the whole guava fruit by calculating the bruised area (black area) ratio to the total area (white area). The RGB images were cropped into a square image of 300×300 pixels and converted into 8-bit grayscale images to determine the degree of guava bruise damage. The FD was calculated using the box-counting method described by Chaiwong et al. (2021).

2.5.2. Estimation of CIELAB color

The pre-processed image was analyzed and RGB color values were extracted from the vibration bruising image of guava peel, calculated to CIEXYZ and converted to CIELAB using the CIE standard color spaces using Eqs. (4) to (12) (Strecker et al., 2010).

$$\text{Var}_R = \left(\frac{\left(\frac{R}{255} + 0.055 \right)}{1.055} \right)^{2.4} \times 100 \quad (4)$$

$$\text{Var}_G = \left(\frac{\left(\frac{G}{255} + 0.055 \right)}{1.055} \right)^{2.4} \times 100 \quad (5)$$

$$\text{Var}_B = \left(\frac{\left(\frac{B}{255} + 0.055 \right)}{1.055} \right)^{2.4} \times 100 \quad (6)$$

RGB values were converted to XYZ values using the following equations:

$$X = (\text{Var}_R \times 0.4124) + (\text{Var}_G \times 0.3576) + (\text{Var}_B \times 0.1805) \quad (7)$$

$$Y = (\text{Var}_R \times 0.2126) + (\text{Var}_G \times 0.7152) + (\text{Var}_B \times 0.0722) \quad (8)$$

$$Z = (\text{Var}_R \times 0.0193) + (\text{Var}_G \times 0.1192) + (\text{Var}_B \times 0.9505) \quad (9)$$

The XYZ values were then converted to CIELAB values using the following equations:

$$L^* = 116f\left(\frac{Y}{Y_n}\right) - 16 \quad (10)$$

$$a^* = 500 \left[f\left(\frac{X}{X_n}\right) - f\left(\frac{Y}{Y_n}\right) \right] \quad (11)$$

$$b^* = 200 \left[f\left(\frac{Y}{Y_n}\right) - f\left(\frac{Z}{Z_n}\right) \right] \quad (12)$$

where Y_n , X_n and Z_n are the tristimulus values of the illuminant and observer angle. For illuminant D65, observer angle 10°, $X_n = 94.83$, $Y_n = 100.0$ and $Z_n = 107.38$.

2.5.3. Browning index (BI) and total color difference (TCD)

The browning index (BI) and total color difference (TCD) were used to characterize the overall changes in browning color on vibration bruising of guava peel. BI and TCD were calculated from the calculation of CIELAB values in section 2.3.1. BI and TCD were calculated using Eqs.

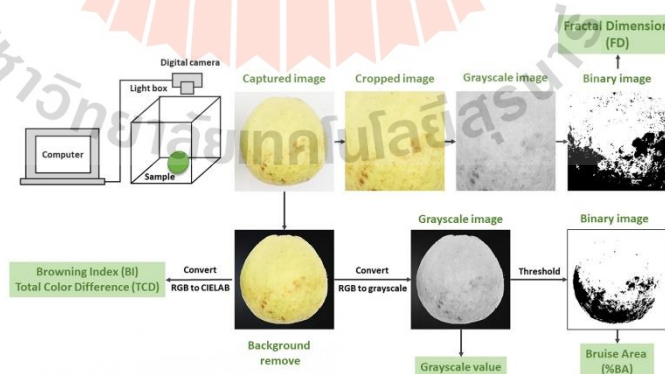


Fig. 2. Experimental flow diagram to determine bruising using the image analysis method.

(13) to (15) (Subhashree et al., 2017).

$$BI = \frac{[100 \times (X - 0.31)]}{0.172} \quad (13)$$

where x = chromaticity coordinate calculated from the L^* , a^* , b^* values, and

$$X = \frac{(a^* + 1.75L^*)}{(5.645L^* + a^* - 3.012b^*)} \quad (14)$$

The total color difference (TCD) was calculated using Eq. (15).

$$TCD = \sqrt{(L_0^* - L^*)^2 + (a_0^* - a^*)^2 + (b_0^* - b^*)^2} \quad (15)$$

where L_0^* , a_0^* and b_0^* are the initial color values of the guava surface while L^* , a^* and b^* are the final values of guava peel after storage at 20 °C under 80% RH for 4 d.

2.6. Statistical analysis

One-way analysis of variance (ANOVA) with a 95% level of confidence was used to compare the data acquired in this experiment. Statistically significant differences were observed between the treatments at $p < 0.05$. All experiments for cushioning material and simulated vibration tests were performed using four replications. All statistical analyses were conducted with SPSS for Windows version 20 (SPSS Inc., Chicago, IL, USA) using Tukey's HSD test. The normality was tested by the Kolmogorov-Smirnov test with SPSS. Also, the normality was performed to ensure the validity of the data and Box-Cox transformation was employed to those that was not normally distributed. This transformation was conducted using MATLAB Software version R2018a (MathWorks Inc., Natick, MA, USA).

3. Results and discussion

3.1. Cushioning properties and percentage transmissibility

Cushion materials of NRL-FN were compared with the commercially available EPE-FN. The thicknesses of the NRL-FNs were in the range of 3.080–3.196 mm thinner than that of the EPE-FN cushion (5.444 mm). The NRL-FN + BLF0.0 and NRL-FN + BLF2.5 treatments gave highest energy (E) values, followed by NRL-FN + BLF5.0 and EPE-FN treatments (Table 1). High E value indicated high potential energy absorption from the vibration force and related to low C values in the NRL-FN + BLF0.0 and NRL-FN + BLF2.5 treatments at strain (ϵ) 0.500 compared to NRL-

Table 1
Cushioning properties (thickness, energy (E), cushion coefficient (C) and percentage transmissibility (P_T) of five treatments.

Treatment	Thickness (mm)	Energy (E) at strain (ϵ) 0.500 (mm/mm)	C at strain (ϵ) 0.500 (mm/mm)	P_T at 13.5 Hz
Control (a bare fruit)	-	-	-	87.393 $\pm 3.491^a$
EPE-FN	5.385 $\pm 0.057^a$	0.004 \pm 0.000 ^c	5.203 $\pm 0.052^a$	69.376 $\pm 2.577^{bc}$
NRL-FN + BLF0.0 phr	3.198 $\pm 0.021^b$	0.012 \pm 0.001 ^a	4.613 $\pm 0.081^c$	58.546 $\pm 2.215^c$
NRL-FN + BLF2.5 phr	3.163 $\pm 0.032^b$	0.012 \pm 0.000 ^a	4.839 $\pm 0.027^b$	79.851 $\pm 7.758^{ab}$
NRL-FN + BLF5.0 phr	3.043 $\pm 0.039^b$	0.010 \pm 0.000 ^b	5.003 $\pm 0.033^{ab}$	74.479 $\pm 2.579^{bc}$

Different letters indicate significant differences at $p < 0.05$. Values are mean \pm S.E. from four replications.
List of Figures

FN + BLF5.0 and EPE-FN treatments (Table 1 and Fig. 3). Song et al. (2018) explained that the best cushioning performance provided the smallest C value in a graph plot of the static cushion coefficient-strain curve indicating the highest absorbed energy. As shown in Fig. 3, the lowest C level was recorded at strain (ϵ / %) (50%). It was found that both NRL-FN + BLF0.0 and NRL-FN + BLF2.5 treatments with thickness of 3 mm exhibited highest cushioning performance in absorbing vibration energy and preventing vibration bruising of guava fruit, as compared to EPE-FN cushion with a thickness of 5 mm. Adding BLF (2.5 phr) had no effect on cushioning performance. However, further increased BLF loading in NRL-FN resulted in increased C value. The result may infer that reduced BLF levels could be applied in NRL-FN cushion as valorization from agricultural waste.

The percentage transmissibility (P_T) value of the five treatments was also investigated at 13.5 Hz in the frequency range of 15–20 Hz caused by tires (Singh et al., 2006) and commonly found in truck transportation in Thailand (Chonhenchob et al., 2010). For the resonance frequency of fresh produce packaging, highest P_T was recorded in MK4 and MK6 package designs (corrugated fiberboard boxes) of apple with frequency range 9–12 Hz (Fadji et al., 2016). The most critical frequencies of apple packaging were between 3 and 15 Hz determined by transmissibility evaluation of corrugated fiberboard boxes (Vursavus and Ozguven, 2004). Khodaei et al. (2019) recorded the P_T of reusable plastic containers for fresh apricot at a frequency of 17 Hz, indicating that the selected frequency at 13.5 Hz was a representative critical range for guava packaging systems (cushion and OPF box). Results showed that P_T of the control (a bare fruit) (87%) exhibited the highest value compared to NRL-FN with BLF 2.5 and 5.0 phr (74–79%), while NRL-FN + BLF0.0 phr and EPE-FN s had the lowest P_T values at 58% and 69%, respectively (Table 1). At higher P_T levels the fruit bounced more inside the package during transportation (Fernando et al., 2018). The cushioning material also reduced the free space inside the package (Kitazawa, 2018) and restricted fruit movement/bounce during the simulated vibration test. The free space (%) of the OPF box was calculated by the length of the box (18.5 cm) and the two fruit horizontal diameters (2×7.5 cm), including four layers of cushioning thickness (Table 1). The free space of a bare fruit was highest at 18.9% box length, followed by all NRL-FN treatments (18.2%) and EPE-FN (17.8%). No significant differences in P_T level were recorded between NRL-FN + BLF0.0 phr and EPE-FN cushioning treatments and were below 100% P_T (Table 1). The NRL-FN + BLF0.0 phr and EPE-FN absorbed vibration force that exhibited a lower acceleration than the vibration shaker. However, adding BLF composition in NRL-FN increased P_T level above 100%. Overall cushioning properties and P_T value of NRL-FN + BLF0.0 phr showed high cushioning performance with reduced thickness, lower C and lower P_T levels than the EPE-FN cushion.

3.2. Vibration bruising area (BA) and fractal dimension (FD)

Cushioning applications to protect vibration bruising reduced BA significantly as compared to the control (a bare fruit) (Fig. 4B). A bare fruit showed a gradual increase in BA% during storage for 3 d while the other four cushioning treatments exhibited a constant BA value (Fig. 5). Browning incidence of guava peel from vibration bruising was observed after storage at 20 °C under 80% RH for 4 d (Fig. 4). As shown in Fig. 5, BA% of vibrated guava was analyzed by image analysis. The control (a bare fruit) had the highest BA (30–45%) followed by NRL-FN + BLF5.0 phr (6–7%) and the other three cushioning treatments ($< 2.5\%$), with no significant difference from EPE-FN cushioning. Adding BLF at 5.0 phr to NRL-FN increased BA due to the higher C value (Table 1 and Fig. 3) and rougher surface (Jitkokkruad et al., 2023) as compared to other treatments. The Thai and ASEAN guava standards state that the defect on guava peel in class II must not exceed 10% of the total fruit surface area (Agricultural Standard TAS 16–2010, 2010; ASEAN Stan 7:2008, 2008). Thus, by BA assessment, all cushioning treatments showed high potential for vibration protection, particularly NRL-FN + BLF0.0 phr,

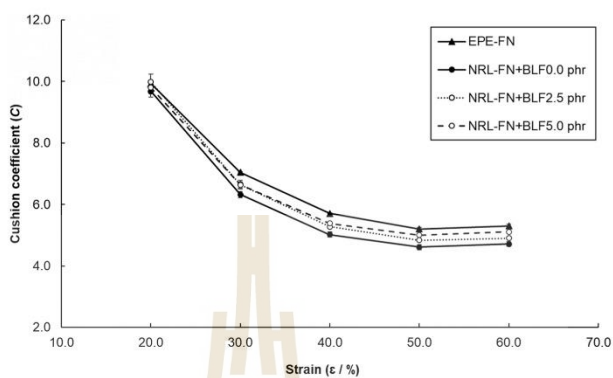


Fig. 3. Static cushion coefficient-strain curves of the four foam net cushioning treatments (EPE-FN, NRL-FN + BLF0.0 phr, NRL-FN + BLF2.5 phr and NRL-FN + BLF5.0 phr). Values are mean \pm S.E. from four replications.



Fig. 4. Browning incidence in the control (a bare fruit) and four cushioning materials from vibration bruising on Glom Sali guava peel under simulated vibration ($8.826 \text{ m s}^{-2} + 13.5 \text{ Hz} + 40 \text{ min}$) after storage at 20°C under 80% RH for 0 d (A) and 4 d (B).

NRL-FN+BLF 2.5 phr and EPE-FN.

Fractal dimension (FD) was assessed by image analysis. The normalized fractal dimension difference ($\Delta \text{FD}/\text{FD}_0$) was used to describe non-homogenous browning incidence on vibration bruising of

guava and provide a more potent evaluation of bruising than BI and TCD by colorimeter (Chaiwong et al., 2021). In this study, $\Delta \text{FD}/\text{FD}_0$ could not classify bruising level on the first day (24 h) after simulated vibration but there was a gradual increase in all $\Delta \text{FD}/\text{FD}_0$ values during storage

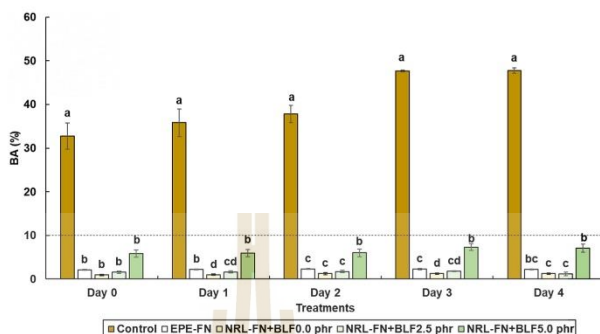


Fig. 5. Vibration bruising area (%) of the control (a bare fruit) and four cushioning materials on Glom Sali guava peel under simulated vibration ($8.826 \text{ m s}^{-2} + 13.5 \text{ Hz} + 40 \text{ min}$) after storage at 20°C under 80% RH for 4 d. Different letters indicate significant differences at $p < 0.05$. Values are mean \pm S.E. from four replications.

for 4 d (Fig. 6). Fractal dimension has been used to characterize various fresh produce and related products including banana (Quevedo et al., 2008), bayberry (Zheng et al., 2011) and fresh-cut pear, mushroom, apple, and papaya (Quevedo et al., 2016; Caez-Ramírez et al., 2017). An increase in FD values indicated the heterogeneity of guava surface color due to the development of vibration bruising. However, a limitation of FD was found on the first day. The efficacy of FD was lower than BA, which determined vibration damage after 24 h. The lower heterogeneity of guava surface color impacted analysis of the FD results. The $\Delta \text{FD}/\text{FD}_0$ of a bare fruit was the highest, while there were no significant differences among the four cushioning treatments. A gradual increase in $\Delta \text{FD}/\text{FD}_0$ values of EPE-FN, NRL-FN+BLF0.0 phr, NRL-FN+BLF2.5 phr and NRL-FN+BLF5.0 phr treatments was observed during storage as compared to BA values that remained in the same range during storage. $\Delta \text{FD}/\text{FD}_0$ showed potential for assessment of vibration bruising and senescence in Glom Sali guava with increased storage duration (Fig. 6). This result concurred with Chaiwong et al. (2021). The $\Delta \text{FD}/\text{FD}_0$ value demonstrated higher reliability and repeatability in predicting vibration bruising in guava than BA.

In this study, NRL-FN+BLF0.0 phr and NRL-FN+BLF2.5 phr exhibited the lowest BA and $\Delta \text{FD}/\text{FD}_0$ levels (Figs. 5 and 6). These NRL-FN cushioning treatments provided good performance in terms of

cushioning properties and vibration protection. NRL-FN had lower thickness, cushion coefficient (C) and P_T with higher energy (E) (Table 1 and Fig. 3). Important functions of cushioning material led to a reduction of vibration force against vibration bruising of Glom Sali guava. The EPE-FN also provided good cushioning performance with low P_T and high thickness that corresponded to less free space inside the OPF box (Table 1). In addition, Eissa et al. (2012) and Zhou et al. (2018) have showed that conventional foam net for apple protection efficiently reduced acceleration intensity as compared to a bare fruit. In this study, thickness and free space were not the only considerations for cushioning properties and C and E variables were also considered when developing cushioning design. Scant reports have investigated conventional foam net and other cushioning materials for vibration protection under simulated transportation. Many studies evaluated scoring by severity level (Chonhenchob et al., 2008; Zhou et al., 2008), vibration damage (%) (Sigalingging et al., 2019) and conventional assessments by calculation of bruise area (BA), bruise volume (BV) (Eissa et al., 2012, 2013; Lin et al., 2020) and browning changes (Tao et al., 2021), with no studies investigating cushioning materials using image analysis for vibration bruising assessment of fruit. This study was the first to apply image analysis to compare vibration bruising under EPE-FN (conventional foam net) and NRL-FN+BLF cushioning packaging during

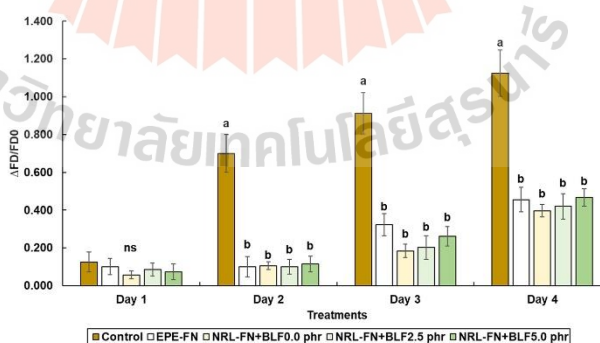


Fig. 6. Normalized fractal dimension difference ($\Delta \text{FD}/\text{FD}_0$) of the control (a bare fruit) and four cushioning materials on Glom Sali guava peel under simulated vibration ($8.826 \text{ m s}^{-2} + 13.5 \text{ Hz} + 40 \text{ min}$) after storage at 20°C under 80% RH for 4 d. Different letters indicate significant differences at $p < 0.05$. Values are mean \pm S.E. from four replications.

simulated transportation, by focusing on alternative material such as NRL-FN combined with BLF to increase valorization from agricultural waste.

Previous studies investigated different cushioning materials to protect fruit from both impact and vibration bruising damage. For vibration testing, most studies investigated apple or pear and compared a cushioning effect of a conventional foam net and paper-wrap which are a commercial practice (Eissa et al., 2012, 2013; Zhou et al., 2008). Conventional foam net exhibited greater protective vibration in Huanghua pear than paper-wrap packaging and no cushion, respectively (Zhou et al., 2008) as well as in apple (Eissa et al., 2012, 2013). Conventional foam net was also used as primary packaging to cover pineapple fruit packed in different secondary packages such as RPC, foam boxes, and corrugated fiberboard boxes (CFB) with a single wall C-flute.

Conventional foam net prevent vibration bruising with less severe and moderate bruise levels as compared to without conventional foam net in all secondary packages (Chonhenchob et al., 2008). For shock testing, the conventional foam net was compared with a two-ply pulp molded tray to protect apple fruit. This pulp molded tray exhibited greater cushioning performance than conventional foam net with reduced impact bruising area at peak acceleration ($490, 735.5$ and 980.7 m s^{-2}) and velocity change (3 and 4 m s^{-1}) (Kitazawa et al., 2018). Impact testing by a ballistic pendulum using a bare fruit gave the highest bruise volume, followed by conventional foam net and single face board with a corrugated flute on the outside. Conventional foam net gave lower cushioning performance than single face corrugated board for impact bruising protection in apple (Jarimopas et al., 2007). Therefore, conventional foam net proved to be a good cushioning material for vibration

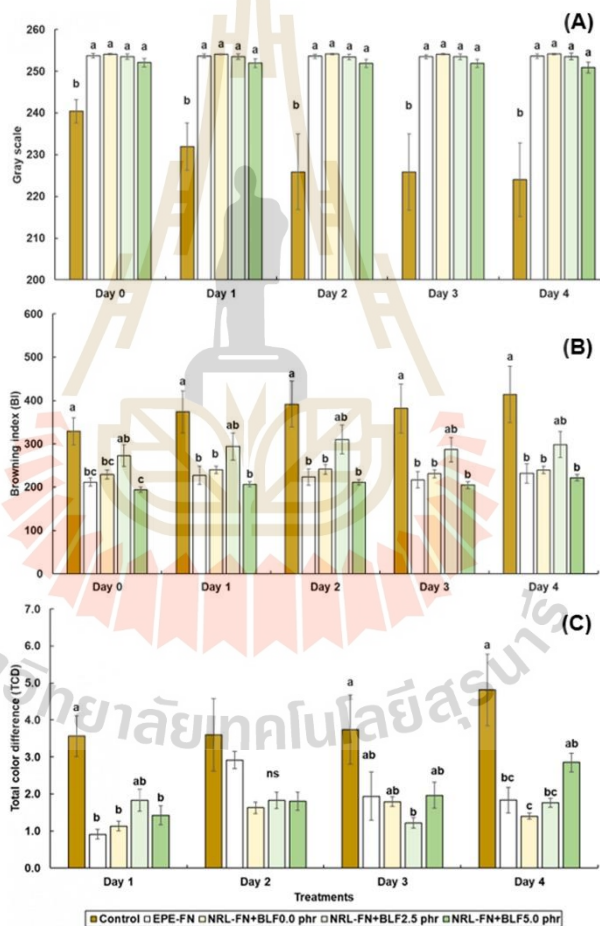


Fig. 7. Gray scale (A), BI (B) and TCD (C) of the control (a bare fruit) and four cushioning materials on Glom Sali guava peel under simulated vibration ($8.826 \text{ m s}^{-2} + 13.5 \text{ Hz} + 40 \text{ min}$) after storage at 20°C under $80\% \text{ RH}$ for 4 d. Different letters indicate significant differences at $p < 0.05$. Values are mean \pm S.E. from four replications.

S. Chaiwong et al.

Postharvest Biology and Technology 199 (2023) 112273

bruising protection of fruit but with lower cushioning performance against impact bruising. In this study, EPE-FN, NRL-FN+BLF0.0 phr and NRL-FN+BLF2.5 phr treatments gave a good protection for guava against vibration bruising as indicated by BA and Δ FD/FD₀ obtained by image analysis.

3.3. Gray scale, BI and TCD

Different color features were determined from the treated guava as grayscale color, BI and TCD. Gray scale of the four cushioning materials exhibited higher value than a bare fruit with no significant differences among the four cushioning materials during storage for 4 d (Fig. 7A). High grayscale levels related to low Δ FD/FD₀ levels in all treatments (Fig. 6). BI and TCD of a bare fruit gave the highest levels compared to the other four cushioning materials (Fig. 7B and C). Changes in grayscale intensity in guava were related to the development of vibrational damage. Generation of vibration brushing created brown scatter patches on the fruit surface, with lower grayscale. Surya Prabha and Satheesh Kumar (2015) reported change in grayscale intensity of banana during fruit development; grayscale intensity increased when the fruit turned pale-green while under-mature (dark green) fruit provided low grayscale intensity. Correlation between the changes in CIELAB and grayscale value was reported by Caez-Ramírez et al. (2017). Increasing a^* value due to the browning of fresh-cut papaya resulted in increasing gray value. For BI and TCD, results showed the same trend. The generation of vibration bruising increased both BI and TCD values. Greater change in CIELAB values in the control samples resulted in higher changes in both BI and TCD. The capability of the cushioning prevented the occurrence of vibration bruising of guava. The sample packed with various cushioning materials gave lower BI and TCD values. BI has been used to indicate that browning occurred according to changes in CIELAB parameters. TCD was also used to characterize changes in color parameters. However, limitations of using BI and TCD were reported by Chaiwong et al. (2021). They stated that the correlation among bruise area, BI and TCD was lower than Δ FD/FD₀ to indicate bruise area. Moreover, the vibration bruising characteristic of guava randomly revealed browning incidence on guava peel around the fruit. A small area with low bruising level is difficult to measure using a colorimeter to represent browning changes from vibration bruising.

4. Conclusions

The cushioning material performance of NRL-FN with different BLF compositions was investigated for vibration bruising of Glom Sali guava fruit and compared with EPE-FN as commercial cushioning material. The NRL-FN either without BLF (0.0 phr) or with BLF (2.5 phr) as well as EPE-FN exhibited the lowest cushioning performance to reduce vibration bruising by image analysis, with < 10% of the total bruising area as the limited defect of Thai and ASEAN guava standards. Increasing BLF composition to 5.0 phr in NRL-FN increased vibration bruising area on guava peel. The normalized fractal dimension difference (Δ FD/FD₀) of NRL-FN was indifferent from that of the EPE-FN after simulated vibration testing and storage at 20 °C under 80% RH for 4 d. NRL-FN+BLF0.0 phr gave lower cushion coefficient and percentage transmissibility than EPE-FN (at strain (ϵ) 0.500 mm/mm). This is the first research reporting that NRL-FN displayed excellent cushioning material and design performance properties against vibration damage in guava and other fruit. Bamboo leaves as a natural fiber were applied in NRL-FN as efficient waste utilization. Future studies should further optimize the potential of active packaging to delay browning incidence and fruit softening from the ripening process.

CRedit authorship contribution statement

Saowapa Chaiwong: Conceptualization, Methodology, Principal investigation, Data curation, Formal analysis, Writing – original draft.

Rattapon Saengrayap: Methodology, Investigation, Visualization, Writing – original draft. **Jutarat Rattanakaran:** Investigation, Data curation. **Arraya Chaithanarueang:** Investigation, Data curation. **Sujitra Arwattchananukul:** Visualization, Writing – review & editing. **Nattapol Aunsri:** Writing, Formal analysis, Writing – review & editing. **Khemapat Tontiwattanukul:** Resources, Software, Writing – review & editing. **Keavalin Jitkokkrud:** Investigation, Data curation. **Hiroaki Kitazawa:** Writing – review & editing. **Tatiya Trongsatitkul:** Methodology, Investigation, Visualization, Writing – original draft.

Declaration of Competing Interest

The authors declare that they have no known competing financial interests or personal relationships that could have appeared to influence the work reported in this paper.

Data Availability

Data will be made available on request.

Acknowledgements

The authors are grateful for the grant from Mae Fah Luang University under the National Science, Research, and Innovation Fund (NSRF) 2022: grant 652A04011, National Science and Technology Development Agency (NSTDA) (JRA-CO-2564-15967-TH) and to Mae Fah Luang University, and Suranaree University of Technology, Thailand for financial support and the provision of experimental sites for this research study.

References

- Acican, T., Alibas, K., Özelkök, I.S., 2007. Mechanical damage to apples during transport in wooden crates. *Biosyst. Eng.* 96 (2), 239–248. <https://doi.org/10.1016/j.biosystemseng.2006.11.002>.
- Agricultural Standard TAS 16-2010, 2010. Thai agricultural standard for guava. <https://www.acfs.go.th/standard/download/eng/guava.pdf> (accessed 28 July 2022).
- Altendorf, S., 2018. Minor tropical fruits. http://www.fao.org/fileadmin/templates/est/Common_Markets_Monitoring/Tropical_fruits/Documents/Minor_Tropical_Fruits_FoodOutlook_1_2018.pdf (accessed 14 July 2018).
- ASEAN Stan 7:2008, 2008. ASEAN standard for guava. <https://asean.org/storage/2012/05/7-ASEAN-STANDARD-FOR-GUAVA-2008.pdf> (accessed 28 July 2022).
- Caez-Ramírez, G., Téllez Medina, D.L., García Armenta, E., Gutiérrez López, G.F., 2017. Digital image analysis and fractal metrics as potential tools to monitor colour changes in fresh-cut papaya (*Carica papaya* L.). *Int. J. Food Prop.* 20, S177–S189. <https://doi.org/10.1080/10942912.2017.1293099>.
- Chaiwong, S., 2016. Effect of impact and vibration on quality and damage in the British strawberries (Doctoral dissertation). University of Essex, Colchester, UK.
- Chaiwong, S., Vaythaisong, P., Arwattchananukul, S., Aunsri, N., Tontiwattanukul, K., Trongsatitkul, T., Kitazawa, H., Saengrayap, R., 2021. Vibration damage in guava during simulated transportation assessed by digital image analysis using response surface methodology. *Postharvest Biol. Technol.* 181, 111641. <https://doi.org/10.1016/j.postharvbio.2021.111641>.
- Chandra, D., Kumar, R., 2012. Qualitative effect of wrapping and cushioning materials on guava fruits during storage. *Hortiflora. Res. Spectr.* 1 (4), 318–322.
- Chonhenchob, V., Singh, S.P., 2004. Testing and comparison of various packages for mango distribution. *J. Test. Eval.* 32 (1), 69–72. <https://doi.org/10.1520/JTE11888>.
- Chonhenchob, V., Kamhangwong, D., Singh, S.P., 2008. Comparison of reusable and single-use plastic and paper shipping containers for distribution of fresh pineapples. *Packag. Technol. Sci.* 21, 73–83. <https://doi.org/10.1002/pts.780>.
- Chonhenchob, V., Singh, S.P., Singh, J.J., Sittipod, S., Swasdee, D., Pratheepthong, S., 2010. Measurement and analysis of truck and rail vibration levels in Thailand. *Packag. Technol. Sci.* 23 (3), 91–100. <https://doi.org/10.1002/pts.881>.
- Dubey, N., Mishra, V., 2019. Cushioning materials for fruits, vegetables and flowers. In: Siddiqui, M.W., Rahman, M.S., Wani, A.A. (Eds.), *Innovative Packaging Fruits and Vegetables Strategies for Safety and Quality Maintenance*. Apple Academic Press, Waretown, pp. 275–314.
- Eissa, A.H.A., Albaloushi, N.S., Azam, M.M., 2013. Vibration analysis influence during crisis transport of the quality of fresh fruit on food security. *Agric. Eng. Int.: CIGR J.* 15 (3), 181–190.
- Eissa, A.H.A., Gomaa, G.R., Gomaa, F.R., Azam, M.M., 2012. Comparison of package-cushioning materials to protect vibration damage to golden delicious apples. *Int. J. Latest Trends Agric. Food Sci.* 2 (1), 36–57.
- Fadji, T., Coetzee, C., Chen, L., Chukwu, O., Opara, U.L., 2016. Susceptibility of apples to bruising inside ventilated corrugated paperboard packages during simulated

- transport damage. *Postharvest Biol. Technol.* 118, 111–119. <https://doi.org/10.1016/j.postharvbio.2016.04.001>.
- Food and Agriculture Organization, 2021. Food and agricultural commodities production: guava, mango, and mangosteen. <http://www.fao.org/faostat/en/#data/QC> (accessed 28 July 2022).
- Fernando, I., Fei, J., Stanley, R., Enshaei, H., 2018. Measurement and evaluation of the effect of vibration on fruits in transit—Review. *Packag. Technol. Sci.* 31 (11), 723–738. <https://doi.org/10.1002/pts.2409>.
- Idah, F.A., Gana, Y.M., Ogbounaya, C., Morenikeji, O.O., 2012. Simulated transport damage study on fresh tomato (*Lycopersicon esculentum*) fruits. *Agric. Eng. Int. CIGR J.* 14 (2), 119–126.
- Ismail, O., El-Moniemi, E., Allah, A., El-Naggar, M., 2010. Influence of some post-harvest treatments on guava fruits. *Agr. Biol. J. N. Am.* 1, 1309–1318 <https://doi.org/10.5251/abjna.2010.1.6.1309.1318>.
- Jarimopas, B., Mahayassan, T., Srianeek, N., 2004. Study of capability of net made of banana string for apple protection against impact. *Eng. J. Kasetsart.* 17 (51), 9–16.
- Jarimopas, B., Singh, S.P., Sayasoonthorn, S., Singh, J., 2007. Comparison of package cushioning materials to protect post-harvest impact damage to apples. *Packag. Technol. Sci.* 20 (5), 315–324. <https://doi.org/10.1002/pts.760>.
- Jitkokkrad, K., Jarukumjorn, K., Chaiwong, S., Trongsatitkul, T., 2021. Effect of foaming time and speed on morphology and mechanical properties of natural rubber latex foam vulcanized by microwave heating. In *SUT International Virtual Conference on Science and Technology, Nakhon-Ratchasima, Thailand*, 6 August 2021, 245–251.
- Kamsiati, E., 2013. Postharvest handling practices in maintaining quality and shelf life of guava (*Psidium guajava*). In *Proceeding of the International Conference on Agricultural Postharvest Handling, and Processing, Jakarta, Indonesia*, 19–21 November 2013, 363–373.
- Jitkokkrad, K., Jarukumjorn, K., Rakskulpiwat, C., Chaiwong, S., Trongsatitkul, T., 2023. Effects of bamboo leaf fiber content on cushion performance and biodegradability of natural rubber latex foam composite. *Polymers* 15 (3), 654. <https://doi.org/10.3390/polym15030654>.
- Katumbi, J.N., Imungi, J.K., Abong, G.O., Gachuri, C.K., Mwangombe, A.W., Omaylo, D.G., Owade, J.O., 2021. Harvesting, postharvest handling, hygiene knowledge and practices of guava fruit farmers: a comparative study of two counties of Kenya. *Afr. J. Food Sci.* 15 (5), 177–189. <https://doi.org/10.5897/AJFS2021.2079>.
- Khodaei, M., Seidielou, S., Sadeghi, M., 2019. The evaluation of vibration damage in fresh apricots during simulated transport. *Res. Agric. Eng.* 65 (4), 112–122. <https://doi.org/10.17221/12/2019-RAE>.
- Kitazawa, H., 2018. Cushioning packaging for fresh produce. *Ref. Modul. Food Sci.* 1–8.
- Kitazawa, H., Saito, K., Ishikawa, Y., 2015. Method for controlling damage to products subjected to cumulative fatigue considering damage degree at each layer in stacked packaging. *J. Pac. Sci. Technol.* 24 (2), 71–78.
- Lin, M., Fawole, O.A., Saeyes, W., Wu, D., Wang, J., Opara, U.I., Nicolai, B., Chen, K., 2022. Mechanical damages and packaging methods along the fresh fruit supply chain: a review. *Crit. Rev. Food Sci. Nutr.* 1–20. <https://doi.org/10.1080/10408398.2022.2078783>.
- Lin, M., Chen, J., Chen, F., Zhu, C., Wu, D., Wang, J., Chen, K., 2020. Effects of cushioning materials and temperature on quality damage of ripe peaches according to the vibration test. *Food Packag. Shelf Life* 25, 100518. <https://doi.org/10.1016/j.foodeng.2020.100518>.
- Mendes, M.S., Chaves, F.M.S., Nascimento, S.S., Pires, L.C.G., Almeida, E.I.B., Sousa, A.N.S., Ferrão, G.E., 2019. Postharvest losses of guava in the retail trade at Chapadinha (MA). *Sci. Electron. Arch.* 12 (5), 57–61.
- Quevedo, R., Mendoza, F., Aguilera, J.M., Chmoua, J., Gutiérrez-López, G., 2008. Determination of senescent spotting in banana (*Musa cavendishii*) using fractal texture Fourier image. *J. Food Eng.* 84 (4), 509–515. <https://doi.org/10.1016/j.jfoodeng.2007.06.013>.
- Quevedo, R., Pedreschi, F., Bastias, J.M., Diaz, O., 2016. Correlation of the fractal enzymatic browning rate with the temperature in mushroom, pear and apple slices. *LWT* 65, 406–413. <https://doi.org/10.1016/j.lwt.2015.08.052>.
- Rolle, R., 2008. Good practice for assuring the post-harvest quality of exotic tree fruit crops produced in Jamaica. <https://www.fao.org/3/ak832e/ak832e.pdf> (accessed 1 August 2022).
- Sigalingging, R., Nasution, H.A., Rindang, A., Ayu, P.C., 2019. Effect of packaging fillers materials on the quality of papaya fruit (*Carica papaya* L.). In *International Conference on Agriculture, Environment, and Food Security, Medan, Indonesia*, 24–25 October 2018, 012036.
- Singh, J., Singh, S.P., Joneson, E., 2006. Measurement and analysis of US truck vibration for leaf spring and air ride suspensions, and development of tests to simulate these conditions. *Packag. Technol. Sci.* 19 (6), 309–323. <https://doi.org/10.1002/pts.732>.
- Singh, S.P., 2011. Guava (*Psidium guajava* L.). In: Yalnia, F.M. (Ed.), *Postharvest Biology and Technology of Tropical and Subtropical Fruits*. Woodhead Publishing Limited, Cambridge, pp. 213–245.
- Sohn, J.S., Kim, H.K., Kim, S.W., Ryu, Y., Cha, S.W., 2019. Biodegradable foam cushions as ecofriendly packaging materials. *Sustainability* 11 (6), 1731. <https://doi.org/10.3390/s11061731>.
- Song, X., Zhang, G., Lu, J., Zhang, L., Zhang, S., 2018. Study on the cushion performance of the cushion material composed of EPE and corrugated paperboard. *Applied Sciences in Graphic Communication and Packaging*, Springer, pp. 467–474.
- Strecker, J., Rodriguez, G., Njanji, I., Thomas, J., Jack, A., Darrigues, A., Hall, J., Dujnovic, N., Gray, S., van der Knaap, E., Francis, D., 2010. Tomato analyzer color test user manual version 3. https://vanderknaaplab.uga.edu/files/Color_Test_3.0_Manual.pdf (accessed 1 May 2022).
- Snbhashree, S.N., Smoj, S., Xue, J., Bora, G.C., 2017. Quantification of browning in apples using colour and textural features by image analysis. *Food Qual. Saf.* 1 (3), 221–226. <https://doi.org/10.1093/foodqual/fyx021>.
- Surya Prabha, D., Satheesh Kumar, J., 2015. Assessment of banana fruit maturity by image processing technique. *J. Food Sci. Technol.* 52 (3), 1316–1327. <https://doi.org/10.1007/s13197-013-1188-3>.
- Tao, F., Chen, W., Jia, Z., 2021. Effect of simulated transport vibration on the quality of shiitake mushroom (*Lentinus edodes*) during storage. *Food Sci. Nutr.* 9 (2), 1152–1159. <https://doi.org/10.1002/fsn3.2094>.
- Vursavus, K., Ozguven, E., 2004. Determining the effects of vibration parameters and packaging method on mechanical damage in golden delicious apples. *Turk. J. Agric. For.* 28 (5), 311–320.
- Yadav, A., Kumar, N., Upadhyay, A., Fawole, O.A., Mahawar, M.K., Jalgaonkar, K., Chandran, D., Rajalingam, S., Zengin, G., Kumar, M., Mekhemar, M., 2022. Recent advances in novel packaging technologies for shelf-life extension of guava fruits for retaining health benefits for longer duration. *Plants* 11 (4), 547. <https://doi.org/10.3390/plants11040547>.
- Zheng, H., Jiang, B., Lu, H., 2011. An adaptive neural fuzzy inference system (ANFIS) for detection of bruises on Chinese bayberry (*Myrica rubra*) based on fractal dimension and RGB intensity color. *J. Food Eng.* 104 (4), 663–667. <https://doi.org/10.1016/j.jfoodeng.2011.01.033>.
- Zhou, R., Su, S., Li, Y., 2008. Effects of cushioning materials on the firmness of Huanghua pears (*Pyrus pyrifolia Nakai* cv. Huanghua) during distribution and storage. *Packag. Technol. Sci.* 21, 1–11. <https://doi.org/10.1002/pts.769>.

BIOGRAPHY

Miss Keavalin Jitkokkrud was born on May 29, 1997, in Nakhon-Ratchasima, Thailand. She earned her Bachelor's Degree in Polymer Engineering from Suranaree University of Technology (SUT) in 2019. She then continued her Master's degree in Materials Engineering (Polymer) at the Institute of Engineering at Suranaree University of Technology. Her fields of interest include cushioning packaging foam from natural rubber latex and microwave-assisted vulcanization. During her Master's degree study, she presented an international conference entitled "Effect of Blowing Agent Content on Compressive Property and Cell Structure of Natural Rubber Foam Prepared using Microwave Heating Process" at the International Polymer Conference of Thailand (PCT-10), Bangkok, Thailand, and "Effect of Foaming Time and Speed on Morphology and Mechanical Properties of Natural Rubber Latex Foam Vulcanized by Microwave Heating" at the SUT International Virtual Conference on Science and Technology 2021 (IVCST 2021), Nakhon-Ratchasima, Thailand, and In addition, she worked on her thesis with the School of Agro-Industry at Mae Fah Luang University, Chiang Rai, Thailand, and published two international journals entitled "Effects of Bamboo Leaf Fiber Content on Cushion Performance and Biodegradability of Natural Rubber Latex Foam Composites" at Polymers Journal (2023) and "Natural Rubber Latex Cushioning Packaging to Reduce Vibration Damage in Guava during Simulated Transportation" in Postharvest Biology and Technology (2023).